Genome-wide study of subcutaneous and visceral adipose tissue reveals novel sex-specific adiposity loci in Mexican Americans: The Insulin Resistance Atherosclerosis Family Study

Chuan Gao[1,2,3], Carl D. Langefeld[3,4], Julie T. Ziegler[3,4], Kent D. Taylor[5], Jill M. Norris[6], Yii-Der I. Chen[5], Jacklyn N. Hellwege[2,8], Xiuqing Guo[5], Matthew A. Allison[11], Elizabeth K. Speliotes[9], Jerome I. Rotter[5,12], Donald W. Bowden[2,8,10], Lynne E. Wagenknecht[7], Nicholette D. Palmer[2,3,8,10*]

[1]Molecular Genetics and Genomics Program; Wake Forest School of Medicine, Winston-Salem, NC

[2]Center for Genomics and Personalized Medicine Research; Wake Forest School of Medicine, Winston-Salem, NC

[3]Center for Public Health Genomics; Wake Forest School of Medicine, Winston-Salem, NC

[4]Department of Biostatistical Sciences; Wake Forest School of Medicine, Winston-Salem, NC

[5]Institute for Translational Genomics and Population Sciences; Los Angeles Biomedical Research Institute at Harbor-UCLA Medical Center, Torrance, CA

[6]Department of Epidemiology, Colorado School of Public Health; University of Colorado, Aurora, CO

[7]Division of Public Health Sciences; Wake Forest School of Medicine, Winston-Salem, NC

[8]Center for Diabetes Research; Wake Forest School of Medicine, Winston-Salem, NC

[9]Department of Internal Medicine, Division of Gastroenterology and Department of Computational Medicine and Bioinformatics; University of Michigan, Ann Arbor, MI

[10]Department of Biochemistry; Wake Forest School of Medicine, Winston-Salem, NC

[11]Department of Family Medicine and Public Health, University of California San Diego, La Jolla CA

[12]Department of Pediatrics; Los Angeles Biomedical Research Institute at Harbor-UCLA Medical Center, Torrance, CA

Keywords: Genetics, Hispanics, Family Studies, Computed Tomography, Obesity

Running title:

Genetics of adipose deposition

Contact info:

*Correspondence to

Nicholette D. Palmer, PhD

Department of Biochemistry

1 Medical Center Blvd

Winston-Salem, NC 27040

Phone: 336-713-7534

E-mail: nallred@wakehealth.edu

Word count:

3,499

Funding:

This research was supported by DK097524 from the National Institute of Diabetes and Digestive and Kidney Diseases (NIDDK), DK053591 from National Institute of Health, and HG007112 from the National Human Genome Research Institute (NHGRI). The provision of GWAS genotyping data was supported in part by UL1TR000124 (CTSI) and DK063491 (DRC). Exome chip genotyping was supported by DK081350, HG007112, DK087914, and the Department of Internal Medicine at the University of Michigan. Computational resources were provided, in part, by the Wake Forest School of Medicine Center for Public Health Genomics. The authors would like to acknowledge the members of the GUARDIAN Consortium with research supported by DK085175 from NIDDK and from the IRASFS grants (HL060944 and HL061019). EKS was supported by NIH grants R01 DK106621, R01 DK107904, The University of Michigan Biological Sciences Scholars Program and The University of Michigan Department of Internal

Medicine. MESA and the MESA SHARe project are conducted and supported by the National Heart, Lung, and Blood Institute (NHLBI) in collaboration with MESA investigators. Support for MESA is provided by contracts HHSN268201500003I, N01-HC-95159, N01-HC-95160, N01-HC-95161, N01-HC-95162, N01-HC-95163, N01-HC-95164, N01-HC-95165, N01-HC-95166, N01-HC-95167, N01-HC-95168, N01-HC-95169, UL1-TR-000040, UL1-TR-001079, UL1-TR-001420, UL1-TR-001881, and DK063491. Funding for SHARe genotyping was provided by NHLBI Contract N02-HL-64278. Genotyping was performed at Affymetrix (Santa Clara, California, USA) and the Broad Institute of Harvard and MIT (Boston, Massachusetts, USA) using the Affymetrix Genome-Wide Human SNP Array 6.0. Funding support for the abdominal aortic CT dataset was provided by grant HL088451.

Disclosure:

The authors declared no conflict of interest.

Study questions:

What is already known about this project:

- Genetic variation contributes to body fat deposition.
- Males and female have distinct fat deposition patterns.
- Regional fat deposition is a strong risk factor for metabolic disease.

What does your study add:

- Novel genetic signals associated with body fat deposition were identified.
- Novel genetic signals with sex-specific fat deposition effects were identified.
- Previously identified fat deposition genetic signals were replicated.

Abstract (200 words):

Objective: This study aimed to explore genetic mechanisms of regional fat deposition, which is a strong risk factor for metabolic diseases beyond total adiposity.

Methods: A genome-wide association study of 7,757,139 SNPs in 983 Mexican Americans (N_{male}=403, N_{female}=580) from the Insulin Resistance Atherosclerosis Family Study (IRASFS) was performed. Association analyses were performed with and without sex stratification for subcutaneous adipose tissue (SAT), visceral adipose tissue (VAT), and visceral-subcutaneous ratio (VSR) obtained from computed tomography (CT).

Results: The strongest signal identified was SNP rs2185405 (MAF=40%, $P_{VAT}=1.98x10^{-8}$) with VAT. It is an intronic variant of the GLIS family zinc finger 3 gene (*GLIS3*). In addition, SNP rs12657394 (MAF=19%) was associated with VAT in males ($P_{male}=2.39x10^{-8}$; $P_{female}=2.5x10^{-3}$). It is located intronically in the serum response factor binding protein 1 gene (*SRFBP1*). On average, male carriers of the variant had 24.6cm^2 increased VAT compared to non-carriers. Subsequently, genome-wide SNP-sex interaction analysis was performed. SNP rs10913233 (MAF=14%, $P_{int}=3.07x10^{-8}$) in *PAPPA2* and rs10923724 (MAF=38%, $P_{int}=2.89x10^{-8}$) upstream of *TBX15* were strongly associated with the interaction effect for VSR.

Conclusions: Six loci were identified with genome-wide significant associations with fat deposition and interactive effects. These results provided genetic evidence for a differential basis of fat deposition between genders.

Introduction

Obesity is a global health epidemic affecting more than 500 million individuals worldwide and responsible for nearly three million deaths each year (1). Previous studies have confirmed obesity as a strong risk factor for many metabolic diseases including cardiovascular disease (CVD), type 2 diabetes (T2D), metabolic syndrome, certain types of cancer, stroke, and hypertension (2, 3). However, the exact mechanisms underlying these associations have been poorly elucidated.

Recent research has suggested obesity is not a homogeneous condition and regional fat distribution affects glucose and lipid metabolism beyond total body adiposity (4). For example, visceral adipose tissue (VAT) has been shown to be responsible for the increased mortality and risk for metabolic disorders while subcutaneous adipose tissue (SAT) is thought to be benign (5). Genetic studies have been successful in identifying genetic loci responsible for regional fat distribution using measures including waist circumference (WAIST) and waist-hip ratio (WHR). However, anthropometric measures can be impacted by skeletal structure and aging (6) and cannot differentiate between regional fat depots, e.g. visceral and subcutaneous adipose tissue, and therefore bias studies. Currently, computed tomography (CT) is considered as the gold standard for the measurement of adipose tissue deposition (7, 8). However, due to cost and accessibility reasons, only one genome-wide association study (GWAS) has been published focusing on directly measured SAT and VAT with genome-wide significant signals (9).

Numerous evidence has suggested strong sex specificity for regional adipose tissue distributions with females having a higher proportion of gluteal-femoral body fat whereas males have more in the abdominal (visceral) region (8, 10). This observation suggests a potentially different mechanism for fat deposition in different genders. In 2015, the Genetic Investigation of Anthropometric Traits (GIANT) consortium published a genetic study of adipose tissue deposition using WHR and identified 49 (33 new)

signals associated with 20 loci demonstrating sex-specific effects (11). Until now, no formal genome-wide SNP-sex interaction analysis has been performed in Mexican Americans.

Here we report a genetic study of sex-specific adipose tissue deposition using CT measures including SAT and VAT in the Insulin Resistance Atherosclerosis Family Study (IRASFS). Genome-wide and exome chip association studies were combined to provide a more comprehensive scan of both common and rare variants. As adiposity deposition differs between genders, sex-stratified analyses as well as genome-wide SNP-sex interaction analyses were performed.

Materials and Methods

Insulin Resistance Atherosclerosis Family Study (IRASFS)

The study design, recruitment, and phenotyping for the IRASFS have been previously described (12, 13). In brief, the IRASFS is a family-based study designed to investigate the genetic and environmental basis of insulin resistance and adiposity. Individuals included in this cohort (N=1,417 individuals, 90 pedigrees) were Mexican Americans recruited from in San Antonio, TX and San Luis Valley, CO. Since a diagnosis of diabetes was not required for participation, about 12.7% of individuals had diabetes. The study protocol was approved by the Institutional Review Board of each participating clinical and analysis site and all participants provided written informed consent.

Phenotypes

Measures of adiposity were obtained using a standardized protocol. BMI was calculated as weight in kilograms divided by height in meters squared. Computed tomography (CT) scans were performed to estimate visceral and subcutaneous fat area (VAT and SAT, respectively; cm^2). This procedure consisted of a single scout of the abdomen followed by a 10-mm thick axial image. Axial images were obtained at L4-L5 disc space using a standard protocol. CT images were sent to a centralized reading center at the

University of Colorado Health Sciences Center. VAT and SAT were computed from these data as previously described (7). Visceral-subcutaneous ratio (VSR) was computed as the ratio of VAT and SAT. In addition, glucose homeostasis traits were also obtained in IRASFS, e.g. acute insulin response (AIR), metabolic clearance rate of insulin (MCRI), fasting plasma glucose (GFAST) and insulin (FINS), and homeostatic model assessment of beta-cell function and insulin resistance ($HOMA_B$ and $HOMA_{IR}$). Phenotype acquisition and variable calculations have been previously described (12, 14).

Genotyping and Quality Control

Genotyping

GWAS genotyping was supported through the Genetics Underlying Diabetes in Hispanics (GUARDIAN) Consortium (15) using the Illumina OmniExpress and 1S arrays (Illumina Inc.; San Diego, CA, USA) and exome chip genotyping was carried out on the Illumina HumanExome Array. A detailed description of genotyping platforms and quality controls has been published (13).

Imputation

Imputation was performed using IMPUTE2 (16) and the 1000G phase I V3 integrated reference panel. All IRASFS samples genotyped on the OmniExpress and 1S arrays were imputed together. Imputed variants were filtered with a confidence score >0.90 and an information score >0.50. Imputation quality was evaluated using 10,000 SNPs with both exome chip and imputation coverage randomly selected from 32,729 overlapping SNPs.

Statistical Analysis

GWAS and Exome Chip

Phenotypes were transformed to approximate the distributional assumptions of normality and homogeneity. Specifically, VSR was natural log transformed and SAT and VAT were square-root transformed. Admixture estimates were calculated using maximum likelihood estimation of individual ancestries as implemented in ADMIXTURE (17). For SNPs available in both GWAS imputation and exome chip, exome chip genotypes were always used for analysis. Imputation quality was evaluated with 10,000 overlapping SNPs between GWAS imputation and exome chip, which were selected based on minor allele frequencies (MAF). Concordance analysis was performed between the two platforms and an r-square value was computed for each variant.

Tests of association between individual variants and quantitative traits were computed using the Wald test from the variance component model implemented in Sequential Oligogenic Linkage Analysis Routines (SOLAR) (18). Rare variants (both genotyped and imputed) with MAF <1% were removed, resulting a total of 7,708,309 variants. Genetic associations were calculated adjusting for age, recruitment center, admixture estimates, and sex (for sex-combined analysis only). The primary inference was the additive model. A lack of fit to the additive model was tested using the orthogonal contrast. If the lack-of-fit test was significant ($P<0.05$), the model with the "best" p-value as the minimum of the dominant, additive, and recessive genetic models was selected. For robust estimation purposes, the dominant and recessive genetic models were not computed if there were less than 10 and 20 individuals homozygous for the minor allele, respectively (this threshold is not applicable for SNPs with the non-significant lack-of-fit test). Interaction analysis was performed to test the beta-coefficient of the interaction variable using the same genetic model as the main effect. Genome-wide significance was defined as a P value less than $5x10^{-8}$ and suggestive significance was defined as a P value less than $5x10^{-7}$. A genetic locus is defined as a genetic region (<1MB) with a cluster of correlated variants ($r^2>0.4$). A novel signal is defined as one that is more than 500kb away from a known CT phenotype-associated locus.

Replication

Replication of loci that attained genome-wide significance in IRASFS was undertaken among Mexican American participants from the Multi-ethnic Study of Atherosclerosis (MESA; n=485). MESA is a multiethnic cohort of participants that were free of clinical cardiovascular disease at enrollment.(19) Protocols were approved by the Institutional Review Board at each participating institution. All participants provided written informed consent. Assessment of adiposity by CT has been previously described.(20) Genotypes from MESA were obtained from the Affymetrix Genome-Wide Human SNP Array 6.0 with imputation to the 1000G phase I V3 integrated reference panel. The statistical analysis in MESA followed the same protocol as described for IRASFS.

Results

A demographic summary of the study samples is shown in **Table S1**. Overall, individuals were overweight with an average BMI greater than 28.3kg/m^2. In total, 983 and 1,205 individuals were analyzed for GWAS imputed and exome chip SNPs, respectively. Compared to GWAS, an additional 222 samples were included in the exome chip data, of which 150 were individuals with T2D. This resulted in modestly increased age and adiposity traits ($P<0.001$). In addition, mean trait values of adiposity phenotypes were significantly different between females and males, i.e. females had significantly larger amounts of SAT ($P<0.0001$) while males had larger amounts of VAT ($P<0.0001$). The ratio between VAT and SAT (VSR) was two times greater in males than females ($P<0.0001$), suggesting males have the predisposition to store fat viscerally. Overall, 7,708,309 SNPs with MAF≥1% were analyzed with SAT, VAT, VSR, and VAT_BMI (VAT with additional adjustment of BMI). A complete list of quantile-quantile (q-q) plots can be found in **Figure S1**.

Imputation quality

The majority of the SNPs analyzed were derived from statistical imputation as opposed to direct genotyping. To evaluate imputation quality, concordance analysis for 10,000 SNPs overlapping between exome chip and imputation was performed. Overall, SNP genotypes were well-matched between the two platforms with an r^2>0.95 (**Figure S2**). However, for rare variants with MAF<1%, the imputation quality varied and therefore these were excluded from analysis.

Association Results

Association analyses were computed for SAT, VAT, VAT_BMI, and VSR adjusting for age, sex, recruitment center, and admixture estimates. The association results are summarized in **Figure S3, Table 1**. The strongest signal identified was SNP rs2185405 (P_{rec}=1.98x10^{-8}, MAF=40%) with VAT. It is an intronic SNP located in the GLIS family zinc finger 3 gene (*GLIS3*). Association of this variant in MESA was non-significant (P=0.63, Table S3). In addition, suggestive evidence of association was observed with SAT (rs2223471 and rs4746598), VAT (rs2131949 and rs78596136), VAT_BMI (rs4243443 and rs12657394), and VSR (rs1504143) (**Table S2**).

Sex-stratified Association Analysis

Results of the sex-stratified association analysis are summarized in **Figure S4 and Table 1**. Overall, five SNPs from two loci reached genome-wide significance (P<5x10^{-8}). Two directly genotyped intronic SNPs (rs12657394, MAF=18.9%, P_{male}=2.39x10^{-8}, P_{female}=4.10x10^{-3}; rs2914610, MAF=19.2%, P_{male}=4.55x10^{-8}, P_{female}=5.58x10^{-3}) within the serum response factor binding protein 1 gene (*SRFBP1*) on chromosome 5 were strongly associated with VAT_BMI in males (r^2=0.98). Three imputed SNPs (rs1002945, rs13247968, and rs1830005, r^2>0.91) located downstream of the sorting nexin 13 gene (*SNX13*) were significantly associated with VAT_BMI in males but not females (rs13247968, MAF=42.9%, P_{male}=7.63x10^{-}

^{9}, P_{female}=0.36). Analysis of significant results in MESA failed to provide replication (P>0.35, Table S3) although a consistent direction of effect was observed for the two variants in *SRFBP1* (rs12657394 and rs2914610). Signals of suggestive significance ($P<5x10^{-7}$) are summarized in **Table S2**.

SNP-sex Interaction Analysis

Results of the SNP-sex interaction are summarized in **Figure S5 and Table 1**. SNP rs9289345 was strongly associated with the interaction variable for VAT_BMI ($P_{int}=3.73x10^{-8}$, MAF=1.3%). It is an intronic SNP located within transmembrane and coiled-coil domain family 1 gene (*TMCC1*). An intronic SNP within pappalysin 2 gene (*PAPPA2*) (rs10913233, $P_{int}=3.07x10^{-8}$, MAF=13.8%) was associated with the interaction variable for VSR. SNP rs10923724, located upstream of T-box 15 gene (*TBX15*), was strongly associated with the interaction variable for VSR ($P_{int}=2.89x10^{-8}$, MAF=38.1%). Association of these variants in MESA was non-significant (P>0.15, Table S3).

Assessment of Previously Identified Signals

Nine previously identified CT loci (9, 21, 22) were evaluated herein (**Table S4**). Consistent with previous findings, the fat mass and obesity-associated gene (*FTO*) signal was modestly associated with SAT in IRASFS (rs9922619, $P_{SAT}=4.01x10^{-3}$, $P_{male}=5.98x10^{-2}$, $P_{female}=6.20x10^{-2}$) yet no interactive effect (P_{SAT_INT}=0.41) was detected. In addition, SNP rs2123685 on chromosome 7 was modestly associated with SAT and VAT in males ($P_{SAT}=4.15x10^{-2}$, $P_{VAT}=3.55x10^{-3}$) and rs7374732 on chromosome 3 was modestly associated with VSR in males ($P_{VSR}=3.21x10^{-2}$). Furthermore, 49 adipose deposition signals identified by GIANT using WHR were evaluated for association with all four phenotypes (**Table S4**). Overall, 21 signals were significantly associated (P<0.05) with at least one of the four CT phenotypes and 18 of the 21 signals exhibited gender-specific effects (P<0.05 for gender stratified or interaction analysis). The strongest signal observed was SNP rs2645294 ($P_{VSR\_INT}=1.20x10^{-5}$). It is located in the 3'-UTR region of the tryptophanyl TRNA synthetase 2 mitochondrial gene (*WARS2*) and has been previously

reported to be associated with WHR (11). Interestingly, SNP rs10923724, which is about 500kb downstream of rs2645294, was identified to have a significant sex-interactive effect ($P_{INT}=2.89x10^{-08}$) with VSR. Further analysis revealed that the two SNPs were in modest linkage disequilibrium (LD) in IRASFS ($r^2=0.59$) and strong LD in Europeans ($r^2=0.93$ in 1000G CEU). However, the previous study revealed no sex specificity for SNP rs2645294 (11), suggesting a potentially different biology represented by WHR and VSR.

Discussion

Here we present a study combining genome-wide and exome chip arrays to investigate the genetic determinants of adipose tissue deposition in Mexican Americans from the IRASFS. The differentiation between SAT and VAT using CT provided more refined adiposity phenotypes compared to anthropometric measures. In addition, as SAT and VAT distributions vary by sex, sex-stratified as well as SNP-sex interaction analyses were performed. Signals with significant sex-specific effects were identified.

SNP rs2185405, an intronic SNP within GLIS family zinc finger 3 gene (*GLIS3*), was found to be genome-wide significant for the main effect with VAT without sex stratification ($P_{dom}=1.98x10^{-8}$, MAF=40%)(**Figure 1**). On average, the carriers of the minor allele T have 19.91 cm^2 less VAT compared to non-carriers. *GLIS3* is a member of the GLI-similar zinc finger protein family and encodes a nuclear protein with five C2H2-type zinc finger domains. It functions as both a repressor and activator of transcription and is specifically involved in the development of pancreatic beta-cells, the thyroid, eye, liver and kidney (23). Previous studies have shown this gene is associated with diabetes in multiple ethnicities (24, 25). *In vitro* experiments suggested *GLIS3* modulates pancreatic beta-cell apoptosis via the regulation of a splice variant of the BH3-only protein Bim (26). Since VAT has been shown to be a risk factor for metabolic disorders (4, 5), it is possible that VAT is involved in the modulation of beta-cell

function through *GLIS3*. Further evaluation of the SNP using glucose homeostasis traits in IRASFS revealed a significant association with insulin clearance (P=0.03) and a suggestive association with fasting insulin (P=0.09). However, acute insulin response (AIR) was not significant (P=0.64).

For sex-stratified analyses, five SNPs from two loci (*SRFBP1*, 7p21.1) reached genome-wide significance. *SRFBP1*, also named as *p49/STRAP*, was associated with VAT_BMI in males. Regional plots indicate long-range LD covering a 200kb region (**Figure 2**). The strongest signal in the region was an intronic SNP rs12657394 under a dominant model (P_{male}=2.39x10^{-8}; P_{female}=0.0041; MAF=18.9%). In males, the minor allele carriers had a 24.6cm^2 increase in VAT compared to common allele homozygous individuals. Conditional analysis using rs12647394 as a covariate abolished the association signal, suggesting only one independent signal exists in *SRFBP1*. Previous studies have shown that the protein encoded by *SRFBP1* specifically interacts with an acidic amino acid motif in the N-terminus of GLUT4 in adipose cells, suggesting a possible role in biosynthesis and/or processing of GLUT4 in adipocytes (27). However, no biological evidence has been identified to explain sex specificity. Further evaluation of glucose homeostasis traits in IRASFS with and without sex stratification revealed modest association signals for rs12657394 with fasting insulin (P_{add}=7.92x10^{-3}), fasting glucose (P_{rec}=0.025), $HOMA_{IR}$ (P_{add}=0.03) and $HOMA_B$ (P_{dom}=0.03). However, no sex-specific patterns were observed. Extended examination of this region in the GIANT consortium with WAIST, BMI, and WHR stratified by sex failed to replicate this signal. This could be due to ethnic heterogeneity as well as the limitations of anthropometric measures compared to CT-derived fat deposition.

At 7p21.1, SNP rs13247968 (MAF=42.5%, P_{male}=7.63x10^{-9}, P_{female}=0.36) as well as two other highly correlated SNPs (r^2≥0.9) were strongly associated with VAT after adjusting for BMI under the dominant model in males. On average, male carriers of the rs13247968 minor allele (G) had a 16.4 cm^2 increase of VAT compared to homozygous major allele carriers. The regional plot (**Figure 3**) reveals a tight cluster of

signals located downstream of *SNX13* (Sorting nexin 13 gene, also known as *RGS-PX1*). The RGS (Regulator of G protein) domain of the encoded protein can function as a GTPase-activating protein for G alpha subunits of heterotrimeric G proteins while the PX (Phox) domain works as a sorting nexin protein involved in intracellular trafficking (28). Studies have shown that the protein can target lysosomes and delay lysosomal degradation of the EGFR (Epidermal growth factor receptor) (28). Further examination of this region in the GIANT consortium identified rs1990467, 100kb proximal to rs13247968, was associated with WC_BMI in males ($P=2.6x10^{-4}$)(**Figure S6**) (29, 30). However, the correlation between rs13247968 and rs1990467 was poor ($r^2=0.00$ in IRASFS, $r^2<0.08$ in 1000G). Previous genetic studies have suggested *SNX13* is strongly associated with HDL cholesterol in European ancestry individuals (31). Evaluation of SNP rs13247968 with circulating cholesterol levels and BMI in IRASFS failed to detect significant associations (P>0.05). Interestingly, rs13247968 is 300kb upstream of histone deacetylase 9 gene (*HDAC9*), which encodes an important histone deacetylase that regulates transcriptional regulation, cell cycle progression, and developmental events. Genetic studies have suggested *HDAC9* is associated with multiple phenotypes including coronary artery disease (CAD), BMI, and vigorous physical activity in European and Hispanic populations (rs2107595, rs2853552, rs12666612, respectively) (32, 33). However, no strong LD was detected between rs13247968 and these previously identified *HDAC9* signals ($r^2<0.01$).

The pappalysin 2 or pregnancy-associated plasma protein A2 gene (*PAPPA2*) located on chromosome 1 (rs10913233, $P_{Add}=3.07x10^{-8}$, MAF=13.8%) was associated with the SNP-sex interaction effect for VSR (**Figure 4**). The protein encoded by *PAPPA2* has been proposed as a biomarker for preeclamptic placentae in pregnant women. It works as a protease specifically cleaving insulin-like growth factor binding protein 5 (IGFBP5) and thus plays an important role in regulating IGFBP5 levels (34). Diseases related to this gene include HELLP-syndrome and developmental dysplasia of hip (35, 36). Human population genetic studies have suggested this gene is associated with height (37). Previous mice studies

have identified this gene to be associated with body size and weight, bone size and shape, postnatal growth retardation with more pronounced phenotypes in female mice compared to male mice (38). Further examination of this region in the GIANT Consortium identified modest signals for WHR and WHR_BMI in females (rs10913190, $P_{WHR}=5.6x10^{-4}$, rs10913282 $P_{WHR\_BMI}=8.6x10^{-4}$; $r^2<0.01$ with rs12090061 in IRASFS) (**Figure S7**).

SNP rs10923724 was significantly associated with the SNP-sex interaction variable with VSR ($P_{add}=2.89x10^{-8}$, MAF=38%) (**Figure 5**). Sex-stratified analysis revealed rs10923724 was nominally associated in males and females with opposite directions of effect ($P_{male}=3.84x10^{-4}$, $\beta_{male}=-0.97$; $P_{female}=2.31x10^{-3}$, $\beta_{female}=0.10$). It is an intergenic SNP located at 1p12, 14kb upstream of *TBX15* and 27kb downstream of the tryptophanyl tRNA synthetase 2 gene (*WARS2*). *WARS2* is one of the two isoforms of mitochondrial aminoacyl-tRNA synthetases that catalyzes the aminoacylation of tRNA (23). The T-box 15 gene (*TBX15*) is a member of the T-box family. The family encodes phylogenetically conserved transcription factors that regulate developmental processes (23). Diseases related to the gene product include Cousin Syndrome and congenital heart malformations (39, 40). Interestingly, this locus has been identified as one of the top WHR genetic signals in multiple ethnicities i.e. rs2645294 ($P=1.7x10^{-19}$) and rs984222 ($P=8.69x10^{-25}$) were associated with WHR without sex-specific patterns (11, 41). In IRASFS, the two SNPs were highly correlated ($r^2=0.87$) with strong associations with the interaction variable of VSR (rs2645294, $P_{VSR\_int}=1.2x10^{-5}$; rs984222, $P_{VSR\_int}=2.63x10^{-7}$). However, they were not associated with non-interactive effects of VSR and WHR (P>0.10). SNP rs10923724 has nominal correlations with the previous two SNPs ($r^2<0.58$) and was not associated with WHR (P=0.60). Analysis of rs10923724 conditioned by rs2645294 and rs984222 revealed nominal association (P=0.040) in males and no association in females (P=0.98). These results suggest there are multiple signals in the region with and without sex-specific heterogeneity. Interestingly, GTEx Portal suggested a strong eQTL signal for rs10923724 with *WARS2* expression in multiple tissues including skeletal muscle and adipose tissue

($P=3.3x10^{-27}$) (42). Taken together, 1p12 is an interesting locus with complicated signals combining sex-specific and non-sex-specific mechanisms.

Although significant signals have been identified, study limitations do exist. First, the majority of the SNPs analyzed were from statistical imputation as opposed to direct genotyping. Although SNP genotypes were highly concordant between platforms, the imputation quality was reduced for rare variants with MAF<1% (**Figure S2**). Therefore, only SNPs with MAF≥1% were included in analysis. More specifically, the most significant results with the exception of one were common variants. Another limitation was the small number of available individuals which largely limited the study power, i.e. interaction and sex-stratified analyses. Replication efforts focused on Mexican American participants from MESA; however, a modest sample size (n=485) likely impacted the lack of replication observed. In addition, limited biological evidence was found to support sex-specific signals identified by genetic studies. This is likely attributed to the small number of biological studies that have been focused on sex-specific mechanisms of adipose deposition.

Increasing evidence has supported disease susceptibility heterogeneity related to adipose tissue depots: subcutaneous adipose tissue is benign while visceral adipose is correlated with metabolic risks (5). The use of CT scans has enabled a more direct estimate of regional adiposity, i.e. differentiate between subcutaneous and visceral adipose tissue. In addition, CT scans are less prone to user bias as all scans were conducted under the same protocol and results were sent to a centralized reading center. In contrast, anthropometric measures can often be biased by age, sex, clinical site, etc. (6). CT measures can include bias as well. For example, females predominantly store body fat in the gluteal-femoral region while males store fat in abdominal region (8). However, CT measures in this study were obtained by axial slices at the L4-L5 disc space and therefore no gluteal adipose tissue was measured. This may explain why fewer female signals were observed.

In summary, we computed a combined study of genome-wide and exome chip arrays in the IRASFS Mexican American cohort. Adiposity phenotypes included were SAT, VAT, VSR, and VAT_BMI. Sex stratification and formal SNP-sex interaction analyses were conducted to search for signals with sex-specific effects. These findings support a genetic basis to the differential mechanism of adipose tissue distribution by sex. Moreover, these results highlighted the importance of using more refined measures of adiposity (CT scans) as well as the added utility of research in minority populations where an increased prevalence of adiposity-related diseases may be associated with a different genetic architecture.

Ethical statement:

Participants included in this study were recruited from clinical centers in San Antonio, TX and San Luis Valley, CO. The Institutional Review Board of each clinical (UT Health Science Center San Antonio Review Board and Colorado Multiple Institutional Review Board, respectively) and analysis (Wake Forest School of Medicine) site approved the study protocol and all participants provided written informed consent.

Conflict of Interest

The authors have no conflict of interest to disclose.

References:

1. Scully T. Public health: Society at large. *Nature* 2014;**508:** S50-51.

2. Narkiewicz K. Obesity and hypertension--the issue is more complex than we thought. *Nephrology Dialysis Transplantation* 2005;**21:** 264-267.

3. Frayling TM, Timpson NJ, Weedon MN, Zeggini E, Freathy RM, Lindgren CM*, et al.* A Common Variant in the FTO Gene Is Associated with Body Mass Index and Predisposes to Childhood and Adult Obesity. *Science* 2007;**316:** 889-894.

4. Wajchenberg BL. Subcutaneous and visceral adipose tissue: their relation to the metabolic syndrome. *Endocr Rev* 2000;**21:** 697-738.

5. Cohen P, Levy JD, Zhang Y, Frontini A, Kolodin DP, Svensson KJ*, et al.* Ablation of PRDM16 and beige adipose causes metabolic dysfunction and a subcutaneous to visceral fat switch. *Cell* 2014;**156:** 304-316.

6. Taylor RW, Jones IE, Williams SM, Goulding A. Evaluation of waist circumference, waist-to-hip ratio, and the conicity index as screening tools for high trunk fat mass, as measured by dual-energy X-ray absorptiometry, in children aged 3-19 y. *Am J Clin Nutr* 2000;**72:** 490-495.

7. Norris JM, Langefeld CD, Scherzinger AL, Rich SS, Bookman E, Beck SR*, et al.* Quantitative trait loci for abdominal fat and BMI in Hispanic-Americans and African-Americans: the IRAS Family study. *Int J Obes (Lond)* 2005;**29:** 67-77.

8. Blaak E. Gender differences in fat metabolism. *Curr Opin Clin Nutr Metab Care* 2001;**4:** 499-502.

9. Fox CS, Liu Y, White CC, Feitosa M, Smith AV, Heard-Costa N*, et al.* Genome-wide association for abdominal subcutaneous and visceral adipose reveals a novel locus for visceral fat in women. *PLoS Genet* 2012;**8:** e1002695.

10. Zillikens MC, Yazdanpanah M, Pardo LM, Rivadeneira F, Aulchenko YS, Oostra BA*, et al.* Sex-specific genetic effects influence variation in body composition. *Diabetologia* 2008;**51:** 2233-2241.

11. Shungin D, Winkler TW, Croteau-Chonka DC, Ferreira T, Locke AE, Magi R*, et al.* New genetic loci link adipose and insulin biology to body fat distribution. *Nature* 2015;**518:** 187-196.

2. Henkin L, Bergman RN, Bowden DW, Ellsworth DL, Haffner SM, Langefeld CD*, et al.* Genetic epidemiology of insulin resistance and visceral adiposity. The IRAS Family Study design and methods. *Ann Epidemiol* 2003;**13:** 211-217.

3. Gao C, Wang N, Guo X, Ziegler JT, Taylor KD, Xiang AH*, et al.* A Comprehensive Analysis of Common and Rare Variants to Identify Adiposity Loci in Hispanic Americans: The IRAS Family Study (IRASFS). *PLoS One* 2015;**10:** e0134649.

4. Gao C, Hsu FC, Dimitrov LM, Okut H, Chen YI, Taylor KD*, et al.* A genome-wide linkage and association analysis of imputed insertions and deletions with cardiometabolic phenotypes in Mexican Americans: The Insulin Resistance Atherosclerosis Family Study. *Genet Epidemiol* 2017;**41:** 353-362.

5. Goodarzi MO, Langefeld CD, Xiang AH, Chen YD, Guo X, Hanley AJ*, et al.* Insulin sensitivity and insulin clearance are heritable and have strong genetic correlation in Mexican Americans. *Obesity (Silver Spring)* 2014;**22:** 1157-1164.

6. Howie BN, Donnelly P, Marchini J. A flexible and accurate genotype imputation method for the next generation of genome-wide association studies. *PLoS Genet* 2009;**5:** e1000529.

7. Alexander DH, Novembre J, Lange K. Fast model-based estimation of ancestry in unrelated individuals. *Genome Res* 2009;**19:** 1655-1664.

8. Almasy L, Blangero J. Multipoint quantitative-trait linkage analysis in general pedigrees. *Am J Hum Genet* 1998;**62:** 1198-1211.

9. Bild DE, Bluemke DA, Burke GL, Detrano R, Diez Roux AV, Folsom AR*, et al.* Multi-Ethnic Study of Atherosclerosis: objectives and design. *Am J Epidemiol* 2002;**156:** 871-881.

0. Shah RV, Murthy VL, Abbasi SA, Blankstein R, Kwong RY, Goldfine AB*, et al.* Visceral adiposity and the risk of metabolic syndrome across body mass index: the MESA Study. *JACC Cardiovasc Imaging* 2014;**7:** 1221-1235.

1. Sung YJ, Perusse L, Sarzynski MA, Fornage M, Sidney S, Sternfeld B*, et al.* Genome-wide association studies suggest sex-specific loci associated with abdominal and visceral fat. *Int J Obes (Lond)* 2016;**40:** 662-674.

2. Chu AY, Deng X, Fisher VA, Drong A, Zhang Y, Feitosa MF*, et al.* Multiethnic genome-wide meta-analysis of ectopic fat depots identifies loci associated with adipocyte development and differentiation. *Nat Genet* 2017;**49:** 125-130.

3. Tatusova T, Ciufo S, Fedorov B, O'Neill K, Tolstoy I. RefSeq microbial genomes database: new representation and annotation strategy. *Nucleic Acids Res* 2015;**43:** 3872.

4. Awata T, Yamashita H, Kurihara S, Morita-Ohkubo T, Miyashita Y, Katayama S*, et al.* A low-frequency GLIS3 variant associated with resistance to Japanese type 1 diabetes. *Biochem Biophys Res Commun* 2013;**437:** 521-525.

5. Rees SD, Hydrie MZ, O'Hare JP, Kumar S, Shera AS, Basit A*, et al.* Effects of 16 genetic variants on fasting glucose and type 2 diabetes in South Asians: ADCY5 and GLIS3 variants may predispose to type 2 diabetes. *PLoS One* 2011;**6:** e24710.

6. Nogueira TC, Paula FM, Villate O, Colli ML, Moura RF, Cunha DA*, et al.* GLIS3, a susceptibility gene for type 1 and type 2 diabetes, modulates pancreatic beta cell apoptosis via regulation of a splice variant of the BH3-only protein Bim. *PLoS Genet* 2013;**9:** e1003532.

7. Lisinski I, Matsumoto H, Yver DR, Schurmann A, Cushman SW, Al-Hasani H. Identification and characterization of p49/STRAP as a novel GLUT4-binding protein. *Biochem Biophys Res Commun* 2006;**344:** 1179-1185.

8. Zheng B, Ma YC, Ostrom RS, Lavoie C, Gill GN, Insel PA*, et al.* RGS-PX1, a GAP for GalphaS and sorting nexin in vesicular trafficking. *Science* 2001;**294:** 1939-1942.

9. Randall JC, Winkler TW, Kutalik Z, Berndt SI, Jackson AU, Monda KL*, et al.* Sex-stratified Genome-wide Association Studies Including 270,000 Individuals Show Sexual Dimorphism in Genetic Loci for Anthropometric Traits. *PLoS Genet* 2013;**9:** e1003500.

0. Berndt SI, Gustafsson S, Magi R, Ganna A, Wheeler E, Feitosa MF*, et al.* Genome-wide meta-analysis identifies 11 new loci for anthropometric traits and provides insights into genetic architecture. *Nat Genet* 2013;**45:** 501-512.

1. Willer CJ, Schmidt EM, Sengupta S, Peloso GM, Gustafsson S, Kanoni S*, et al.* Discovery and refinement of loci associated with lipid levels. *Nat Genet* 2013;**45:** 1274-1283.

2. Comuzzie AG, Cole SA, Laston SL, Voruganti VS, Haack K, Gibbs RA*, et al.* Novel genetic loci identified for the pathophysiology of childhood obesity in the Hispanic population. *PLoS One* 2012;**7:** e51954.

3. Dichgans M, Malik R, Konig IR, Rosand J, Clarke R, Gretarsdottir S*, et al.* Shared genetic susceptibility to ischemic stroke and coronary artery disease: a genome-wide analysis of common variants. *Stroke* 2014;**45:** 24-36.

4. Overgaard MT, Boldt HB, Laursen LS, Sottrup-Jensen L, Conover CA, Oxvig C. Pregnancy-associated plasma protein-A2 (PAPP-A2), a novel insulin-like growth factor-binding protein-5 proteinase. *J Biol Chem* 2001;**276:** 21849-21853.

5. Jia J, Li L, Zhao Q, Zhang L, Ru J, Liu X*, et al.* Association of a single nucleotide polymorphism in pregnancy-associated plasma protein-A2 with developmental dysplasia of the hip: a case-control study. *Osteoarthritis Cartilage* 2012;**20:** 60-63.

6. Buimer M, Keijser R, Jebbink JM, Wehkamp D, van Kampen AH, Boer K*, et al.* Seven placental transcripts characterize HELLP-syndrome. *Placenta* 2008;**29:** 444-453.

7. Lango Allen H, Estrada K, Lettre G, Berndt SI, Weedon MN, Rivadeneira F*, et al.* Hundreds of variants clustered in genomic loci and biological pathways affect human height. *Nature* 2010;**467:** 832-838.

8. Christians JK, de Zwaan DR, Fung SH. Pregnancy associated plasma protein A2 (PAPP-A2) affects bone size and shape and contributes to natural variation in postnatal growth in mice. *PLoS One* 2013;**8:** e56260.

9. Hu Z, Shi Y, Mo X, Xu J, Zhao B, Lin Y*, et al.* A genome-wide association study identifies two risk loci for congenital heart malformations in Han Chinese populations. *Nat Genet* 2013;**45:** 818-821.

0. Dikoglu E, Simsek-Kiper PO, Utine GE, Campos-Xavier B, Boduroglu K, Bonafe L*, et al.* Homozygosity for a novel truncating mutation confirms TBX15 deficiency as the cause of Cousin syndrome. *Am J Med Genet A* 2013;**161A:** 3161-3165.

1. Heid IM, Jackson AU, Randall JC, Winkler TW, Qi L, Steinthorsdottir V*, et al.* Meta-analysis identifies 13 new loci associated with waist-hip ratio and reveals sexual dimorphism in the genetic basis of fat distribution. *Nat Genet* 2010;**42:** 949-960.

2. Carithers LJ, Moore HM. The Genotype-Tissue Expression (GTEx) Project. *Biopreserv Biobank* 2015;**13:** 307-308.

Titles and legends to table and figures

Table Legends

Table 1. Summary of the genome-wide significant signals.

Figure 1. Regional plots of *GLIS3* for association with visceral adipose tissue (VAT) in IRASFS Mexican Americans combining genome-wide and exome chip datasets.

Figure 2. Regional plots of *SRFBP1* for association with visceral adipose tissue adjusted by BMI in IRASFS Mexican Americans combining genome-wide and exome chip datasets. **A.** without sex stratification, **B.** females only, **C.** males only.

Figure 3. Regional plots of the rs13247968 locus for association with visceral adipose tissue adjusted by BMI in IRASFS Mexican Americans combining genome-wide and exome chip datasets. **A.** without sex stratification, **B.** females only, **C.** males only.

Figure 4. SNP rs10913233 was associated with the SNP-sex interaction variable for VSR. **A.** Regional plots of the rs10913233 locus for interaction analysis, **B.** genotypic means of rs10913233 SNP-sex interaction analysis results stratified by sex.

Figure 5. SNP rs10923724 was associated with the SNP-sex interaction variable for VSR. **A.** Regional plots of the rs10923724 locus for interaction analysis, **B.** genotypic means of rs10923724 SNP-sex interaction analysis results stratified by sex.

Table S1. Demographic characteristics of the study population.

Table S2. Table of signals with suggestive significance.

Table S3. Table of previously identified fat deposition signals.

Table S4. Number of variants rejected the lack-of-fit model.

Figure S1. QQ plots of genome-wide and exome chip association analysis for SNPs with MAF greater than 0.01.

Figure S2. Assessment of imputation quality.

Figure S3. Manhattan plots for association analysis in IRASFS Mexican Americans: **A**. Subcutaneous adipose tissue (SAT), **B**. Visceral adipose tissue (VAT), **C**. Visceral adipose tissue adjusted for body mass index (VAT_BMI), **D**. Visceral-subcutaneous adipose tissue ratio (VSR). Results were adjusted for age, sex, recruitment center (San Antonio, TX or San Luis Valley, CO), and admixture estimates. P-values are shown under the best fit model. The lower line at $-\log_{10}(PVAL)=5$ represents the suggestive P-value=1.00×10^{-5} and the upper line represents the genome-wide significance threshold ($P=5.00\times10^{-8}$).

Figure S4. Manhattan Plots for genome-wide and exome chip sex-stratified association analysis in IRASFS Mexican Americans: **A**. Subcutaneous Adipose Tissue (SAT), **B**. Visceral Adipose Tissue (VAT), **C**. Visceral Adipose Tissue adjusted for Body Mass Index (VAT_BMI), **D**. Visceral-Subcutaneous adipose tissue ratio (VSR).

Figure S5. Manhattan plots for genome-wide SNP-sex interaction analysis in IRASFS Mexican Americans: **A**. Subcutaneous adipose tissue (SAT), **B**. Visceral adipose tissue (VAT), **C**. Visceral adipose tissue adjusted for body mass index (VAT_BMI), **D**. Visceral-subcutaneous adipose tissue ratio (VSR). Results were adjusted for age, recruitment center (San Antonio, TX or San Luis Valley, CO), and admixture estimates.

Figure S6. Regional plots for *SNX13* locus from GIANT. **A**. Waist Circumference Female, **B**. Waist circumference males, **C**. BMI females, **D**. BMI males, **E**. Waist circumference adjusted by BMI females, **F**.

Waist circumference adjusted by BMI males, **G**. Waist-hip ratio females, **H**. Waist-hip ratio males, **I**. Waist-hip ratio adjusted by BMI females, **J**. Waist-hip ratio adjusted by BMI males.

Figure S7. Regional plots for *PAPPA2* from GIANT indexed by interaction analysis significant SNP rs10913233. **A**. Waist circumference females, **B**. Waist circumference males, **C**. BMI females, **D**. BMI males, **E**. Waist circumference adjusted by BMI Females, **F**. Waist circumference adjusted by BMI males, **G**. Waist-hip ratio females, **H**. Waist-hip ratio males, **I**. Waist-hip ratio adjusted by BMI females, **J**. Waist-hip ratio adjusted by BMI males.

Table 1. Genome-wide significant signals from SNP association analyses

SNP[a]	Chr:Pos	Gene	Alleles[e]	RAF[f]	Beta	P_overall (N=983)	Beta	P_female (N=580)	Beta	P_male (N=403)	P_interaction (N=983)
Visceral Adipose Tissue (VAT)											
rs2185405	9:4078851	*GLIS3*	T/C	0.40	-0.90	**1.98E-08[d]**	-0.76	1.36E-04[d]	1.11	1.10E-05[d]	0.69[d]
Visceral Adipose Tissue adjusted by BMI (VAT_BMI)											
rs12657394	5:121308199	*SRFBP1*	A/G	0.19	0.62	3.68E-07[c]	0.35	4.10E-03[b]	1.09	**2.39E-08[c]**	1.10E-03[c]
rs2914610	5:121314168	*SRFBP1*	A/G	0.19	0.59	9.78E-07[c]	0.34	5.58E-03[b]	1.07	**4.55E-08[c]**	1.53E-03[c]
rs1002945	7:17796659	*AHR-SNX13*	A/T	0.43	0.50	2.80E-05[c]	0.10	0.33[b]	1.09	**1.17E-08[c]**	1.37E-04[c]
rs13247968	7:17806817	*AHR-SNX13*	G/T	0.42	0.53	1.30E-05[c]	0.10	0.36[b]	1.11	**7.63E-09[c]**	1.59E-04[c]
rs1830005	7:17807563	*AHR-SNX13*	C/T	0.43	0.55	6.72E-06[c]	0.15	0.18[b]	1.07	**3.67E-08[c]**	8.70E-04[c]
rs9289345	3:129579506	*TMCC1*	G/A	0.01	0.35	0.51[b]	1.40	0.017[c]	-4.59	2.90E-04[c]	**3.73E-08[b]**
Visceral Subcutaneous Adipose Ratio (VSR)											
rs10913233	1:176625427	*PAPPA2*	T/A	0.14	-0.011	0.68[b]	-0.087	4.94E-03[b]	0.13	4.66E-03[c]	**3.07E-08[b]**
rs10923724	1:119546842	*TBX15/WARS2*	C/T	0.38	-0.0078	0.68[b]	0.099	2.30E-03[c]	-0.098	3.84E-04[b]	**2.89E-08[b]**

[a]SNP in build GRCh37/hg19; [b]Additive model; [c]Dominant model; [d]Recessive model; [e]Minor/Major allele; [f]Reference allele based on minor allele.

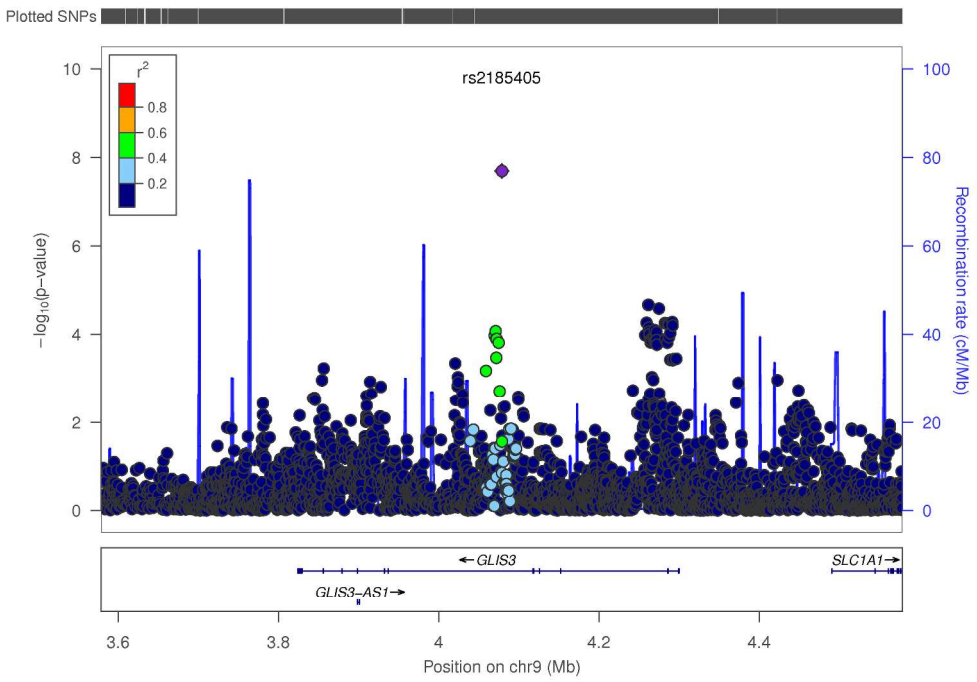

Figure 1

254x177mm (300 x 300 DPI)

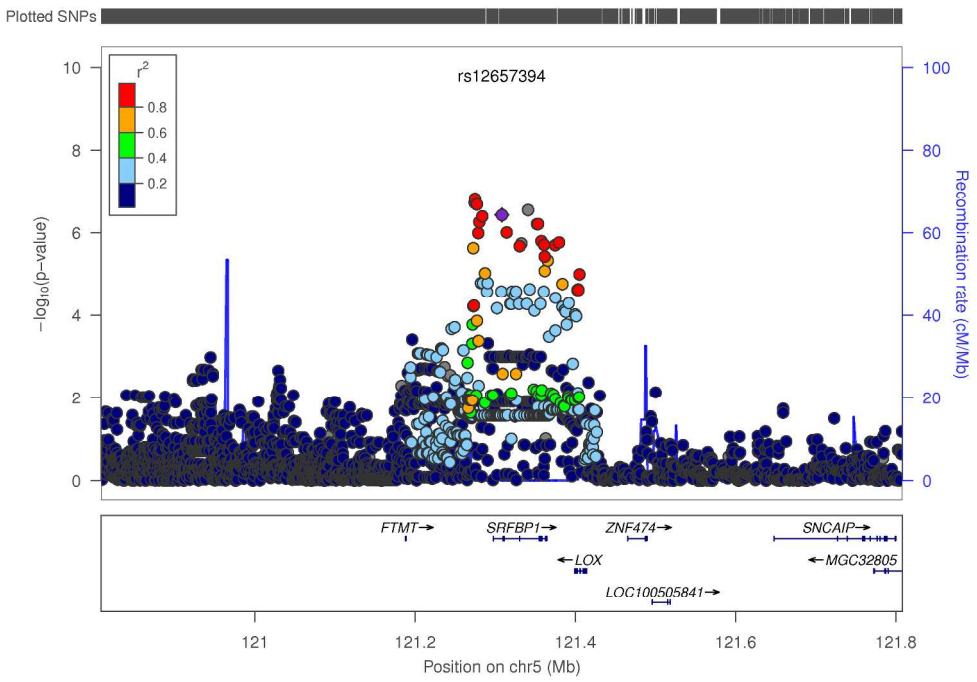

Figure 2a

254x177mm (300 x 300 DPI)

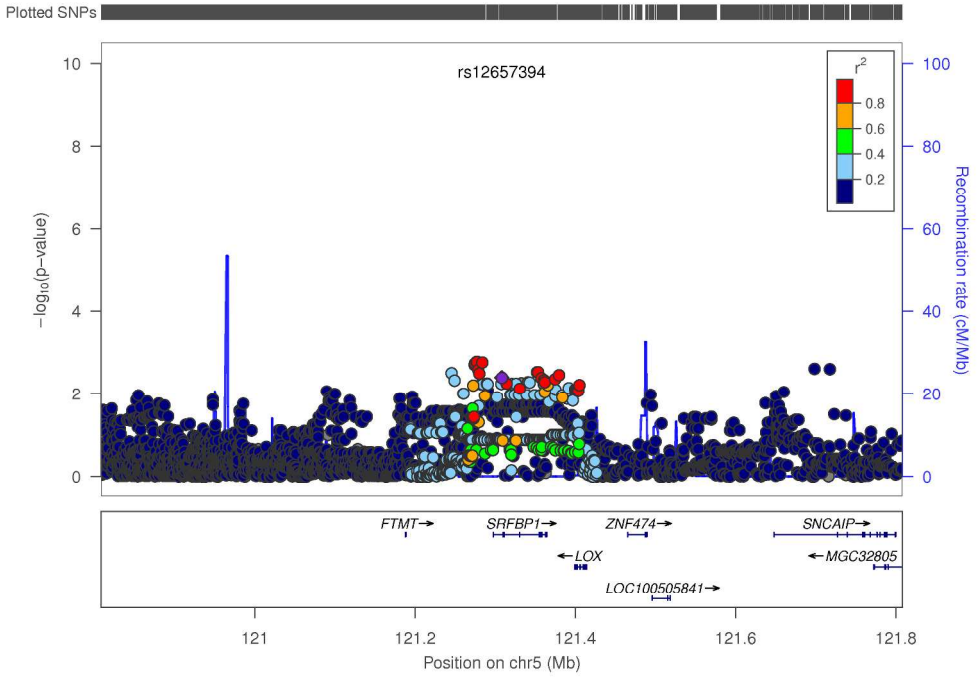

Figure 2b

254x177mm (300 x 300 DPI)

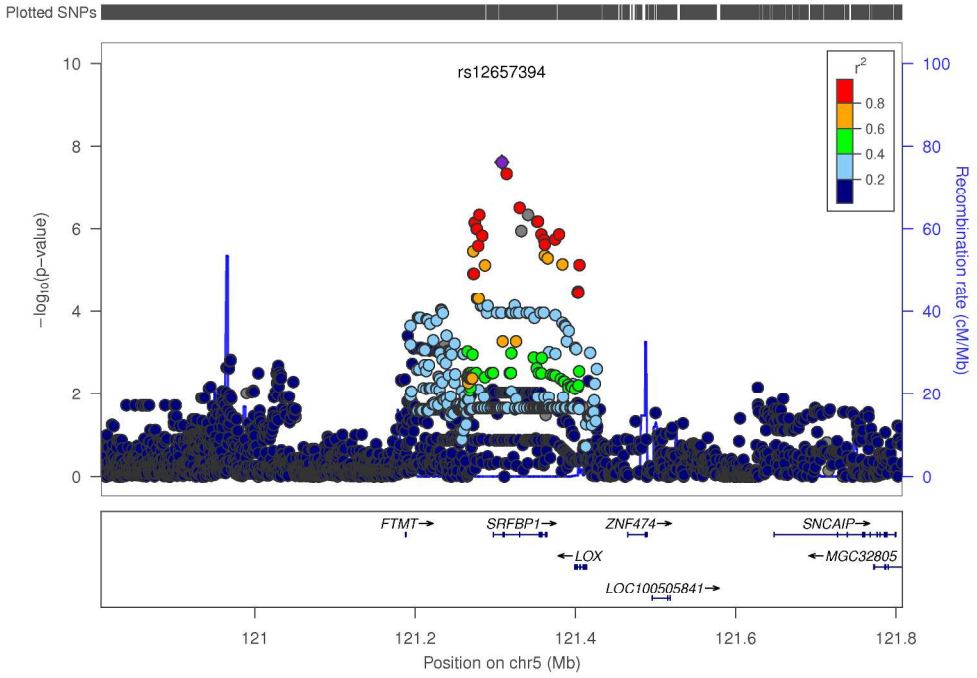

Figure 2c

254x177mm (300 x 300 DPI)

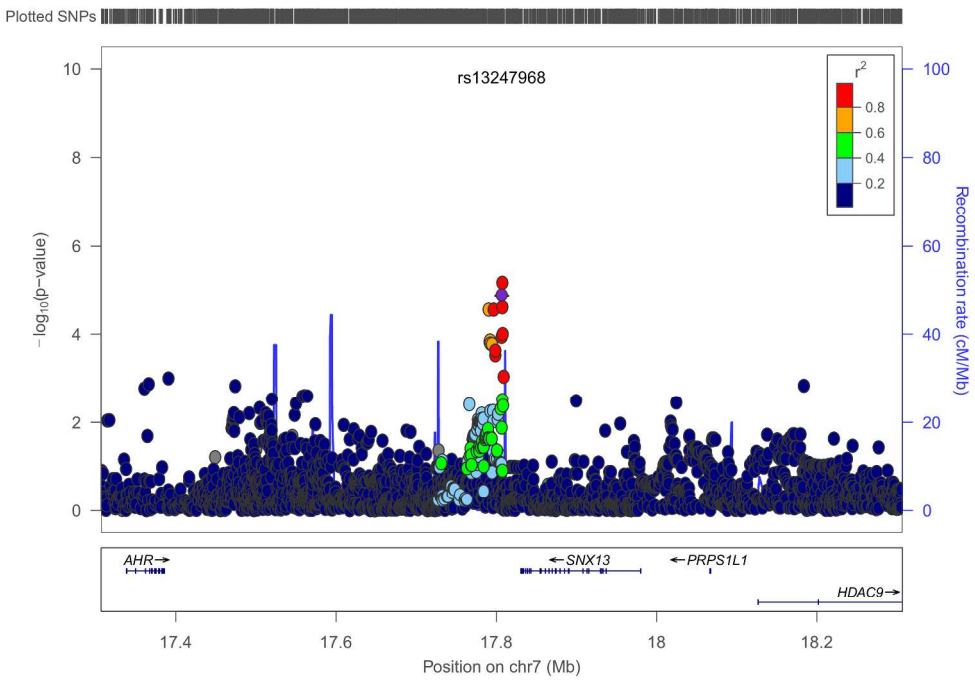

Figure 3a

254x177mm (300 x 300 DPI)

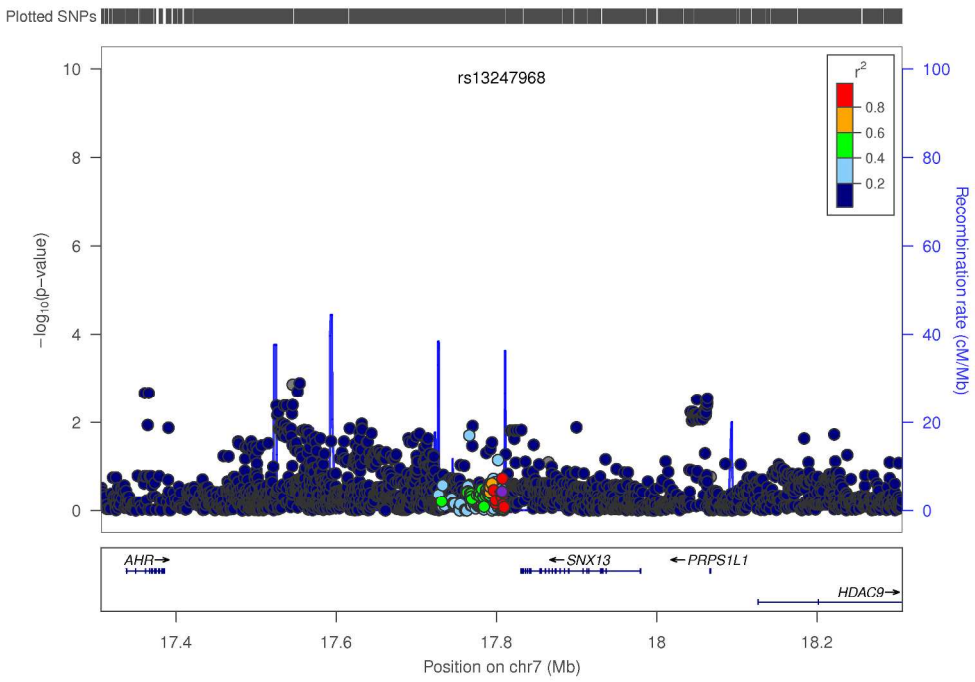

Figure 3b

254x177mm (300 x 300 DPI)

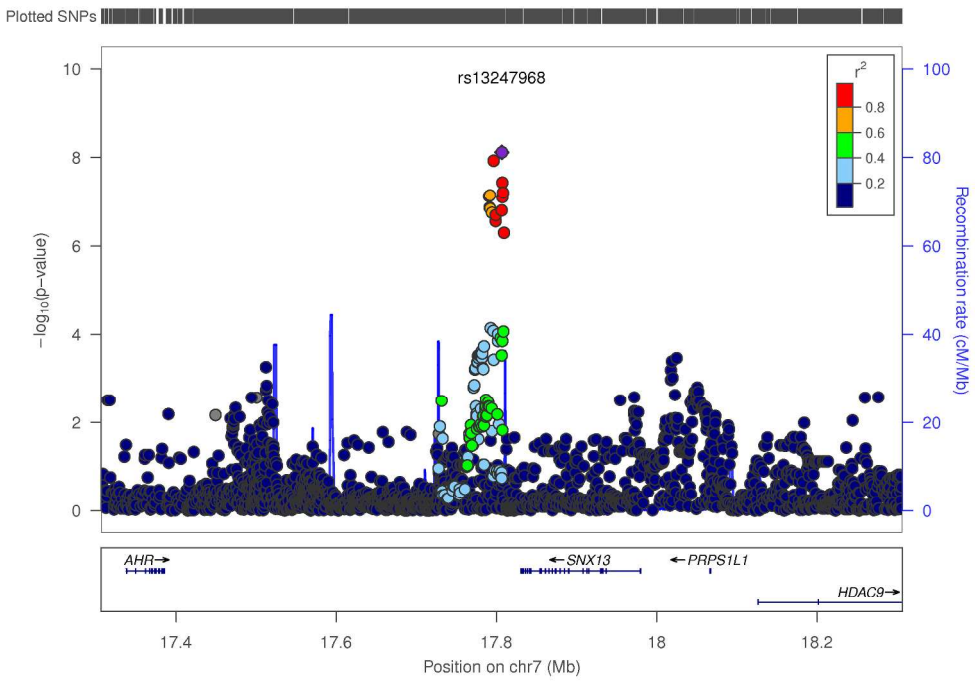

Figure 3c

254x177mm (300 x 300 DPI)

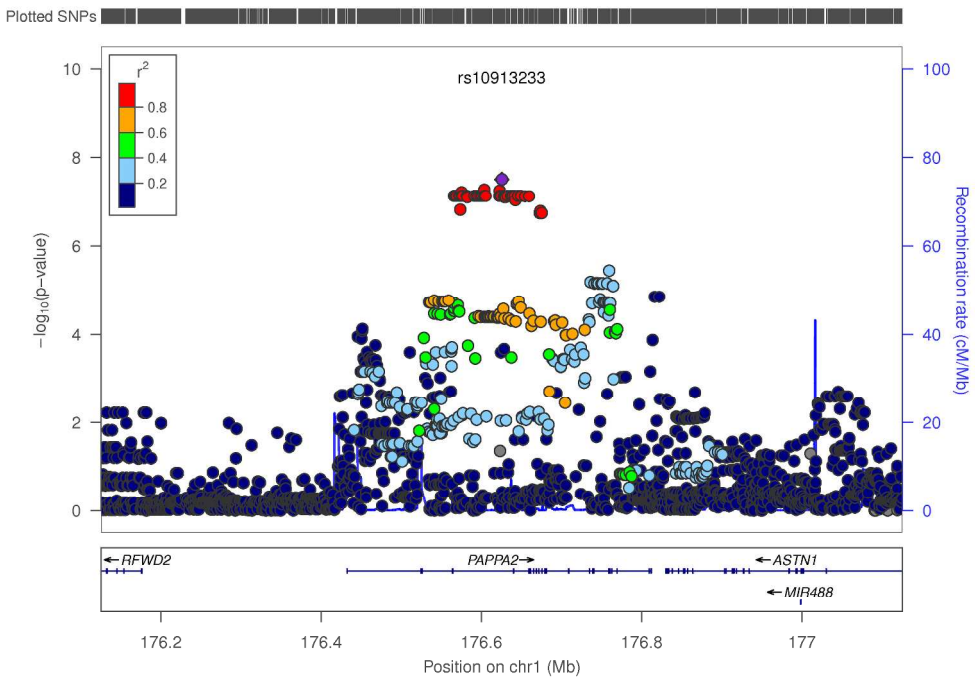

Figure 4a

254x177mm (300 x 300 DPI)

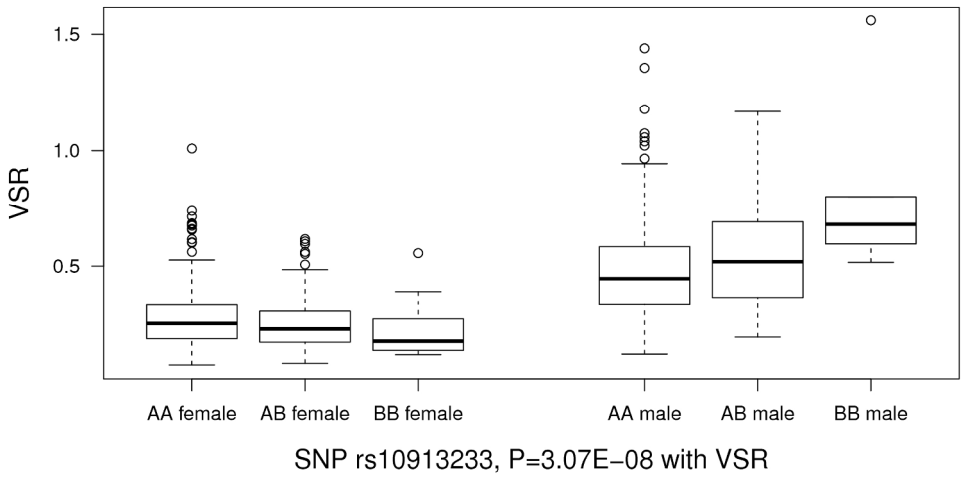

Figure 4b

215x127mm (300 x 300 DPI)

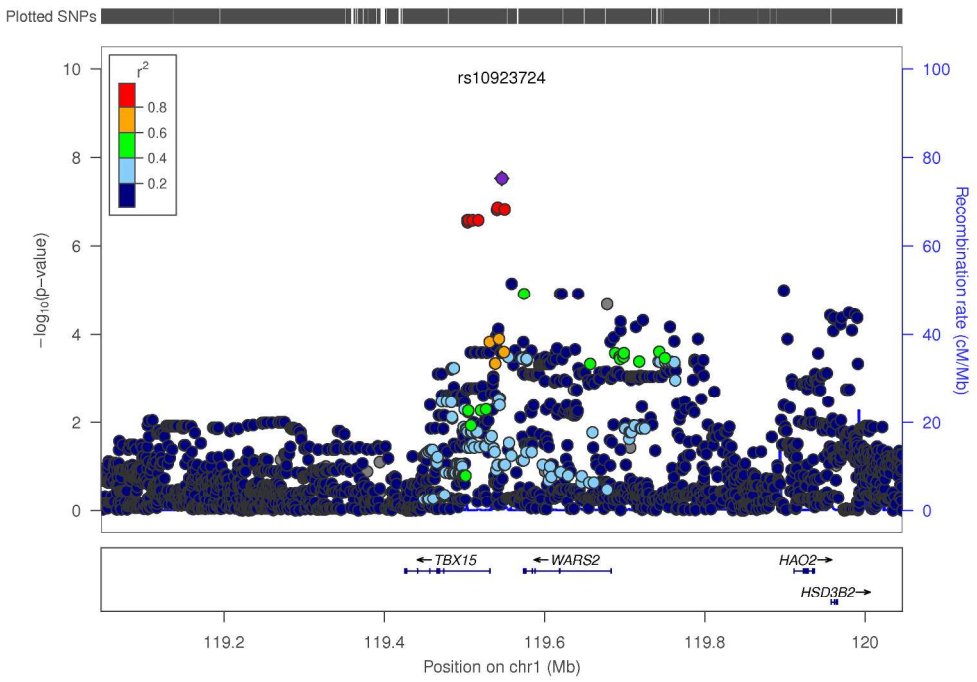

Figure 5a

254x177mm (300 x 300 DPI)

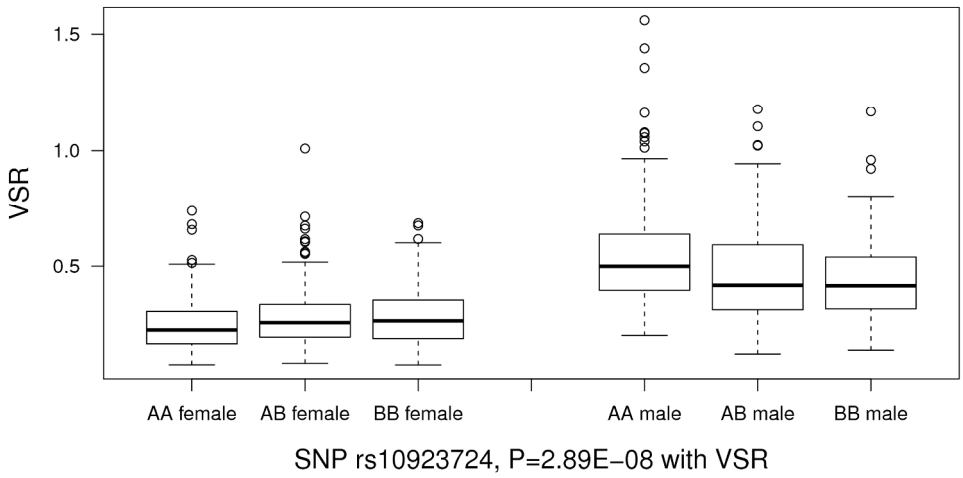

Figure 5b

215x127mm (300 x 300 DPI)

Table S1. Demographic characteristics of the study population.

	GWAS			
	overall	male	female	overall
N	983	403	580	1205
BMI (kg/m^2)	28.3±5.8	27.9±5.1	28.5±6.2	28.9±6.1
Age (years)	40.6±13.6	39.5±14.1*	41.4±13.3*	42.6±14.6
SAT (cm^2)	329.7±151.7	263.7±129.2†	375.7±149.4†	339.1±154.7
VAT (cm^2)	106.6±57.0	120.3±59.9†	97.1±52.9†	114.0±61.3
VSR	0.35±0.21	0.49±0.22†	0.25±0.13†	0.36±0.22

Significant difference was observed between sexes: * (P<0.001), † (P<0.000

Exome Chip	
male	female
498	707
28.4±5.4	29.2±6.6
41.6±14.9*	43.4±14.3*
272.9±132.2†	386.1±152.1†
127.3±63.7†	104.8±57.8†
0.50±0.23†	0.27±0.15†

)1).

Table S2. Table of signals with suggestive significance.

SNP	Chr	Position	Mapped Genes	sat_female			sa
				model	P	beta	model
rs12749490	1	41095597	RIMS3	add	3.92E-01	0.43	dom
rs10913233	1	176625427	PAPPA2	add	1.25E-01	-0.51	add
rs12712385	2	34624135	.-.	add	9.54E-01	-0.01	add
rs231784	2	204696982	CD28 (102487)-CTLA4 (35528)	dom	2.70E-07	-2.36	dom
rs2675289	3	2754005	CNTN4	add	7.84E-01	0.07	add
rs2131949	3	107542605	BBX (50122)-LOC151658 (17903)	add	7.31E-04	0.82	add
rs72941731	3	108203190	MYH15	add	2.15E-01	0.64	add
rs59058901	3	115307630	.-GAP43 (34520)	add	6.75E-01	-0.31	add
rs79669032	3	119689657	GSK3B	dom	1.05E-02	-1.43	add
rs9289345	3	129579506	TMCC1	add	7.22E-01	0.50	add
rs6775869	3	186698711	ST6GAL1	add	8.60E-01	-0.05	add
rs4862258	4	184754906	TRAPPC11 (120159)-STOX2 (71602)	add	3.17E-01	-1.16	add
rs117565216	5	43726800	NNT (21132)-.	add	5.77E-01	0.45	dom
rs4243443	5	121274650	.-SRFBP1 (23005)	add	8.56E-01	0.05	add
rs78596136	5	121292889	.-SRFBP1 (4766)	add	9.92E-02	1.01	dom
rs12657394	5	121308199	SRFBP1	add	4.86E-01	0.21	add
rs3958879	5	127569918	SLC12A2 (44538)-FBN2 (23682)	add	5.63E-02	0.74	add
rs145623349	5	132732902	FSTL4	add	3.32E-01	0.40	add
rs115635403	5	135332131	LECT2 (41408)-TGFBI (32452)	add	1.19E-01	-0.92	dom
rs1363220	5	143822828	KCTD16	add	9.24E-01	-0.03	add
rs2223471	6	50733648	TFAP2D	dom	4.90E-04	-1.17	dom
rs12529451	6	167089261	RPS6KA2	dom	2.30E-02	3.46	add
rs77185402	7	7849703	LOC729852	add	9.42E-01	0.05	add
rs13247968	7	17806817	.-SNX13 (23567)	add	1.86E-01	-0.35	add
rs143132638	7	76835987	CCDC146	add	2.98E-01	-0.32	add
rs115347982	8	102372518	.-AK291701 (1503)	add	8.85E-01	0.12	add
rs2185405	9	4078851	GLIS3	add	2.75E-02	0.54	rec
rs4879907	9	35566752	FAM166B (2856)-TESK1 (38528)	add	5.31E-01	0.20	add
rs78113377	9	88261634	AGTPBP1	add	7.54E-02	-1.50	add
rs62577244	9	138428077	LCN1 (9691)-OBP2A (9907)	add	5.50E-01	-0.23	add
rs4746598	10	68309168	CTNNA3	dom	6.18E-06	-2.33	dom
rs11172896	12	40017154	ABCD2 (3311)-C12orf40 (2817)	add	6.64E-01	0.18	add
rs181102206	12	41068946	MUC19 (170699)-CNTN1 (17411)	add	1.09E-01	-8.23	dom
rs11174701	12	63263130	PPM1H	add	5.74E-03	0.67	add
rs1504143	12	91220774	.-C12orf37 (91025)	add	5.72E-01	0.21	add
rs74240149	12	100892127	NR1H4	add	1.99E-01	-1.21	dom
rs10871403	16	81193156	PKD1L2	add	7.23E-01	-0.09	add
rs9903536	17	30878748	MYO1D	add	7.24E-01	0.09	add
rs7222268	17	72263867	Z49982 (5708)-DNAI2 (6518)	add	6.31E-01	0.14	add
rs143595390	19	53366633	ZNF468 (5731)-ZNF320 (485)	add	9.52E-01	0.03	add
rs2142795	20	41034985	PTPRT	add	5.04E-01	0.27	add
rs72645213	20	46215767	NCOA3	add	8.37E-01	-0.72	add
rs3827043	20	50215820	ATP9A	add	6.70E-01	-0.17	add
rs460014	21	16091441	SAMSN1 (172777)-NRIP1 (242114)	add	2.37E-01	0.29	add

Models used: sat_female: stratified analysis with females only
sat_male: stratified analysis with males only
sat_sex_int: sex-SNP interaction analysis
sat: sex-combined analysis
vat_bmi_female: stratified analysis with females only
vat_bmi_male: stratified analysis with males only
vat_bmi_sex_int: sex-SNP interaction analysis
vat_bmi: sex-combined analysis
vat_female: stratified analysis with females only
vat_male: stratified analysis with males only
vat_sex_int: sex-SNP interaction analysis
vat: sex-combined analysis
vsr_female: stratified analysis with females only
vsr_male: stratified analysis with males only
vsr_sex_int: sex-SNP interaction analysis
vsr: sex-combined analysis

at_sex_int			sat_male			sat			vat.bmi_female			vat.bmi_sex_i
P	beta	model	P	beta	model	P	beta	model	P	beta	model	P
1.69E-02	-1.85	dom	3.12E-04	2.45	dom	1.64E-02	1.05	add	4.55E-02	0.42	dom	8.76E-02
5.20E-01	0.31	add	1.24E-01	-0.70	add	8.32E-02	-0.48	add	1.97E-03	-0.42	add	2.87E-06
7.62E-01	-0.10	add	4.76E-01	0.22	add	7.88E-01	0.05	dom	4.66E-07	-0.75	dom	6.12E-03
1.60E-03	-2.02	add	2.10E-01	-0.66	dom	2.30E-05	-1.54	add	8.56E-01	-0.03	add	3.50E-01
4.48E-01	0.28	add	4.45E-01	-0.26	add	8.08E-01	-0.05	dom	8.13E-04	0.46	add	4.86E-07
3.14E-01	0.34	add	6.71E-02	0.58	add	1.95E-04	0.74	add	7.03E-04	0.34	add	9.70E-01
2.08E-01	0.86	add	9.31E-01	0.06	add	2.19E-01	0.51	dom	5.92E-03	-0.64	add	1.06E-04
2.50E-01	1.09	add	3.99E-01	-0.72	add	3.25E-01	-0.56	add	1.55E-01	-0.43	add	3.90E-05
2.20E-05	-3.36	dom	6.10E-04	2.37	add	9.75E-01	0.01	add	4.78E-01	-0.17	add	9.15E-03
5.62E-02	4.75	dom	2.82E-02	-6.18	add	7.71E-01	-0.38	dom	1.75E-02	1.40	add	3.73E-08
6.03E-01	-0.17	add	3.04E-01	0.30	add	7.57E-01	0.06	add	4.53E-01	-0.08	add	6.00E-05
3.19E-01	2.08	add	7.49E-02	-3.92	add	1.39E-01	-1.57	add	2.07E-01	0.63	add	1.87E-07
4.83E-04	-3.88	dom	2.88E-07	4.70	dom	3.33E-04	2.20	add	1.90E-01	0.43	add	3.03E-01
3.96E-01	-0.36	add	8.23E-02	0.67	add	2.19E-01	0.30	add	1.82E-03	0.38	add	8.80E-03
6.65E-01	-0.41	dom	3.01E-02	1.80	dom	1.24E-02	1.24	dom	1.85E-02	0.60	dom	1.80E-01
7.22E-01	-0.15	add	8.37E-02	0.69	add	1.15E-01	0.39	add	4.01E-03	0.36	dom	1.10E-03
8.03E-04	1.73	dom	2.35E-03	-1.45	add	8.33E-01	-0.06	dom	4.02E-02	0.35	add	8.37E-06
3.72E-02	1.21	dom	3.83E-02	-1.10	add	9.48E-01	-0.02	add	7.05E-02	0.31	add	1.26E-07
2.14E-01	1.09	dom	8.08E-03	-2.07	dom	1.03E-02	-1.29	add	1.52E-01	0.36	dom	3.26E-02
5.17E-01	0.27	add	6.44E-01	-0.17	add	8.65E-01	-0.04	add	8.53E-03	0.31	add	3.80E-07
4.69E-01	0.34	dom	1.12E-04	-1.61	dom	4.51E-07	-1.37	add	6.77E-01	0.04	add	3.08E-01
7.65E-03	5.07	add	1.80E-01	-2.18	add	4.47E-01	0.91	dom	9.64E-07	3.06	dom	3.00E-03
3.70E-01	0.75	add	7.62E-01	-0.21	add	7.99E-01	-0.12	dom	3.75E-03	0.76	add	2.04E-07
4.73E-01	-0.25	add	6.60E-01	-0.13	add	4.19E-01	-0.16	add	3.61E-01	-0.10	rec	1.59E-04
2.11E-01	-0.53	add	9.60E-01	0.02	add	4.55E-01	-0.18	add	2.62E-02	0.28	add	4.13E-04
8.43E-01	-0.21	add	2.99E-01	1.02	add	6.09E-01	0.33	dom	1.16E-03	-1.32	add	4.94E-07
4.80E-01	0.34	dom	1.05E-02	-1.40	rec	3.35E-03	0.78	rec	2.15E-02	0.33	rec	6.89E-02
8.77E-01	0.07	add	7.50E-01	0.12	add	5.42E-01	0.15	add	2.02E-01	0.17	add	3.12E-04
7.14E-03	-3.29	add	9.32E-02	1.74	add	8.93E-01	-0.09	add	6.10E-02	-0.65	dom	2.63E-02
1.32E-07	-2.87	dom	1.42E-06	2.63	add	7.33E-02	0.59	add	3.74E-01	-0.14	add	4.87E-01
7.14E-01	0.26	dom	9.46E-04	-2.14	dom	2.11E-07	-2.19	add	5.94E-01	0.11	add	1.14E-01
7.22E-01	0.20	add	9.33E-01	0.04	add	6.80E-01	0.14	add	1.97E-01	-0.22	add	1.30E-05
5.86E-01	3.98	add	1.11E-01	-9.97	dom	2.98E-02	-9.26	dom	3.70E-06	9.82	dom	1.23E-08
1.75E-04	1.26	add	1.43E-01	-0.44	add	2.52E-01	0.22	add	2.29E-02	0.23	add	5.79E-06
4.68E-03	1.38	dom	4.80E-03	-1.44	add	2.40E-01	-0.35	dom	1.30E-05	0.74	dom	9.14E-01
1.85E-01	1.56	dom	9.54E-04	-3.13	dom	1.09E-02	-1.78	add	1.46E-01	-0.56	dom	2.47E-02
5.17E-01	-0.22	add	6.53E-01	0.14	add	8.88E-01	-0.03	add	2.67E-01	-0.12	add	1.81E-07
1.29E-02	0.84	add	3.45E-03	-0.88	add	1.11E-01	-0.31	add	3.65E-03	0.29	add	1.95E-06
8.73E-02	-0.62	add	4.09E-03	0.90	add	1.30E-02	0.54	add	5.37E-02	0.22	add	1.34E-03
3.06E-02	1.25	dom	1.00E-02	-1.52	add	7.82E-02	-0.63	add	5.05E-02	-0.37	add	9.11E-04
4.82E-01	-0.39	add	3.73E-01	0.43	add	4.21E-01	0.26	add	2.76E-01	-0.19	dom	3.44E-03
9.17E-01	-0.45	add	6.45E-01	1.23	add	8.16E-01	0.48	dom	3.44E-07	7.30	dom	5.48E-06
7.03E-01	0.21	add	5.04E-01	-0.33	add	5.53E-01	-0.19	dom	2.78E-02	0.38	add	3.29E-07
5.64E-01	0.19	add	6.29E-01	0.15	add	1.80E-01	0.27	dom	1.12E-07	-0.75	dom	4.71E-06

int		vat.bmi_male			vat.bmi			vat_female			vat_sex_int	
beta	model	P	beta	model	P	beta	model	P	beta	model	P	beta
-0.59	dom	6.18E-03	0.85	dom	9.49E-03	0.49	add	3.14E-02	0.63	dom	4.63E-03	-1.36
-1.02	add	4.44E-03	0.57	add	4.98E-01	-0.08	dom	3.79E-03	-0.64	add	4.78E-04	-1.06
-0.61	add	5.96E-01	0.07	dom	1.54E-03	-0.39	dom	1.09E-04	-0.81	dom	7.27E-02	-0.56
0.26	add	1.07E-01	-0.39	add	3.27E-01	-0.15	dom	3.09E-03	-0.80	dom	2.00E-01	-0.52
0.84	add	1.30E-02	-0.37	add	5.16E-01	0.06	dom	1.53E-02	0.47	dom	3.91E-03	0.84
-0.01	add	4.03E-03	0.40	add	5.30E-05	0.34	add	6.66E-06	0.63	rec	2.33E-01	0.51
-1.19	add	3.23E-01	0.28	add	1.92E-01	-0.23	add	4.56E-02	-0.59	add	3.13E-03	-1.26
-1.76	dom	5.97E-03	1.02	add	4.94E-01	0.17	add	9.87E-02	-0.71	add	1.07E-02	-1.53
-0.93	add	2.23E-01	0.38	add	7.35E-01	0.06	dom	1.83E-02	-0.77	add	3.92E-07	-2.49
6.26	dom	2.90E-04	-4.59	add	5.14E-01	0.35	add	2.76E-01	0.87	add	7.18E-06	7.16
-0.60	rec	1.27E-07	1.06	add	3.43E-03	0.25	add	5.66E-01	-0.09	add	2.98E-03	-0.62
4.92	dom	4.10E-05	-3.82	add	3.07E-01	-0.47	add	8.89E-01	-0.09	dom	1.07E-04	5.09
0.52	add	2.84E-01	-0.46	add	5.43E-01	0.16	add	4.02E-01	0.39	dom	9.21E-02	-1.18
-0.49	dom	7.15E-07	0.97	add	1.47E-07	0.53	add	3.18E-03	0.50	rec	6.78E-01	-0.31
-0.57	dom	9.38E-03	0.98	dom	1.01E-03	0.71	dom	9.70E-05	1.40	dom	5.75E-01	-0.33
-0.72	dom	2.39E-08	1.09	dom	3.68E-07	0.62	add	3.77E-03	0.50	add	6.92E-02	-0.49
1.03	dom	2.29E-03	-0.66	add	1.37E-01	-0.19	dom	5.76E-03	0.65	add	3.75E-07	1.63
1.38	dom	4.90E-05	-0.98	add	1.81E-01	-0.19	dom	6.08E-02	0.51	add	2.56E-06	1.71
-0.84	dom	5.30E-04	1.18	dom	1.63E-03	0.68	add	7.73E-01	-0.10	add	2.75E-01	-0.58
0.92	dom	8.00E-05	-0.77	add	7.11E-01	-0.04	add	2.76E-02	0.36	add	4.57E-04	0.89
0.16	add	7.80E-01	-0.04	add	9.45E-01	-0.01	dom	7.22E-03	-0.53	dom	7.29E-01	0.10
2.56	add	4.88E-01	0.49	dom	1.46E-03	1.57	dom	3.76E-08	4.80	dom	4.50E-05	4.88
1.94	dom	6.54E-04	-1.03	add	8.77E-01	-0.03	add	1.29E-01	0.57	add	5.89E-04	1.80
0.85	rec	7.63E-09	-1.11	rec	1.30E-05	-0.53	add	7.08E-02	-0.28	rec	8.06E-02	0.55
0.67	add	1.16E-01	-0.27	add	5.17E-01	0.07	add	2.85E-01	0.19	add	1.03E-02	0.68
-2.38	add	5.96E-02	0.83	add	3.03E-01	-0.29	dom	2.41E-02	-1.30	add	1.53E-04	-2.52
-0.40	rec	1.10E-05	0.83	rec	2.10E-05	0.50	rec	1.36E-04	0.76	rec	6.92E-01	-0.12
-0.71	dom	1.33E-07	1.02	add	1.53E-04	0.41	add	3.75E-01	0.16	add	2.71E-02	-0.61
1.21	dom	7.90E-05	-1.84	dom	3.32E-04	-1.01	dom	1.47E-02	-1.19	dom	8.40E-01	0.15
-0.17	add	1.00E+00	0.00	add	6.28E-01	-0.07	add	8.29E-01	-0.05	add	1.58E-02	-0.83
0.48	add	6.25E-01	-0.14	add	7.85E-01	-0.05	dom	1.01E-02	-0.77	dom	2.99E-01	0.46
-1.08	add	3.14E-03	0.68	add	3.85E-01	0.13	add	2.26E-01	-0.29	add	6.48E-04	-1.19
19.17	dom	9.08E-03	-7.93	dom	8.17E-02	3.19	add	1.01E-01	5.00	add	8.99E-04	15.27
0.68	add	3.61E-04	-0.47	add	4.26E-01	-0.07	add	9.21E-04	0.46	add	1.34E-07	1.10
-0.03	dom	2.52E-03	0.67	dom	2.94E-06	0.65	dom	3.75E-04	0.84	dom	1.04E-01	0.57
1.18	dom	5.30E-04	-1.46	dom	1.95E-04	-1.09	add	1.16E-01	-0.86	dom	6.67E-03	1.99
-0.78	add	1.40E-05	0.57	add	1.20E-01	0.13	add	3.81E-01	-0.13	add	1.50E-05	-0.91
0.73	add	2.05E-02	-0.31	add	9.41E-01	0.01	add	2.19E-02	0.32	add	1.57E-07	1.11
0.53	add	7.93E-03	-0.37	add	7.30E-01	-0.03	add	3.76E-02	0.34	add	7.30E-02	0.41
-0.87	add	8.41E-02	0.40	add	7.40E-01	-0.05	add	7.46E-02	-0.47	add	5.72E-02	-0.69
0.81	dom	1.91E-06	-1.14	dom	1.07E-04	-0.59	add	7.33E-01	-0.08	dom	9.98E-02	0.64
8.62	add	6.38E-01	-0.58	dom	9.22E-03	2.39	dom	5.48E-03	5.74	add	1.70E-02	6.36
1.28	dom	8.84E-04	-0.77	add	6.09E-01	-0.07	add	3.36E-01	0.23	add	3.94E-04	1.25
-0.98	add	2.90E-01	0.14	dom	1.29E-03	-0.38	dom	1.40E-03	-0.64	dom	1.11E-03	-0.98

vat_male			vat			vsr_female			vsr_sex_int		
model	P	beta	model	P	beta	model	P	beta	model	P	beta	model
dom	2.31E-07	2.09	dom	5.00E-05	1.04	add	1.47E-01	0.07	add	9.26E-01	0.01	add
add	2.30E-01	0.32	add	9.17E-02	-0.27	add	4.94E-03	-0.09	add	3.07E-08	-0.26	dom
add	9.42E-01	0.01	dom	5.80E-03	-0.47	dom	3.98E-04	-0.12	dom	1.39E-01	-0.07	add
add	6.32E-02	-0.60	dom	1.49E-03	-0.69	add	9.61E-02	0.07	add	6.14E-01	0.03	add
add	7.87E-02	-0.35	rec	7.41E-02	-0.56	add	8.88E-03	0.07	add	1.99E-04	0.14	add
add	8.14E-03	0.50	add	4.68E-07	0.58	add	1.68E-02	0.06	add	3.62E-01	0.03	add
add	1.72E-01	0.51	add	7.08E-01	-0.09	dom	5.50E-04	-0.18	add	2.62E-07	-0.34	add
add	2.47E-01	0.58	add	6.86E-01	-0.14	dom	3.83E-02	-0.14	add	1.74E-07	-0.48	dom
dom	9.30E-05	1.60	add	6.87E-01	0.11	add	8.88E-01	-0.01	add	3.40E-01	-0.07	add
dom	1.45E-04	-6.51	add	7.98E-01	-0.19	add	1.69E-01	0.18	add	1.35E-04	0.92	dom
add	3.20E-05	0.71	add	3.38E-02	0.25	add	2.33E-01	-0.03	add	3.98E-03	-0.09	add
dom	3.10E-05	-5.19	dom	5.11E-02	-1.20	add	3.52E-01	0.10	add	4.80E-05	0.82	dom
dom	6.90E-03	1.53	dom	2.05E-02	0.86	add	5.64E-01	0.04	add	3.82E-02	0.23	dom
dom	9.49E-06	1.18	add	1.03E-06	0.69	add	1.81E-03	0.09	rec	4.35E-01	-0.09	dom
dom	1.85E-04	1.88	dom	3.39E-07	1.51	dom	2.48E-03	0.18	dom	5.28E-01	0.06	add
dom	2.28E-06	1.24	add	2.01E-06	0.69	add	5.14E-03	0.08	dom	1.07E-01	-0.08	dom
dom	1.62E-04	-1.11	add	3.80E-01	-0.15	dom	2.33E-02	0.09	add	3.12E-04	0.18	add
dom	3.70E-05	-1.37	add	2.35E-01	-0.23	add	4.58E-01	0.03	add	1.86E-03	0.17	dom
add	6.00E-01	0.24	add	7.29E-01	0.10	add	3.07E-01	0.06	dom	2.40E-05	-0.35	dom
add	4.29E-02	-0.45	add	6.01E-01	0.07	add	3.21E-03	0.08	add	3.10E-05	0.16	dom
dom	1.64E-02	-0.60	dom	4.38E-04	-0.56	add	5.01E-01	0.02	add	4.36E-01	-0.03	add
add	8.74E-01	-0.15	dom	4.96E-04	2.38	dom	1.94E-04	0.53	dom	6.77E-02	0.33	add
dom	1.67E-02	-0.98	add	6.48E-01	-0.13	add	9.93E-02	0.10	add	2.21E-04	0.30	dom
rec	2.24E-04	-0.99	rec	2.01E-04	-0.63	add	5.20E-01	-0.02	rec	9.30E-03	0.13	rec
add	1.22E-01	-0.36	add	9.77E-01	0.00	add	4.16E-03	0.08	add	1.71E-07	0.22	add
add	3.31E-02	1.28	add	6.97E-01	-0.15	dom	3.05E-04	-0.33	add	8.68E-06	-0.45	add
rec	1.10E-05	1.11	rec	1.98E-08	0.90	rec	2.32E-02	0.07	rec	8.92E-01	-0.01	add
dom	1.31E-03	0.85	add	1.37E-02	0.36	add	9.57E-01	0.00	add	6.18E-04	-0.15	dom
add	5.59E-02	-1.20	dom	3.50E-03	-1.14	add	9.78E-02	-0.13	dom	1.77E-03	0.37	dom
dom	6.74E-03	0.89	add	1.76E-01	0.25	add	9.81E-01	0.00	add	2.95E-03	0.16	dom
dom	3.23E-03	-1.14	dom	2.06E-04	-0.91	add	4.48E-01	0.04	add	2.52E-01	-0.08	add
add	2.56E-02	0.69	add	6.44E-01	0.09	dom	1.88E-02	-0.10	add	1.79E-07	-0.28	add
dom	1.20E-02	-10.52	add	7.79E-01	-0.70	dom	1.60E-05	2.05	dom	1.31E-04	2.72	add
add	3.66E-04	-0.63	add	6.62E-01	0.05	add	9.59E-02	0.04	add	1.21E-02	0.08	add
add	8.47E-01	-0.05	dom	8.84E-03	0.51	dom	2.86E-04	0.14	dom	2.52E-02	-0.12	dom
dom	2.27E-07	-2.87	dom	8.54E-06	-1.80	add	1.97E-01	-0.12	dom	5.31E-01	0.07	dom
add	1.91E-04	0.66	add	2.08E-01	0.15	add	3.26E-01	-0.02	add	3.43E-06	-0.15	add
add	2.40E-05	-0.75	add	2.77E-01	-0.13	add	9.91E-03	0.06	add	3.38E-04	0.12	add
add	5.84E-01	-0.10	add	1.95E-01	0.16	add	3.72E-02	0.06	add	4.01E-07	0.18	add
add	8.00E-01	0.08	add	2.40E-01	-0.24	add	2.71E-02	-0.09	add	1.25E-07	-0.30	dom
dom	1.97E-03	-1.01	dom	1.81E-02	-0.50	add	3.29E-01	-0.04	dom	6.27E-04	0.21	dom
add	7.81E-01	0.47	add	7.80E-02	2.26	dom	1.86E-04	1.21	add	3.87E-04	1.45	add
dom	4.62E-03	-0.89	add	3.36E-01	-0.18	add	1.85E-01	0.05	add	2.50E-05	0.23	dom
add	1.66E-01	0.25	dom	8.26E-02	-0.28	dom	5.49E-04	-0.11	dom	1.06E-04	-0.18	add

vsr_male			vsr	
P	beta	model	P	beta
1.71E-01	0.09	add	1.85E-01	0.05
4.66E-03	0.13	add	6.81E-01	-0.01
6.48E-01	-0.01	dom	6.53E-03	-0.07
9.38E-01	0.00	add	1.74E-01	0.05
3.69E-01	-0.03	add	1.76E-01	0.03
2.68E-01	0.03	add	2.39E-02	0.04
1.86E-01	0.08	add	7.76E-02	-0.07
2.05E-02	0.18	add	7.73E-01	0.02
9.94E-01	0.00	add	6.86E-01	-0.02
4.14E-02	-0.53	add	4.40E-01	0.09
2.06E-03	0.08	add	2.73E-01	0.02
8.78E-04	-0.68	add	3.88E-01	-0.09
9.96E-03	-0.22	add	2.64E-01	-0.07
3.02E-03	0.12	add	5.30E-05	0.09
1.60E-01	0.11	dom	1.82E-03	0.15
5.64E-04	0.14	dom	9.80E-05	0.11
7.89E-02	-0.07	add	1.00E+00	0.00
7.63E-03	-0.13	add	3.04E-01	-0.03
3.54E-07	0.36	dom	1.28E-04	0.18
1.77E-02	-0.10	add	4.40E-01	0.02
6.82E-02	0.05	add	1.02E-01	0.03
1.02E-01	0.25	dom	1.01E-03	0.36
1.62E-02	-0.15	add	6.71E-01	-0.02
1.21E-04	-0.16	rec	1.41E-03	-0.09
2.23E-02	-0.08	add	3.15E-01	0.02
5.99E-01	0.05	add	3.21E-02	-0.13
7.09E-03	0.08	rec	2.79E-03	0.08
3.20E-05	0.17	add	8.76E-02	0.04
4.08E-07	-0.48	dom	2.00E-05	-0.26
1.63E-02	-0.13	add	1.90E-01	-0.04
1.32E-01	0.09	add	3.88E-01	0.03
1.16E-02	0.12	add	6.70E-01	-0.01
4.23E-01	-0.47	dom	8.00E-03	1.06
1.65E-01	-0.04	add	7.51E-01	0.01
2.70E-05	0.20	dom	8.35E-08	0.17
4.77E-02	-0.17	dom	3.63E-02	-0.14
8.75E-04	0.09	add	3.42E-01	0.02
2.00E-01	-0.04	add	3.72E-01	0.02
6.50E-06	-0.13	add	1.11E-01	-0.03
2.16E-03	0.17	add	4.73E-01	0.02
1.44E-07	-0.27	dom	1.01E-04	-0.13
7.12E-01	-0.09	add	6.64E-02	0.36
1.02E-02	-0.13	add	4.92E-01	-0.02
1.34E-01	0.04	dom	2.43E-02	-0.06

Table S3. Replication of genome-wide significant signals from IRASFS in MESA

SNP[a]	Chr:Pos	Gene	Alleles[e]	RAF[f]	Beta	P_overall (N=485)
Visceral Adipose Tissue (VAT)						
rs2185405	9:4078851	*GLIS3*	T/C	0.4	2.27	0.63
Visceral Adipose Tissue adjusted by BMI (VAT_BMI)						
rs12657394	5:121308199	*SRFBP1*	A/G	0.2	-1.87	0.68
rs2914610	5:121314168	*SRFBP1*	A/G	0.22	-2.39	0.58
rs1002945	7:17796659	*AHR-SNX13*	A/T	0.44	-3.42	0.35
rs13247968	7:17806817	*AHR-SNX13*	G/T	0.46	-3.24	0.38
rs1830005	7:17807563	*AHR-SNX13*	C/T	0.46	-3.44	0.35
rs9289345	3:129579506	*TMCC1*	G/A	0.07	15.67	0.061
Visceral Subcutaneous Adipose Ratio (VSR)						
rs10913233	1:176625427	*PAPPA2*	T/A	0.11	-0.034	0.48
rs10923724	1:119546842	*TBX15/WARS2*	C/T	0.48	-0.0094	0.74

[a]SNP in build GRCh37/hg19; [b]Additive model; [c]Dominant model; [d]Recessive model; [e]Minor/Major allele; [f]Re

Beta	P_female (N=238)	Beta	P_male (N=247)	P_interaction (N=485)
9.38	0.11	-4.7	0.53	0.53
1.29	0.82	-2.39	0.71	0.56
3.76	0.47	-4.79	0.44	0.2
-2.03	0.67	-4.82	0.35	0.84
-0.88	0.85	-5.9	0.27	0.9
-1.08	0.81	-5.91	0.27	0.89
13.97	0.24	5.73	0.64	0.35
-0.011	0.88	-0.047	0.44	0.9
0.028	0.5	-0.045	0.25	0.15

ference allele based on minor allele.

Table S4. Table of previously identified fat deVition signals.

Previously associated	SNP†	Chr	Vition	Mapped Genes
SAT	rs9922619	16	53831771	FTO
SAT_FE	rs2123685	17	38053889	ZPBP2 (19740)-GSDMB (6958)
SAT_FE	rs7919823	10	22036491	MLLT10 (3932)-DNAJC1 (8985)
VAT_BMI	rs2842895	6	7106316	.-RREB1 (1513)
VAT_BMI_FE	rs10060123	5	125683910	.-GRAMD3 (11877)
VAT_FE	rs1659258	2	88659588	THNSL2 (173432)-FOXI3 (88137)
VSR	rs11118316	1	219657163	.-.
VSR	rs7374732	3	23203454	.-UBE2E2 (41198)
VSR	rs912056	6	6736197	BC039678 (6056)-.
WHR	rs10245353	7	25858614	.-.
WHR	rs10842707	12	26471364	SSPN (65511)-ITPR2 (16920)
WHR	rs10991437	9	107735920	AK311445 (43770)-.
WHR	rs12608504	19	18389135	KIAA1683 (3816)-JUND (1427)
WHR	rs12679556	8	72514228	BC048982 (54336)-MSC (239548)
WHR	rs1294410	6	6738752	BC039678 (8611)-.
WHR	rs1385167	2	66200648	FLJ16124
WHR	rs1440372	15	67033151	SMAD6
WHR	rs1569135	2	188115398	.-CALCRL (92450)
WHR	rs17451107	3	156797609	LEKR1 (154564)-LOC339894 (1846)
WHR	rs1936805	6	127452116	RSPO3
WHR	rs2276824	3	52637486	PBRM1
WHR	rs2294239	22	29449477	ZNRF3
WHR	rs2645294	1	119574587	WARS2
WHR	rs303084	4	124066948	SPATA5
WHR	rs4081724	19	33824946	LOC80054 (28983)-CEBPG (39628)
WHR	rs4646404	17	17420199	PEMT
WHR	rs4765219	12	124440110	CCDC92
WHR	rs6090583	20	45558831	EYA2
WHR	rs6556301	5	176527577	FGFR4 (2451)-NSD1 (32502)
WHR	rs714515	1	172352990	DNM3
WHR	rs7705502	5	173320815	CPEB4
WHR	rs7759742	6	32381736	BTNL2 (6836)-HLA-DRA (25882)
WHR	rs7801581	7	27223771	HOXA11
WHR	rs8030605	15	56504598	RFX7
WHR	rs8042543	15	31708263	AK093758 (12152)-OTUD7A (67065)
WHR	rs979012	20	6623374	.-.
WHR_FE	rs10195252	2	165513091	GRB14 (88074)-COBLL1 (28166)
WHR_FE	rs1045241	5	118729286	TNFAIP8
WHR_FE	rs10804591	3	129334233	PLXND1 (8651)-TMCC1 (32401)
WHR_FE	rs10919388	1	170372503	LOC284688 (119154)-AK096329 (57090)
WHR_FE	rs11231693	11	63862612	MACROD1
WHR_FE	rs12454712	18	60845884	BCL2
WHR_FE	rs1358980	6	43764551	VEGFA (10328)-AK097853 (48056)
WHR_FE	rs1443512	12	54342684	HOXC13 (2356)-HOXC12 (6029)

WHR_FE	rs1534696	7	26397239	SNX10
WHR_FE	rs1776897	6	34195011	GRM4 (81142)-HMGA1 (9565)
WHR_FE	rs17819328	3	12489342	PPARG (67912)-TSEN2 (36588)
WHR_FE	rs2371767	3	64718258	ADAMTS9-AS2
WHR_FE	rs2820443	1	219753509	.-.
WHR_FE	rs2925979	16	81534790	CMIP
WHR_FE	rs3805389	4	56482750	NMU
WHR_FE	rs7830933	8	23603324	NKX2-6 (39213)-.
WHR_FE	rs7917772	10	104487443	SFXN2
WHR_FE	rs8066985	17	68453345	.-.
WHR_FE	rs905938	1	154991389	DCST2
WHR_FE	rs9687846	5	55861894	.-.
WHR_FE	rs9991328	4	89713121	FAM13A
WHR_MA	rs224333	20	34023962	GDF5

†Previously identified genome-wide significant SNPs.

*SNP used for replication in IRASFS (proxy variants were used if original ones are

‡R-square between originally identified and proxy variant in IRASFS.

√ Consistent direction of effects observed

X Inconsistent direction of effects observed

Directions of previously identified non-CT signals were evaluated based on the √i

SNPFunction	proxy snp*	r2 to original snp‡	sat_female			sat_gender_ir	
			model	P	beta	model	P
intron	rs9922619	1	add	6.20E-02	0.49	add	4.18E-01
unknown	rs2123685	1	add	9.56E-01	-0.03[v]	dom	8.41E-02
unknown	rs7919823	1	add	1.60E-01	-1.27[x]	add	9.28E-01
near-gene-5	rs2842895	1	add	2.69E-01	0.26	add	3.14E-01
unknown	rs10060123	1	add	5.90E-01	-0.17	add	2.14E-01
unknown	rs1659258	1	add	7.17E-02	1.15	add	7.97E-01
unknown	rs11118316	1	add	2.75E-01	0.27	add	9.60E-01
unknown	rs7374732	1	add	2.29E-01	-0.34	dom	7.43E-01
unknown	rs912056	1	add	5.15E-01	-0.15	add	8.36E-01
unknown	rs10245353	1	add	2.72E-01	-0.33	add	5.36E-01
unknown	rs10842707	1	add	2.91E-01	-0.27	rec	6.69E-01
unknown	rs10991437	1	add	6.18E-01	-0.20	add	2.21E-01
unknown	rs12608504	1	add	1.22E-01	0.40	add	9.47E-01
unknown	rs12679556	1	add	6.11E-01	0.13	add	8.65E-01
unknown	rs1294410	1	add	5.10E-01	-0.16	add	8.17E-01
unknown	rs1385167	1	add	8.18E-01	0.08	add	7.95E-01
intron	rs1440372	1	add	1.93E-01	-0.43	add	3.21E-01
unknown	rs1569135	1	add	6.83E-01	0.10	add	9.73E-01
unknown	rs17451107	1	add	1.87E-01	0.31	add	2.17E-02
intron	rs1936805	1	add	6.56E-01	0.11	add	4.53E-01
intron	rs2276824	1	add	1.19E-01	-0.39	add	5.75E-02
intron	rs2294239	1	add	9.08E-01	-0.03	add	1.23E-01
untranslated-3	rs2645294	1	add	9.56E-01	-0.01	add	1.72E-01
intron	rs303084	1	add	4.81E-01	-0.19	add	2.10E-01
unknown	rs4081724	1	add	8.89E-01	0.05	add	3.10E-02
intron	rs897453	0.64	add	9.07E-02	0.45	add	6.17E-01
intron	rs4765219	1	add	3.90E-01	-0.21	add	3.10E-01
intron	rs6018188	0.87	add	9.75E-02	0.41	add	2.10E-01
unknown	rs6556301	1	add	8.00E-01	-0.07	add	4.38E-01
intron	rs714515	1	add	4.02E-01	-0.26	add	2.95E-01
intron	rs7705502	1	add	6.06E-01	0.15	add	8.80E-01
unknown	NA	NA	NA	NA	NA	NA	NA
intron;near-gene-5	rs7801581	1	add	2.41E-01	0.37	add	1.00E-01
intron	rs8030605	1	add	1.65E-01	-0.37	add	4.87E-01
unknown	rs8042543	1	add	1.77E-01	-0.34	add	5.31E-01
unknown	rs979012	1	add	8.81E-01	0.04	add	1.56E-01
unknown	rs10195252	1	dom	9.63E-02	0.58	add	5.69E-01
untranslated-3	rs1045241	1	add	4.16E-01	0.23	add	4.95E-01
unknown	rs10804591	1	add	7.83E-01	-0.07	add	4.44E-01
unknown	rs10919388	1	add	8.15E-01	0.06	add	8.04E-01
intron	rs11231693	1	add	9.51E-01	0.03	add	4.88E-01
intron	rs12454712	1	add	9.12E-01	-0.03	add	8.62E-01
unknown	rs1358980	1	add	5.06E-01	0.16	add	2.01E-01
unknown	rs1443512	1	add	3.33E-01	-0.29	add	7.95E-01

intron	rs1534696	1	add	6.56E-01	-0.10	add	6.41E-01
unknown	rs1776897	1	add	5.54E-01	-0.16	add	3.96E-01
unknown	rs17819328	1	add	5.33E-01	0.16	add	4.45E-01
intron	rs2371767	1	dom	1.06E-02	-0.89	rec	1.80E-01
unknown	rs2820443	1	add	6.91E-02	0.45	add	2.77E-01
intron	rs2925979	1	add	1.10E-01	-0.53	add	1.34E-01
intron	rs3805389	1	add	9.11E-01	0.03	add	9.54E-01
unknown	rs7830933	1	add	3.98E-01	0.20	add	1.09E-01
intron	rs7917772	1	add	9.53E-01	-0.02	add	5.88E-01
unknown	rs8066985	1	add	3.81E-01	-0.22	add	8.17E-01
intron;near-gene-3	rs905938	1	add	8.10E-01	-0.08	add	6.67E-01
unknown	rs9687846	1	add	8.87E-01	0.05	add	9.89E-01
intron	rs9991328	1	add	2.80E-01	0.27	add	4.39E-01
intron	rs224333	1	add	2.97E-01	0.26	add	5.28E-01

not available)

tive correlation between WHR and VAT (r2=0.36) and VSR (r2=0.33). Directions for SAT were not evaluated due t

ıt		sat_male			sat			vat.bmi_female		vat.l
beta	model	P	beta	model	P	beta	model	P	beta	model
-0.29	add	5.98E-02	0.62	add	4.01E-03	0.62	add	8.73E-01	0.02	add
1.72	dom	1.17E-02	-2.43	dom	4.15E-02	-1.14	add	1.76E-01	-0.35	dom
0.11	add	3.13E-01	-1.08	add	1.53E-01	-1.05	add	6.99E-01	0.14	add
0.34	add	9.55E-01	-0.02	add	5.35E-01	0.12	add	8.60E-01	-0.02	add
-0.58	add	3.57E-01	0.38	add	6.19E-01	0.13	add	4.50E-01	-0.10 x	add
0.23	add	7.39E-01	0.26	add	3.13E-01	0.51	add	8.68E-01	0.05	add
-0.02	add	7.13E-01	0.11	add	2.10E-01	0.25	add	2.25E-01	0.12	add
0.31	add	1.59E-01	-0.46	dom	4.45E-02	-0.53	dom	2.78E-02	-0.31	add
0.07	add	3.65E-01	-0.26	add	2.51E-01	-0.22	add	8.71E-02	-0.17	add
0.25	add	1.32E-01	-0.54	add	1.72E-01	-0.33	add	4.03E-01	0.10	add
-0.28	add	4.58E-01	0.22	rec	2.68E-02	-0.78	add	4.61E-01	-0.08	add
-0.61	add	9.36E-01	0.04	add	5.37E-01	-0.20	add	3.80E-01	-0.15	add
-0.02	add	2.81E-01	0.35	add	7.41E-02	0.37	add	8.63E-01	-0.02	add
-0.06	add	2.19E-01	0.36	add	2.15E-01	0.24	add	6.74E-01	-0.04	add
0.07	add	3.45E-01	-0.27	add	2.42E-01	-0.22	add	9.24E-02	-0.16	add
0.13	add	6.39E-01	-0.22	add	9.78E-01	-0.01	add	6.36E-01	-0.07	add
-0.45	add	8.14E-01	0.10	add	3.21E-01	-0.26	add	2.44E-01	-0.16	add
-0.01	add	8.28E-01	0.06	add	5.54E-01	0.11	add	7.04E-01	-0.04	add
0.71	add	1.40E-01	-0.42	add	9.44E-01	-0.01	add	2.50E-03	0.29 X	add
-0.24	add	1.49E-01	0.42	add	4.40E-01	0.15	add	9.28E-01	0.01	add
-0.67	add	4.00E-01	0.27	add	4.56E-01	-0.15	add	1.16E-01	0.16	add
-0.50	add	2.29E-01	0.36	add	5.24E-01	0.12	add	2.72E-01	-0.11	add
-0.49	add	2.76E-01	0.35	add	3.99E-01	0.18	dom	7.65E-02	0.25	add
-0.49	add	2.56E-01	0.40	add	8.62E-01	0.04	add	7.64E-01	-0.03	add
-1.10	add	2.53E-02	1.07	add	1.65E-01	0.41	add	2.32E-01	-0.18	add
0.19	add	4.12E-01	0.27	add	6.13E-02	0.40	add	5.51E-01	0.07	add
-0.35	add	9.50E-01	-0.02	add	2.26E-01	-0.24	add	1.05E-01	0.16	add
0.43	add	9.78E-01	0.01	add	3.28E-01	0.19	add	6.36E-01	0.05	add
0.29	add	3.08E-01	-0.32	add	3.68E-01	-0.19	add	8.97E-01	0.01	add
0.46	add	1.59E-01	-0.52	add	1.60E-01	-0.35	add	4.43E-01	0.10	add
-0.06	add	4.60E-01	0.25	add	3.45E-01	0.21	add	3.53E-01	0.11	add
NA	NA	NA	NA	NA	NA	NA	NA	NA	NA	NA
0.70	add	3.38E-01	-0.36	add	6.73E-01	0.11	add	4.19E-01	-0.11	add
-0.26	add	7.93E-01	-0.08	add	2.38E-01	-0.24	add	4.94E-02	-0.22 X	add
-0.21	add	8.24E-01	0.07	add	2.98E-01	-0.20	add	9.07E-01	-0.01	add
-0.58	add	1.93E-01	0.49	add	4.31E-01	0.19	add	9.85E-01	0.00	add
0.22	add	4.59E-01	0.25	add	1.44E-01	0.33	add	9.63E-01	-0.01	add
-0.26	add	3.04E-01	0.34	add	2.21E-01	0.27	add	3.38E-01	0.11	add
0.28	add	1.74E-01	-0.44	add	3.25E-01	-0.20	add	9.29E-01	-0.01	add
0.09	add	9.08E-01	-0.04	add	9.56E-01	0.01	add	1.20E-01	0.17	add
0.46	add	3.80E-01	-0.51	add	8.41E-01	-0.08	add	3.81E-01	-0.19	add
0.06	add	4.60E-01	-0.23	add	7.04E-01	-0.08	add	2.94E-01	0.11	add
0.42	add	4.85E-01	-0.20	add	9.76E-01	-0.01	add	5.44E-01	-0.06	add
-0.11	add	8.38E-01	0.08	add	8.43E-01	-0.05	add	5.53E-01	0.07	add

0.16	add	5.54E-01	-0.18	add	7.29E-01	-0.07	add	8.34E-01	0.02	add		
-0.30	add	7.29E-01	0.11	add	7.32E-01	-0.07	add	3.04E-01	0.11	add		
-0.26	add	5.21E-01	0.19	add	3.46E-01	0.19	add	6.61E-01	0.05	add		
1.36	add	9.43E-02	-0.57	dom	4.30E-03	-0.78	add	1.67E-01	-0.16	add		
-0.35	add	1.19E-02	0.74	add	3.39E-03	0.58	add	9.77E-01	0.00	add		
-0.64	add	7.88E-01	0.10	add	3.14E-01	-0.25	add	6.08E-01	-0.07	add		
0.02	add	6.04E-01	0.19	add	8.61E-01	0.04	add	7.32E-01	0.04	add		
0.51	add	2.34E-01	-0.34	add	6.11E-01	-0.10	add	6.02E-01	-0.05	add		
0.23	add	9.22E-01	-0.04	add	7.48E-01	0.08	add	9.76E-01	0.00	add		
0.08	add	2.96E-01	-0.33	add	1.84E-01	-0.27	add	1.43E-01	-0.15	add		
-0.19	add	5.26E-01	0.25	add	7.96E-01	0.07	add	3.59E-01	0.12	add		
0.01	add	2.82E-01	-0.42	add	5.72E-01	-0.14	add	7.72E-01	0.04	add		
0.26	add	5.12E-01	-0.19	add	6.00E-01	0.10	add	5.56E-01	0.06	add		
0.22	add	8.67E-01	-0.05	add	7.25E-01	0.07	dom	4.50E-02	-0.28v		add	

:o the low correlation (r2=0.0012). No directional effects were evaluated for interaction models.

bmi_gender_int			vat.bmi_male			vat.bmi			vat_femal
P	beta	model	P	beta	model	P	beta	model	P
5.42E-01	0.10	add	3.09E-01	-0.15	add	5.64E-01	-0.05	dom	3.30E-02
3.14E-01	0.45	add	2.60E-01	-0.42	dom	5.06E-02	-0.46	add	3.74E-01
3.39E-01	0.52	add	8.15E-01	-0.11	add	5.08E-01	0.20	add	3.95E-01
2.84E-01	0.16	add	1.38E-01	-0.20	add	2.40E-01	-0.09[v]	add	4.12E-01
4.13E-01	-0.17	add	3.85E-01	0.16	add	9.86E-01	0.00	add	4.75E-01
7.27E-01	-0.14	add	8.68E-01	0.06	add	8.88E-01	-0.03	add	1.19E-01
8.00E-02	0.27	add	4.81E-01	-0.09	add	7.99E-01	0.02	add	9.73E-02
1.59E-01	-0.24	add	8.19E-02	0.25	add	6.13E-01	0.05	dom	2.48E-02
4.55E-01	-0.11	add	7.76E-01	-0.04	add	9.92E-02	-0.13	add	1.60E-01
2.83E-01	0.20	add	8.16E-01	0.04	add	3.45E-01	0.10	add	7.71E-01
6.08E-01	-0.08	add	2.51E-01	0.15	add	6.46E-01	0.04	add	1.53E-01
9.39E-01	0.02	add	5.16E-01	-0.13	add	3.74E-01	-0.12	add	3.56E-01
9.72E-01	0.01	add	5.38E-01	-0.09	add	5.23E-01	-0.06	add	1.43E-01
5.83E-01	-0.09	add	7.89E-01	0.04	add	9.82E-01	0.00	add	8.11E-01
5.13E-01	-0.09	add	7.05E-01	-0.05	add	8.92E-02	-0.14	add	1.54E-01
9.66E-02	-0.38	add	4.66E-01	0.15	add	7.93E-01	-0.03	add	8.78E-01
2.74E-01	-0.23	add	2.58E-01	0.21	add	8.89E-01	0.02	add	3.22E-02
7.21E-01	0.05	add	4.19E-01	-0.10	add	6.62E-01	-0.04	add	9.50E-01
4.13E-03	0.40	add	1.14E-01	-0.20	add	3.37E-01	0.08	add	1.25E-02
8.67E-01	-0.02	add	7.33E-01	-0.04	add	7.89E-01	0.02	add	9.55E-01
1.85E-01	0.21	add	9.04E-01	-0.02	add	1.13E-01	0.14	add	9.75E-01
6.38E-01	0.07	dom	6.75E-02	-0.35	add	2.32E-01	-0.10	add	3.09E-01
1.64E-03	0.51	add	5.30E-04	-0.48[v]	add	1.56E-01	-0.13	dom	7.00E-03
5.24E-01	0.11	add	4.81E-01	-0.11	add	5.35E-01	-0.06	add	3.20E-01
7.03E-01	-0.09	add	6.73E-01	0.09	add	3.76E-01	-0.11	add	8.62E-01
6.98E-01	-0.07	add	9.89E-01	0.00	add	6.82E-01	0.04	add	1.56E-01
4.29E-01	0.12	add	9.76E-01	0.00	add	3.59E-01	0.08	add	3.64E-01
3.81E-01	0.13	add	6.63E-01	-0.06	add	8.68E-01	0.01	add	1.82E-01
5.69E-01	-0.10	add	5.36E-01	0.09	add	6.13E-01	0.05	add	7.51E-01
1.69E-01	0.27	add	8.86E-01	-0.02	add	3.03E-01	0.11	add	7.22E-01
5.64E-01	0.10	add	9.38E-01	0.01	add	5.55E-01	0.06	add	5.71E-01
NA	NA	NA	NA	NA	NA	NA	NA	NA	NA
1.29E-01	-0.29	add	4.99E-01	0.11	add	7.53E-01	-0.03	add	8.36E-01
3.59E-01	-0.16	add	4.52E-01	-0.11	add	1.06E-01	-0.15	add	9.60E-03
8.19E-01	-0.04	add	7.39E-01	-0.04	add	8.04E-01	-0.02	add	1.24E-01
2.01E-01	-0.24	add	4.30E-01	0.13	add	5.18E-01	0.07	add	7.98E-01
6.00E-01	0.09	add	2.39E-01	-0.17	add	3.75E-01	-0.08	add	6.98E-01
4.69E-01	0.12	add	3.18E-01	-0.15	add	7.32E-01	0.03	add	3.77E-01
5.01E-01	-0.11	add	7.39E-01	0.05	add	8.72E-01	-0.01	add	3.04E-01
5.35E-01	0.10	add	2.96E-01	0.15	add	1.59E-01	0.13	add	1.43E-01
9.78E-01	-0.01	add	2.54E-01	-0.29	add	1.31E-01	-0.26	add	5.47E-01
8.58E-01	-0.03	add	4.50E-01	0.10	add	2.40E-01	0.10	add	6.71E-01
7.62E-01	0.04	add	3.62E-01	-0.12	add	2.67E-01	-0.09	add	4.29E-01
3.09E-01	0.19	dom	4.67E-02	-0.38 X	add	8.85E-01	-0.01	add	6.84E-01

5.48E-01	-0.09	add	9.59E-02	0.23	add	2.48E-01	0.10	add	9.93E-01
1.76E-01	0.22	add	8.25E-01	0.03	add	4.92E-01	0.06	add	3.10E-01
4.06E-01	-0.13	add	1.03E-01	0.22	add	1.21E-01	0.13	add	7.38E-01
8.40E-01	-0.04	add	1.91E-01	-0.20	add	9.43E-02	-0.16	dom	9.31E-03
1.10E-01	0.24	add	3.20E-01	-0.13	add	6.12E-01	-0.04	add	3.22E-01
5.14E-03	-0.54	dom	2.29E-04	0.69	X add	5.23E-02	0.21	add	5.19E-01
7.80E-01	-0.05	add	9.68E-01	0.01	add	8.45E-01	0.02	add	5.29E-01
2.93E-01	-0.15	add	4.35E-01	0.10	add	8.43E-01	-0.02	add	7.60E-01
8.60E-01	0.03	add	6.10E-01	0.08	add	7.82E-01	0.03	add	7.42E-01
9.62E-01	-0.01	add	4.17E-02	-0.28	√ add	1.36E-02	-0.21	√ add	4.38E-02
1.67E-01	0.27	add	2.53E-01	-0.20	add	9.97E-01	0.00	add	5.34E-01
6.18E-01	0.10	add	8.28E-01	0.04	add	8.89E-01	0.02	add	7.23E-01
3.09E-01	0.16	add	4.33E-01	-0.10	add	8.17E-01	-0.02	add	1.47E-01
7.80E-02	-0.27	add	7.17E-01	0.05	add	5.74E-01	-0.05	rec	2.29E-02

e	vat_gender_int			vat_male			vat		
	beta	model	P	beta	model	P	beta	model	P	beta	model
	0.43	add	6.81E-01	0.09	add	8.86E-01	0.03	add	1.36E-01	0.19	add
	-0.32	dom	4.85E-02	1.22	dom	3.55E-03	-1.62	dom	1.02E-02	-0.83	add
	-0.44	add	5.90E-01	0.41	add	3.34E-01	-0.62	add	3.57E-01	-0.39	add
	0.11	add	7.00E-02	0.39	add	1.19E-01	-0.29	add	7.46E-01	-0.04	add
	-0.13	add	3.04E-01	-0.30	add	3.97E-01	0.21	add	9.20E-01	0.02	add
	0.59	add	8.29E-01	0.12	add	4.52E-01	0.35	add	1.87E-01	0.40	add
	0.24	add	1.41E-01	0.31	add	9.60E-01	0.01	add	2.40E-01	0.14	add
	-0.44	dom	1.14E-01	-0.46	add	6.36E-01	0.09	rec	1.33E-01	0.46	dom
	-0.19	add	9.18E-01	-0.02	add	3.54E-01	-0.16	add	7.31E-02	-0.20	add
	0.05	add	2.80E-01	0.27	add	4.89E-01	-0.15	add	9.90E-01	0.00	add
	-0.21	rec	4.13E-01	-0.33	add	2.42E-01	0.21	rec	4.35E-02	-0.43	X add
	-0.21	add	2.92E-01	-0.33	add	9.28E-01	0.02	add	4.59E-01	-0.14	add
	0.22	add	4.92E-01	0.16	add	8.36E-01	0.04	add	2.37E-01	0.14	add
	-0.04	add	3.04E-01	-0.22	add	1.62E-01	0.25	add	3.97E-01	0.10	add
	-0.20	add	9.74E-01	-0.01	add	2.98E-01	-0.18	add	5.95E-02	-0.21	add
	-0.03	add	4.94E-01	-0.22	add	9.66E-01	0.01	add	7.73E-01	-0.05	add
	-0.41√	add	2.09E-01	-0.36	add	9.55E-01	0.01	add	1.79E-01	-0.21	add
	-0.01	add	6.59E-01	0.09	add	4.18E-01	-0.14	add	7.68E-01	-0.03	add
	0.34	X add	3.55E-03	0.57	add	5.00E-02	-0.33√	add	5.24E-01	0.07	add
	-0.01	add	4.84E-01	-0.14	add	5.48E-01	0.10	add	5.72E-01	0.06	add
	0.00	add	8.97E-01	-0.03	add	7.10E-01	0.07	add	5.46E-01	0.07	add
	-0.14	rec	2.75E-01	-0.42	rec	8.78E-02	0.54	dom	6.64E-02	-0.30	add
	0.53	X add	6.14E-02	0.42	add	2.27E-01	-0.23	add	7.25E-01	0.04	dom
	-0.16	add	7.63E-01	-0.07	add	8.55E-01	0.04	add	4.82E-01	-0.09	add
	0.04	add	7.18E-01	-0.12	add	2.12E-01	0.35	add	5.10E-01	0.11	add
	0.22	add	9.29E-01	0.02	add	5.60E-01	0.12	add	1.98E-01	0.16	add
	0.13	add	7.94E-01	0.06	add	7.66E-01	0.05	add	5.60E-01	0.07	add
	0.19	add	1.59E-01	0.30	add	6.15E-01	-0.09	add	4.53E-01	0.09	add
	0.05	add	7.39E-01	-0.08	add	6.09E-01	0.10	add	6.11E-01	0.06	add
	0.07	add	1.51E-01	0.39	add	3.15E-01	-0.23	add	8.99E-01	-0.02	add
	0.10	add	4.02E-01	0.21	add	5.88E-01	-0.11	add	9.18E-01	0.01	add
NA	NA		NA	NA		NA	NA		NA	NA	
	0.04	add	9.72E-01	0.01	add	7.03E-01	-0.09	add	9.37E-01	-0.01	add
	-0.41	X add	1.02E-01	-0.39	add	6.61E-01	-0.08	add	3.82E-02	-0.26	X add
	-0.22	add	2.43E-01	-0.25	add	8.96E-01	0.02	add	2.76E-01	-0.13	add
	0.04	add	2.63E-01	-0.29	add	3.25E-01	0.22	add	3.85E-01	0.12	add
	0.06	add	4.72E-01	0.17	add	4.26E-01	-0.16	add	9.50E-01	-0.01	add
	0.14	add	7.06E-01	-0.09	add	5.31E-01	0.13	add	2.83E-01	0.14	add
	-0.15	dom	9.86E-01	-0.01	add	2.30E-01	-0.23	dom	3.84E-02	-0.33√	add
	0.23	add	3.68E-01	0.21	add	8.23E-01	0.04	add	2.63E-01	0.14	add
	-0.18	add	6.03E-01	0.22	add	1.68E-01	-0.47	add	2.29E-01	-0.28	add
	0.06	add	9.26E-01	-0.02	add	9.68E-01	0.01	add	6.65E-01	0.05	add
	0.11	add	1.13E-01	0.32	add	1.88E-01	-0.23	add	8.23E-01	-0.03	add
	-0.07	add	7.65E-01	0.08	dom	1.28E-01	-0.39	add	5.17E-01	-0.09	add

	0.00	add	8.37E-01	-0.04	add	4.19E-01	0.15	add	5.91E-01	0.06	add
	0.16	add	2.66E-01	0.25	add	6.58E-01	0.09	add	3.95E-01	0.11	add
	0.05	add	3.43E-01	-0.20	add	1.06E-01	0.29	add	1.99E-01	0.15	add
-0.52√		dom	6.83E-01	-0.12	add	4.27E-02	-0.42√	dom	1.84E-03	-0.50√	add
	0.14	add	3.49E-01	0.19	add	6.62E-01	0.08	add	3.15E-01	0.12	add
	-0.12	add	4.39E-02	-0.54	add	4.98E-02	0.42 X		add	4.75E-01	0.11	add
	0.11	add	9.78E-01	0.01	add	8.80E-01	0.03	add	6.48E-01	0.06	add
	0.04	add	6.50E-01	0.09	add	8.84E-01	-0.02	add	9.28E-01	-0.01	add
	0.06	add	6.02E-01	0.14	add	9.81E-01	-0.01	add	7.20E-01	0.05	add
-0.29√		add	6.71E-01	-0.09	add	6.06E-02	-0.34	add	5.84E-03	-0.32√	add
	0.12	add	4.77E-01	0.20	add	8.39E-01	-0.05	add	7.98E-01	0.04	add
	-0.07	add	6.94E-01	0.11	add	4.55E-01	-0.17	add	3.99E-01	-0.13	add
	0.21	add	6.51E-02	0.39	add	8.61E-02	-0.30	add	9.68E-01	0.00	add
0.64 X		add	5.27E-01	-0.14	add	5.33E-01	0.11	add	5.89E-01	0.06	dom

vsr_female			vsr_gender_int			vsr_male			vsr
P	beta	model	P	beta	model	P	beta	model	P
7.59E-01	0.01	add	2.38E-01	0.04	add	1.27E-01	-0.05	add	4.68E-01
2.14E-01	-0.07	add	9.38E-01	-0.01	add	7.42E-01	-0.03	add	3.27E-01
3.57E-01	0.08	add	3.16E-01	0.12	add	9.64E-01	0.00	add	3.83E-01
7.34E-01	0.01	add	5.41E-01	0.02	add	3.27E-01	-0.03	add	8.14E-01
1.69E-01	-0.04	add	9.06E-01	-0.01	add	7.86E-01	-0.01	add	2.16E-01
2.93E-01	0.07	add	4.97E-01	0.06	add	8.11E-01	0.02	add	5.51E-01
1.35E-01	0.04	add	1.19E-02	0.08	add	4.70E-01	-0.02	add	6.85E-01
6.56E-02	-0.06	add	1.92E-01	-0.05	dom	3.21E-02	0.08	add	8.12E-01
3.03E-01	-0.02	add	8.27E-01	-0.01	add	4.46E-01	-0.02	add	2.61E-01
1.05E-01	0.05	add	7.87E-01	0.01	add	1.84E-01	0.04	add	3.11E-02
7.60E-01	-0.01	add	9.76E-01	0.00	add	4.69E-01	0.02	add	9.44E-01
2.23E-01	-0.05	add	6.56E-01	-0.02	add	7.43E-01	0.01	add	5.50E-01
7.30E-01	0.01	add	3.20E-01	0.04	add	3.30E-01	-0.03	add	6.75E-01
7.43E-01	-0.01	add	4.69E-01	-0.02	add	4.71E-01	0.02	add	8.43E-01
2.90E-01	-0.02	add	8.50E-01	-0.01	add	4.05E-01	-0.02	add	2.33E-01
7.68E-01	-0.01	add	2.90E-01	-0.05	add	7.99E-01	-0.01	add	6.03E-01
3.40E-02	-0.066√	add	2.16E-01	-0.05	add	7.77E-01	0.01	add	3.93E-01
6.61E-01	-0.01	add	4.97E-01	0.02	add	1.45E-01	-0.04	add	3.90E-01
1.24E-01	0.03	rec	9.04E-01	-0.01	dom	1.93E-01	-0.05	rec	2.12E-02
4.49E-01	-0.02	add	8.31E-01	-0.01	add	4.80E-01	-0.02	add	6.72E-01
1.88E-01	0.03	add	3.04E-02	0.08	add	3.73E-01	-0.03	add	3.57E-01
6.53E-01	-0.01	add	1.21E-01	0.05	add	1.15E-01	-0.04	add	2.74E-01
1.48E-03	0.10 X	add	1.20E-05	0.15	add	6.68E-04	-0.099√	add	5.63E-01
3.45E-01	-0.02	add	4.73E-01	0.03	add	3.36E-01	-0.03	add	1.88E-01
7.92E-01	0.01	add	3.22E-02	0.11	add	1.20E-01	-0.07	add	3.30E-01
9.90E-01	0.00	add	6.96E-01	-0.01	add	3.86E-01	-0.03	add	4.73E-01
1.51E-01	0.03	add	3.79E-01	0.03	add	7.73E-01	0.01	add	2.94E-01
8.90E-01	0.00	add	5.90E-01	0.02	add	6.86E-01	-0.01	add	7.56E-01
8.89E-01	0.00	add	7.39E-02	-0.07	dom	1.15E-02	0.093√	add	1.11E-01
7.22E-01	0.01	add	7.15E-01	0.02	add	4.05E-01	0.03	add	2.99E-01
9.28E-01	0.00	add	2.92E-01	0.04	add	3.55E-02	-0.065 X	add	1.83E-01
NA	NA	NA	NA	NA	NA	NA	NA	NA	NA
3.07E-01	-0.03	add	2.49E-02	-0.09	dom	1.45E-01	0.06	add	9.56E-01
1.69E-02	-0.061 X	add	2.45E-02	-0.08	add	9.87E-01	0.00	add	9.80E-02
5.83E-01	-0.01	add	2.69E-01	-0.04	add	8.50E-01	0.01	add	8.00E-01
8.82E-01	0.00	add	7.81E-01	0.01	add	5.79E-01	-0.02	add	8.84E-01
8.94E-01	0.00	add	7.85E-01	0.01	add	2.18E-01	-0.04	add	3.05E-01
4.49E-01	0.02	add	3.54E-01	0.03	add	4.25E-01	-0.02	add	8.52E-01
2.39E-01	-0.03	add	1.38E-01	-0.05	add	8.68E-01	0.01	add	4.83E-01
1.76E-02	0.061 X	add	2.72E-01	0.04	add	2.97E-01	0.03	add	1.41E-02
2.77E-01	-0.06	add	5.31E-01	-0.04	add	4.54E-01	-0.04	add	2.25E-01
2.35E-01	0.03	add	7.58E-01	-0.01	add	1.84E-01	0.04	add	8.69E-02
3.59E-01	0.02	add	3.64E-01	0.03	add	5.49E-01	-0.02	add	7.45E-01
6.63E-01	0.01	add	6.25E-01	0.02	add	2.43E-01	-0.04	add	6.65E-01

9.27E-01	0.00	add	2.92E-01	-0.04	add	4.85E-02	0.056	X	add	3.31E-01
1.18E-01	0.04	dom	5.57E-02	0.09	add	7.56E-01	0.01		dom	7.26E-02
9.06E-01	0.00	add	9.29E-01	0.00	add	5.05E-01	0.02		add	6.43E-01
8.22E-01	-0.01	add	7.36E-01	-0.01	add	7.65E-01	-0.01		add	6.27E-01
7.27E-01	0.01	add	3.38E-04	0.11	add	9.99E-03	-0.070	V	add	1.21E-01
5.54E-01	0.02	add	4.49E-01	-0.03	add	7.88E-02	0.06		add	1.47E-01
6.39E-01	0.01	add	9.55E-01	0.00	add	7.19E-01	-0.01		add	9.44E-01
4.35E-01	-0.02	add	1.46E-01	-0.05	add	3.46E-01	0.03		add	7.73E-01
5.87E-01	0.02	add	9.26E-01	0.00	add	9.60E-01	0.00		add	9.15E-01
1.35E-01	-0.04	add	2.11E-01	-0.04	add	4.81E-01	-0.02		add	9.45E-02
1.31E-01	0.05	add	1.03E-01	0.07	add	4.36E-01	-0.03		add	6.54E-01
4.01E-01	-0.03	dom	5.58E-01	0.03	add	6.56E-01	0.02		dom	1.81E-01
5.44E-01	0.01	add	2.61E-01	0.04	add	5.11E-01	-0.02		add	9.58E-01
5.63E-02	-0.06	add	1.42E-01	-0.05	add	5.57E-01	0.02		add	7.93E-01

beta
-0.01
-0.05
0.06
0.00
-0.03
0.03
0.01
0.01√
-0.02√
0.049√
0.00
-0.02
-0.01
0.00
-0.02
-0.01
-0.02
-0.02
0.071√
-0.01
0.02
-0.02
-0.01
-0.03
-0.03
-0.01
0.02
-0.01
0.03
0.02
-0.03
NA
0.00
-0.03
0.00
0.00
-0.02
0.00
-0.01
0.051 X
-0.05
0.03
0.01
-0.01

0.02
0.05
0.01
-0.01
-0.03
0.04
0.00
0.01
0.00
-0.03
0.01
-0.04
0.00
0.00

Figure S1. QQ plots for genome-wide sex-combined, female, male, SNP-sex interaction analyses: **A**. Subcutaneous Adipose Tissue (SAT), **B**. Visceral Adipose Tissue adjusted for Body Mass Index (VAT_BMI), **C**. Visceral Adipose Tissue (VAT), **D**. Visceral-Subcutaneous adipose tissue ratio (VSR).

A

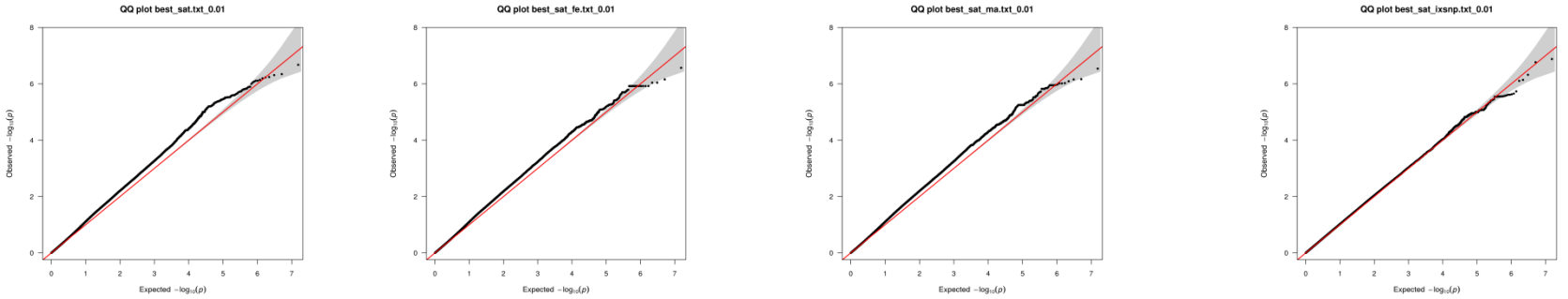

Figure S1. A.
QQ plots for Subcutaneous Adipose Tissue (MAF≥0.01). From left to right: sex-combined analysis, female only, male only, sex-SNP interaction.

Figure S1. QQ plots for genome-wide sex-combined, female, male, SNP-sex interaction analyses: **A**. Subcutaneous Adipose Tissue (SAT), **B**. Visceral Adipose Tissue adjusted for Body Mass Index (VAT_BMI), **C**. Visceral Adipose Tissue (VAT), **D**. Visceral-Subcutaneous adipose tissue ratio (VSR).

B

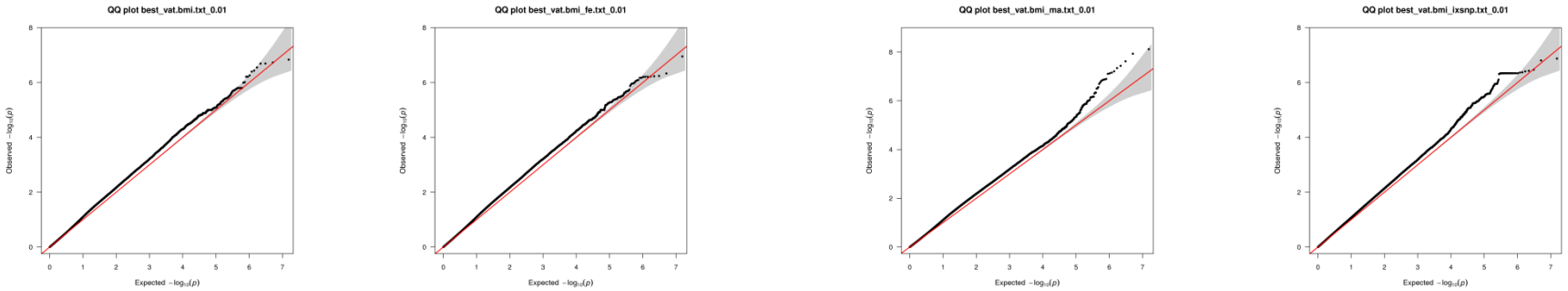

Figure S1. B.
QQ plots for Visceral Adipose Tissue with BMI adjustment (MAF≥0.01).
From left to right: sex-combined analysis, female only, male only, sex-SNP interaction.

Figure S1. QQ plots for genome-wide sex-combined, female, male, SNP-sex interaction analyses: **A**. Subcutaneous Adipose Tissue (SAT), **B**. Visceral Adipose Tissue adjusted for Body Mass Index (VAT_BMI), **C**. Visceral Adipose Tissue (VAT), **D**. Visceral-Subcutaneous adipose tissue ratio (VSR).

C

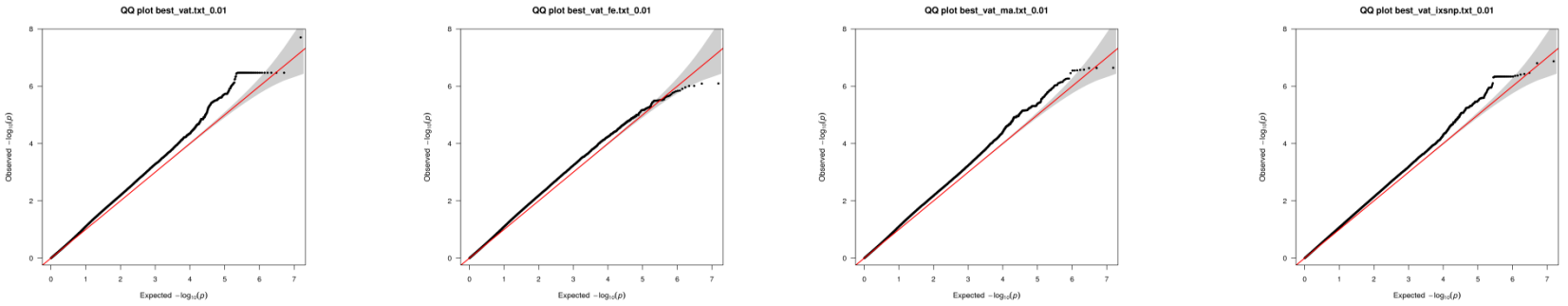

Figure S1. C.
QQ plots for Visceral Adipose Tissue (MAF≥0.01). From left to right: sex-combined analysis, female only, male only, sex-SNP interaction.

Figure S1. QQ plots for genome-wide sex-combined, female, male, SNP-sex interaction analyses: **A**. Subcutaneous Adipose Tissue (SAT), **B**. Visceral Adipose Tissue adjusted for Body Mass Index (VAT_BMI), **C**. Visceral Adipose Tissue (VAT), **D**. Visceral-Subcutaneous adipose tissue ratio (VSR).

D

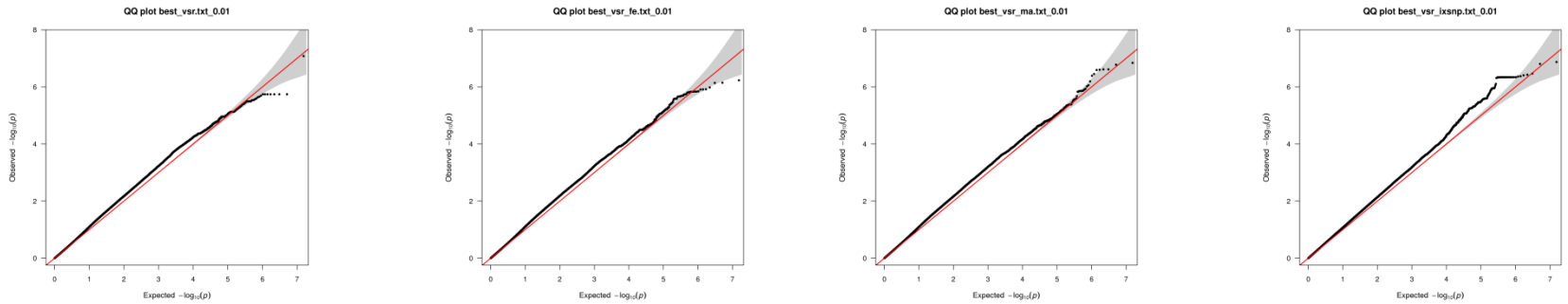

Figure S1. D.
QQ plots for Visceral-subcutaneous Adipose Tissue ratio (MAF≥0.01). From left to right: sex-combined analysis, female only, male only, sex-SNP interaction.

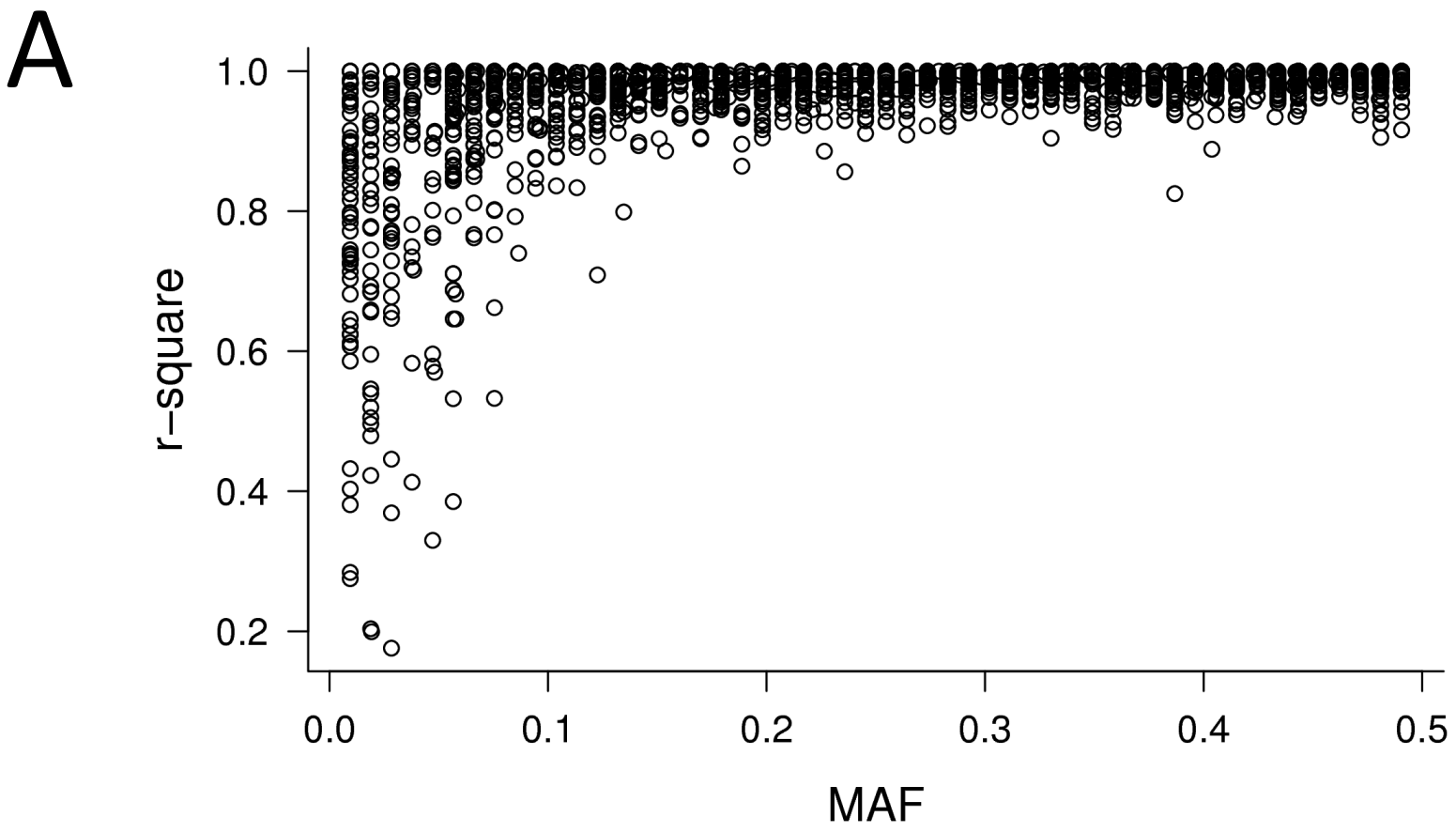

Figure S2. Assessment of imputation quality. **A**. r^2 between imputed and genotyped genotypes, **B**. confidence score for imputation.

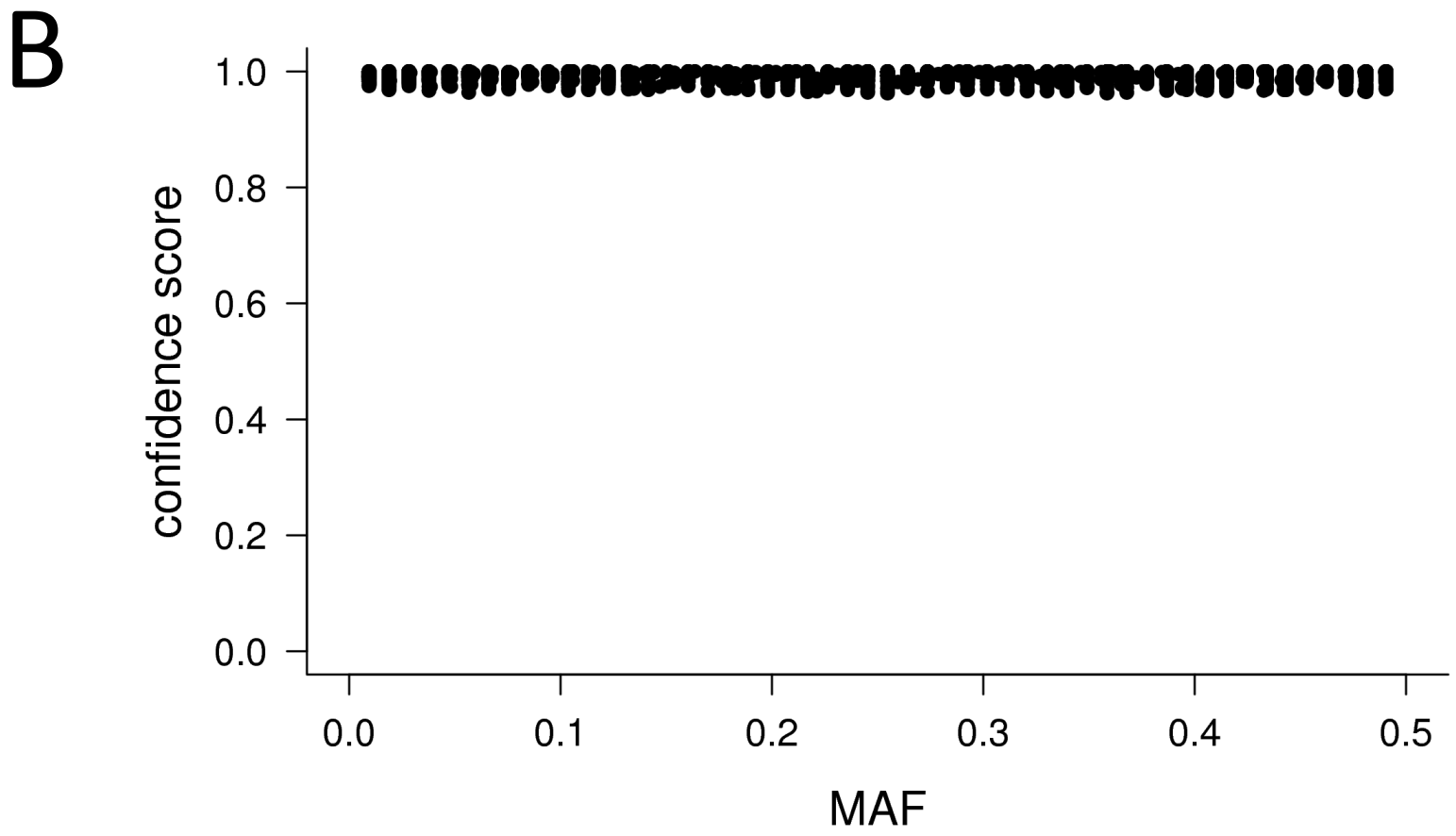

Figure S2. Assessment of imputation quality. **A**. r^2 between imputed and genotyped genotypes, **B**. confidence score for imputation.

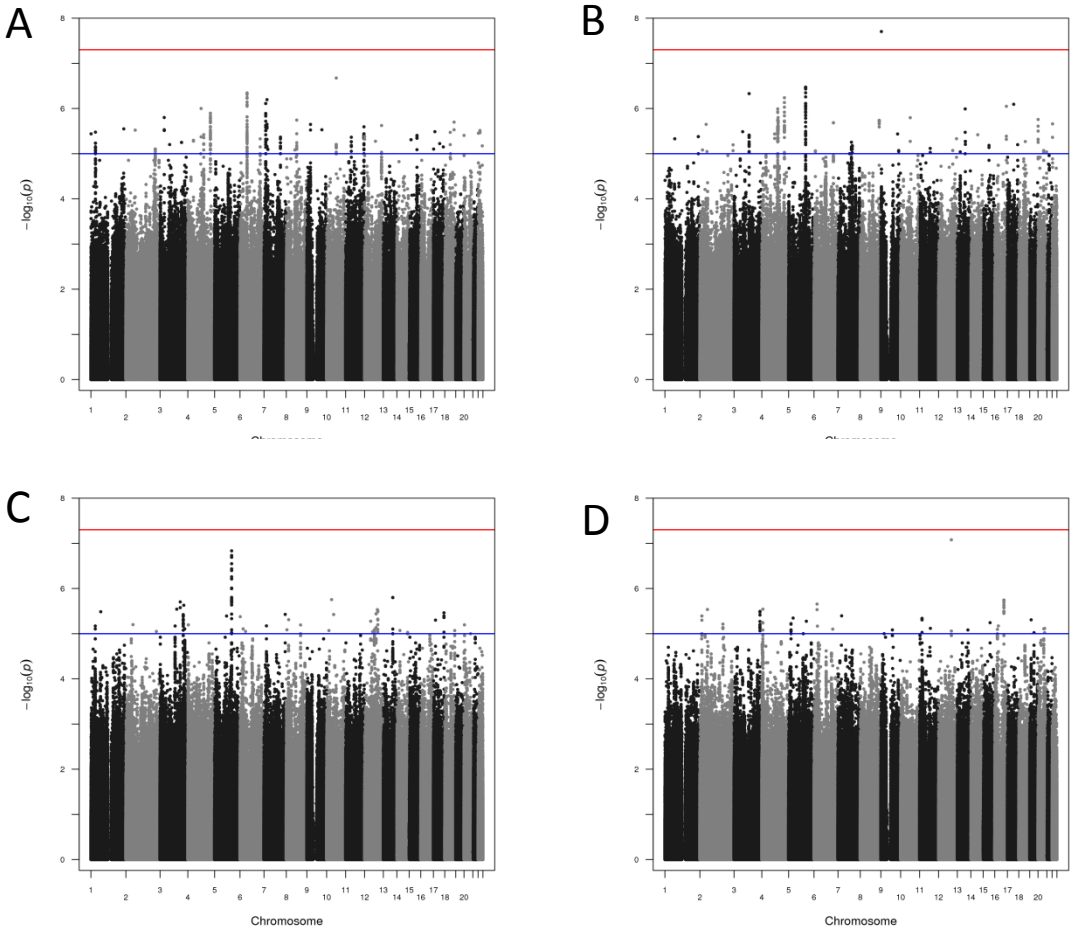

Figure S3. Manhattan plots for association analysis in IRASFS Mexican Americans: **A**. Subcutaneous adipose tissue (SAT), **B**. Visceral adipose tissue (VAT), **C**. Visceral adipose tissue adjusted for body mass index (VAT_BMI), **D**. Visceral-subcutaneous adipose tissue ratio (VSR). Results were adjusted for age, sex, recruitment center, and admixture estimates. P-values are shown under the best fit model. The lower line at $-\log_{10}(PVAL)=5$ represents the suggestive P-value=1.00×10^{-5} and the upper line represents the genome-wide significance threshold (P=5.00×10^{-8}).

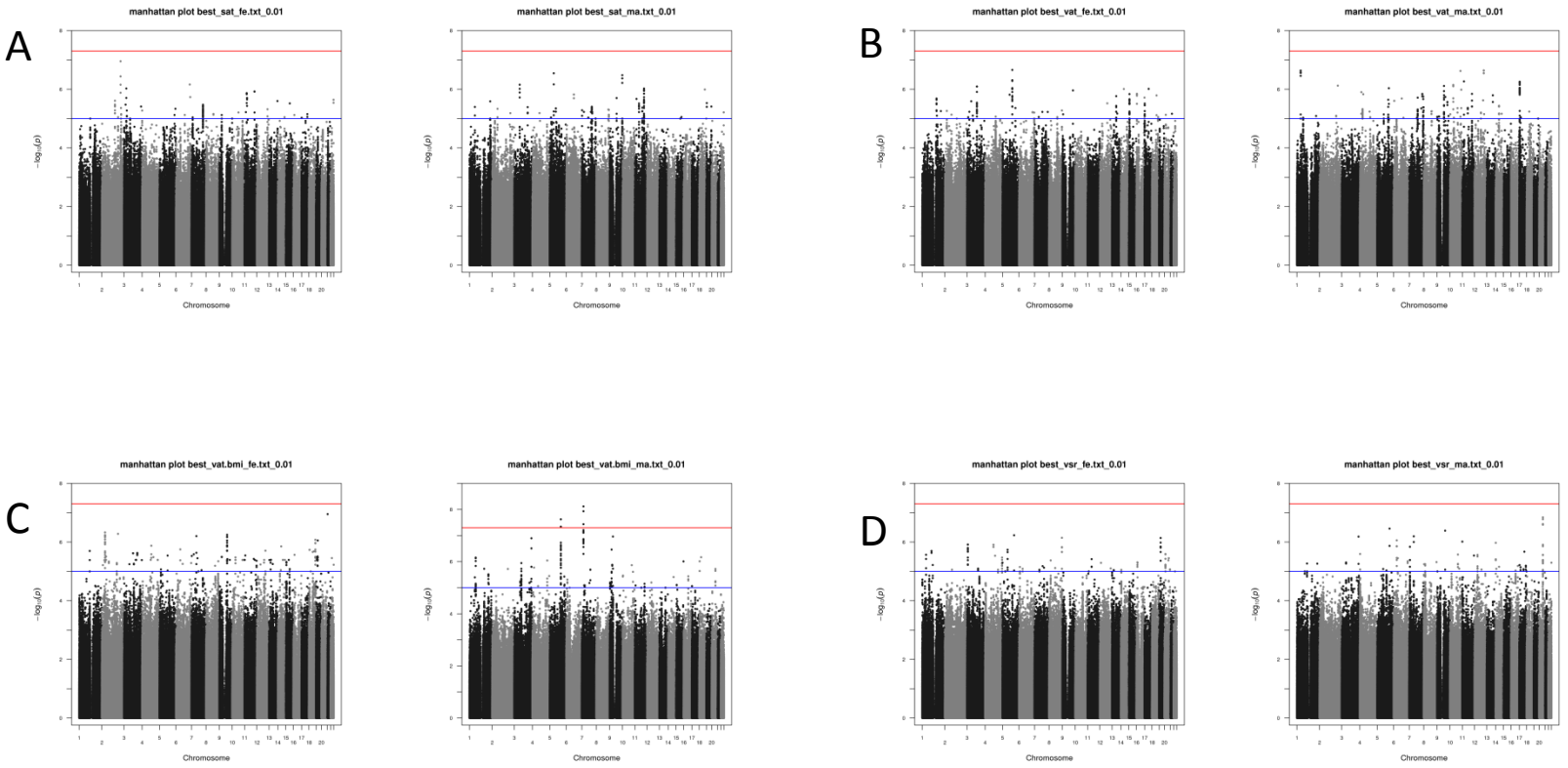

Figure S4. Manhattan Plots for genome-wide and exome chip sex-stratified association analysis in IRASFS Mexican Americans: **A**. Subcutaneous Adipose Tissue (SAT), **B**. Visceral Adipose Tissue (VAT), **C**. Visceral Adipose Tissue adjusted for Body Mass Index (VAT_BMI), **D**. Visceral-Subcutaneous adipose tissue ratio (VSR). (females on the left, males on the right)

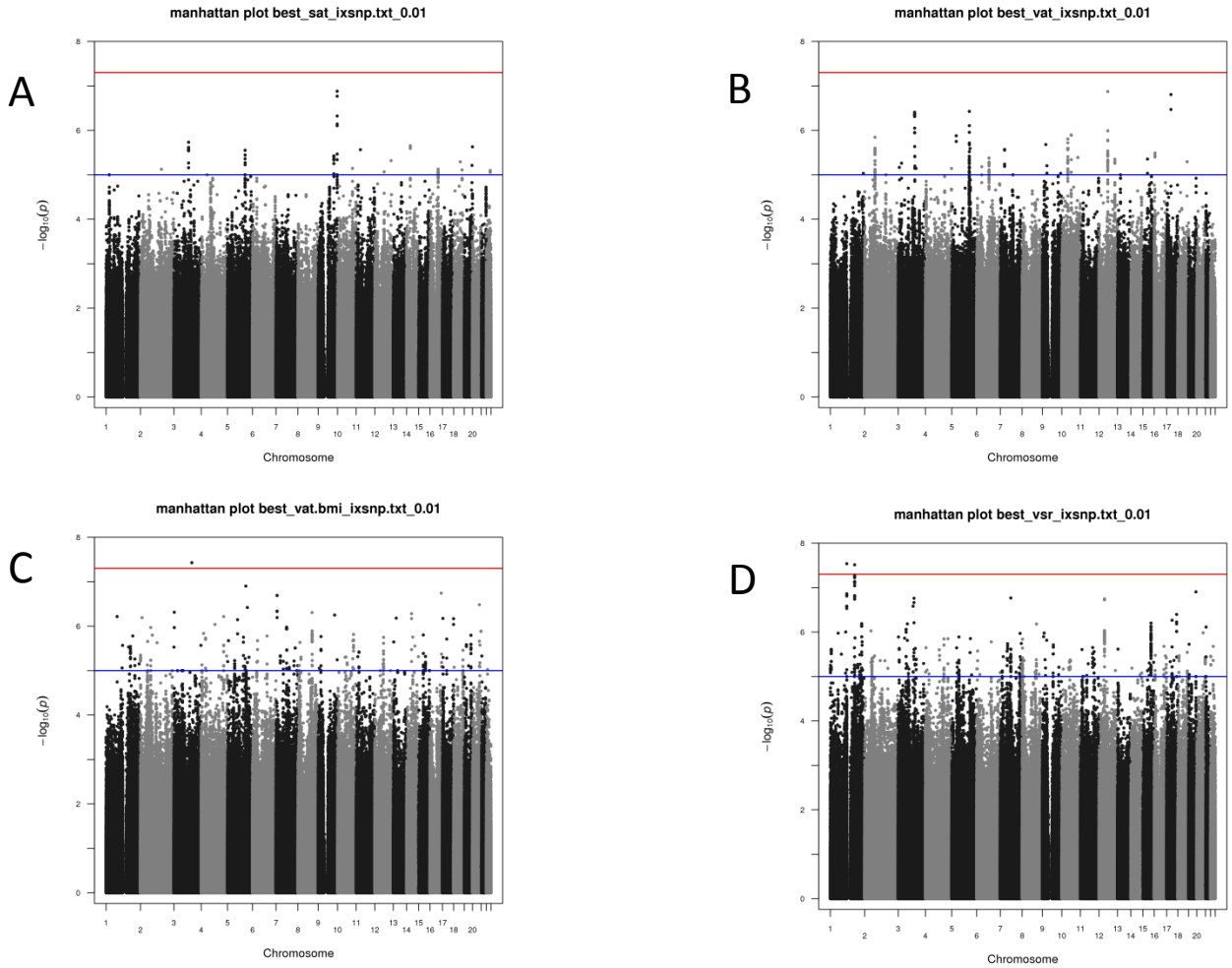

Figure S5. Manhattan plots for genome-wide SNP-sex interaction analysis in IRASFS Mexican Americans: **A**. Subcutaneous adipose tissue (SAT), **B**. Visceral adipose tissue (VAT), **C**. Visceral adipose tissue adjusted for body mass index (VAT_BMI), **D**. Visceral-subcutaneous adipose tissue ratio (VSR). Results were adjusted for age, recruitment center, and admixture estimates.

A

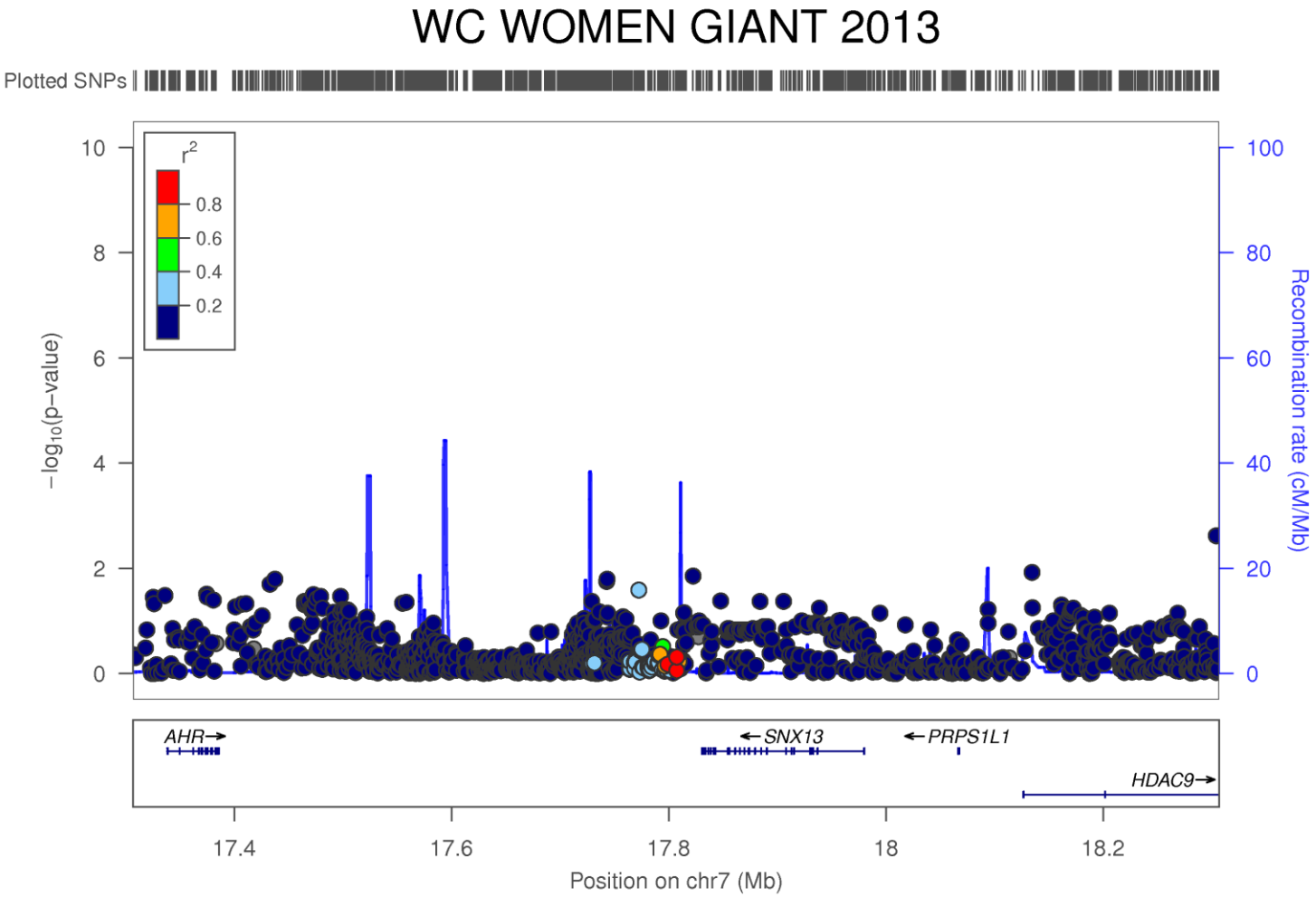

Figure S6. Regional plots for *SNX13* locus from GIANT. **A**. Waist Circumference Women, **B**. Waist Circumference Men, **C**. BMI Women, **D**. BMI Men, **E**. Waist Circumference adjusted by BMI Women, **F**. Waist Circumference adjusted by BMI Men, **G**. Waist-Hip Ratio Women, **H**. Waist-Hip Ratio Men, **I**. Waist-Hip Ratio adjusted by BMI Women, **J**. Waist-Hip Ratio adjusted by BMI Men.

B

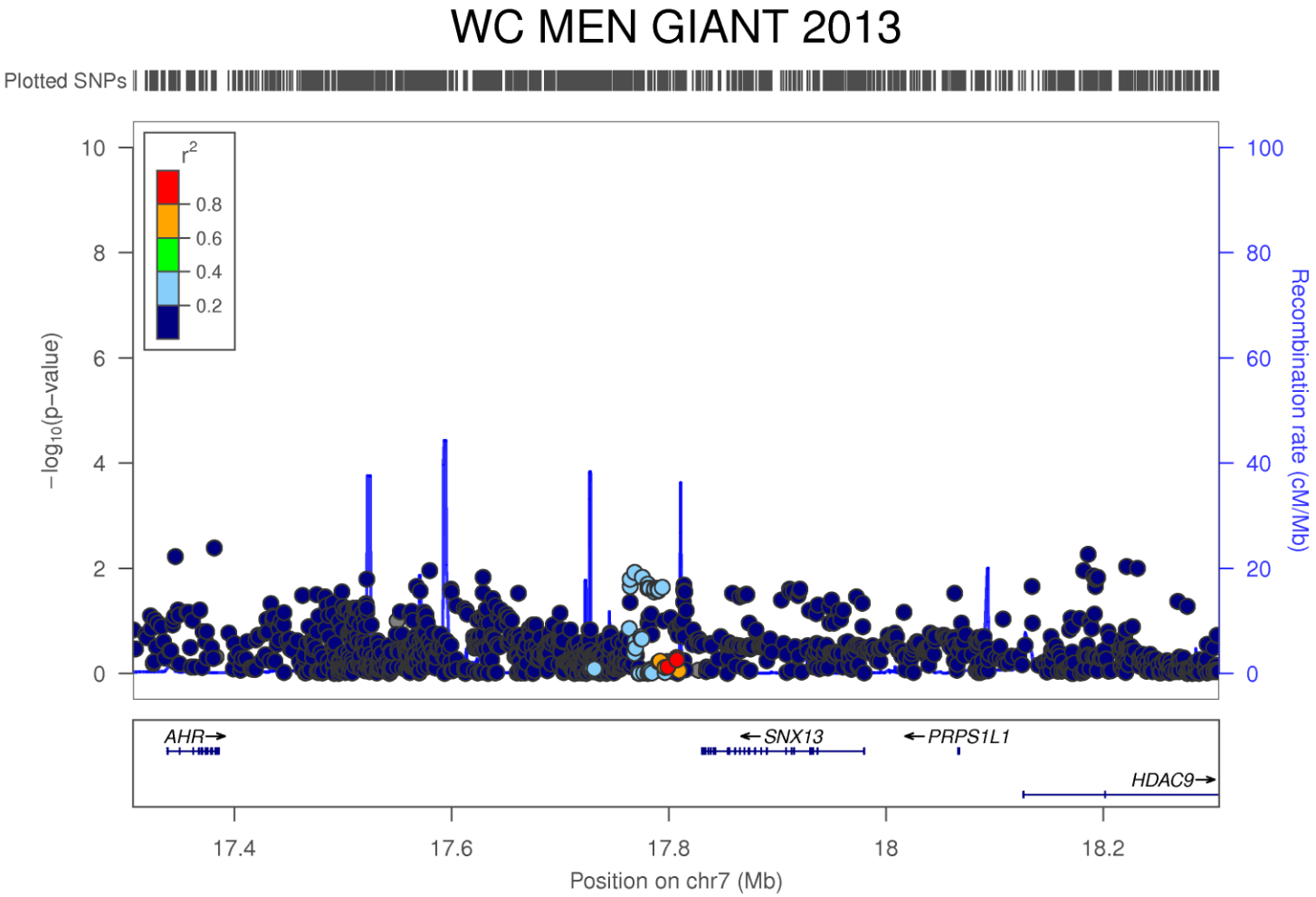

Figure S6. Regional plots for *SNX13* locus from GIANT. **A**. Waist Circumference Women, **B**. Waist Circumference Men, **C**. BMI Women, **D**. BMI Men, **E**. Waist Circumference adjusted by BMI Women, **F**. Waist Circumference adjusted by BMI Men, **G**. Waist-Hip Ratio Women, **H**. Waist-Hip Ratio Men, **I**. Waist-Hip Ratio adjusted by BMI Women, **J**. Waist-Hip Ratio adjusted by BMI Men.

C

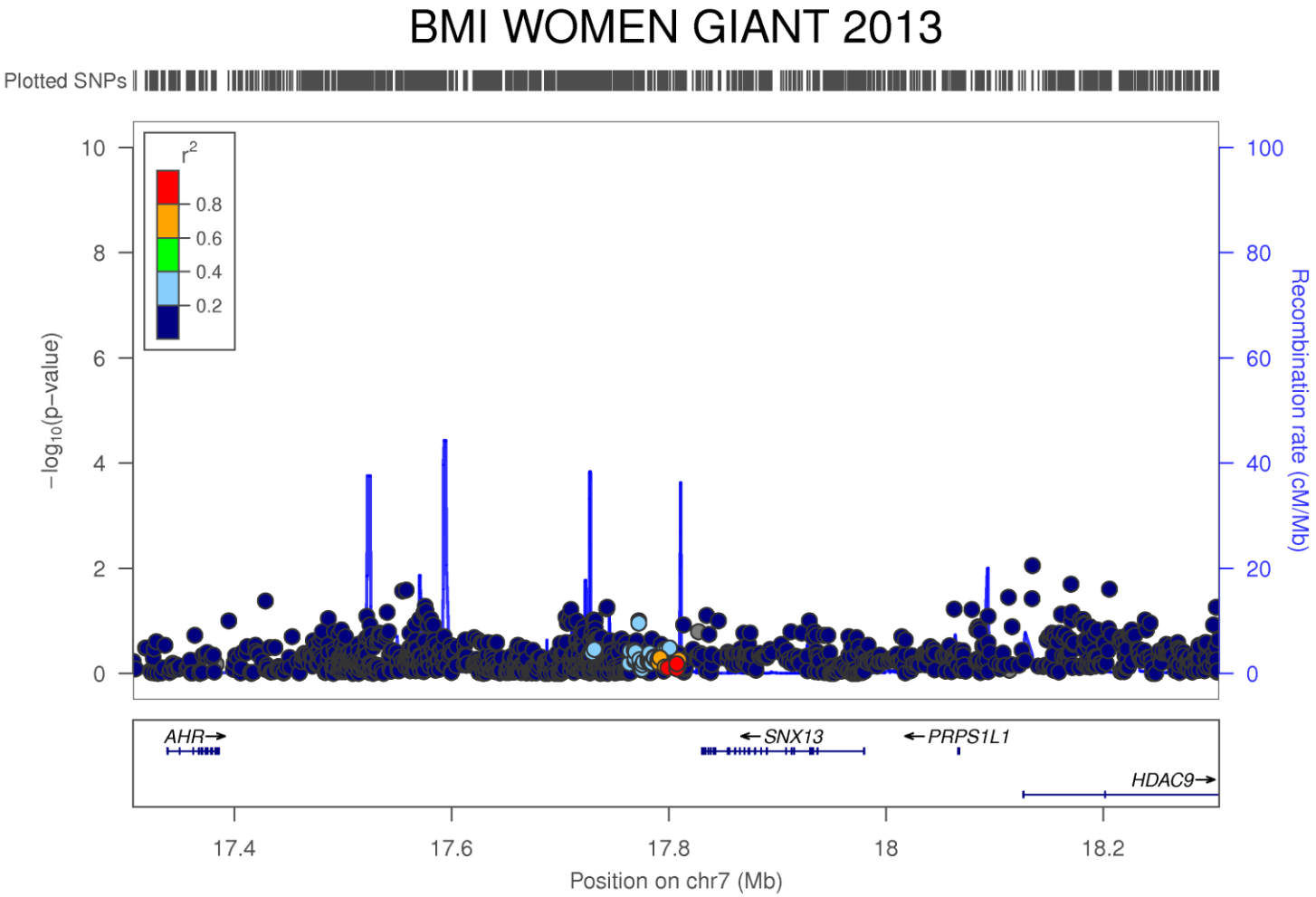

Figure S6. Regional plots for *SNX13* locus from GIANT. **A**. Waist Circumference Women, **B**. Waist Circumference Men, **C**. BMI Women, **D**. BMI Men, **E**. Waist Circumference adjusted by BMI Women, **F**. Waist Circumference adjusted by BMI Men, **G**. Waist-Hip Ratio Women, **H**. Waist-Hip Ratio Men, **I**. Waist-Hip Ratio adjusted by BMI Women, **J**. Waist-Hip Ratio adjusted by BMI Men.

D

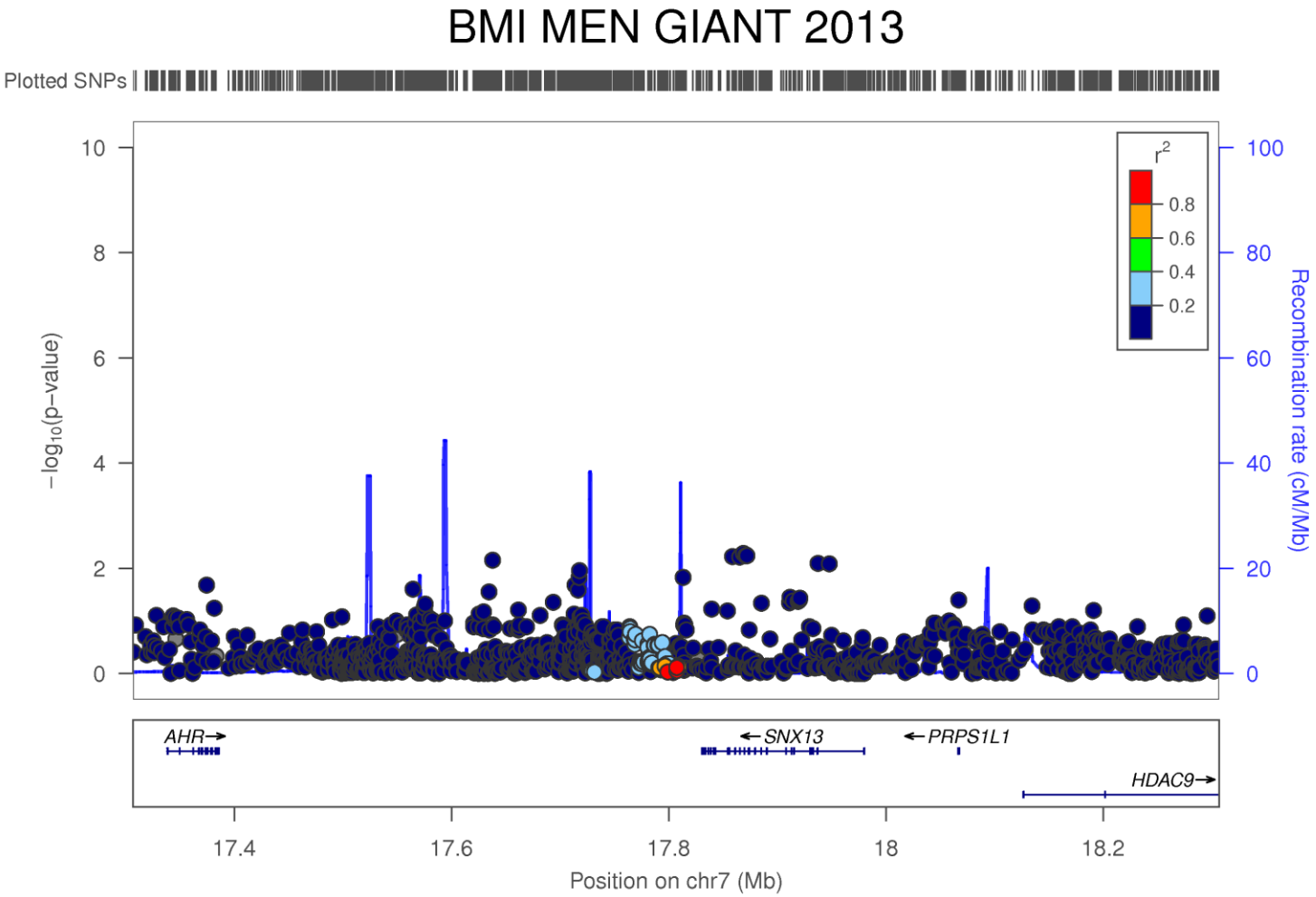

Figure S6. Regional plots for *SNX13* locus from GIANT. **A**. Waist Circumference Women, **B**. Waist Circumference Men, **C**. BMI Women, **D**. BMI Men, **E**. Waist Circumference adjusted by BMI Women, **F**. Waist Circumference adjusted by BMI Men, **G**. Waist-Hip Ratio Women, **H**. Waist-Hip Ratio Men, **I**. Waist-Hip Ratio adjusted by BMI Women, **J**. Waist-Hip Ratio adjusted by BMI Men.

E

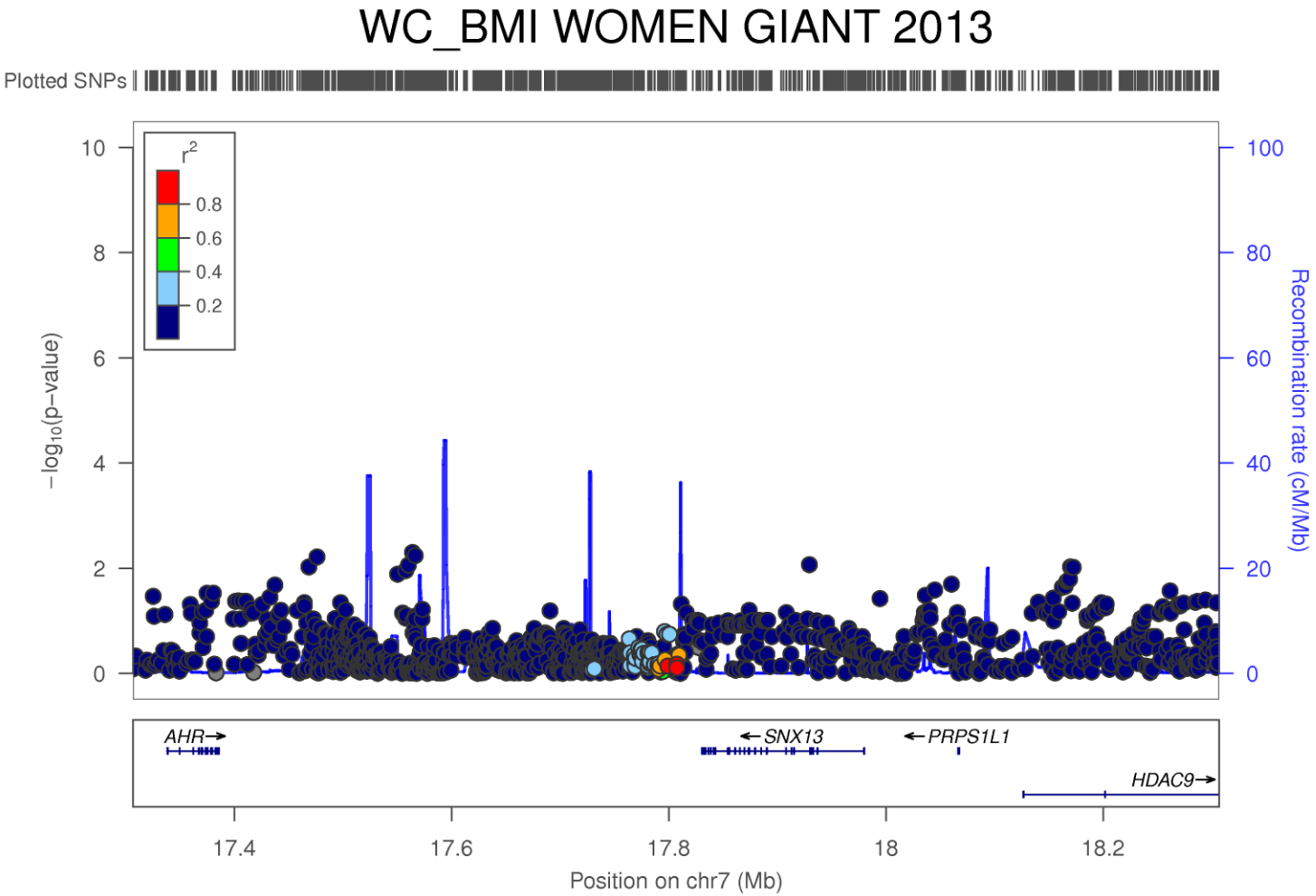

Figure S6. Regional plots for *SNX13* locus from GIANT. **A**. Waist Circumference Women, **B**. Waist Circumference Men, **C**. BMI Women, **D**. BMI Men, **E**. Waist Circumference adjusted by BMI Women, **F**. Waist Circumference adjusted by BMI Men, **G**. Waist-Hip Ratio Women, **H**. Waist-Hip Ratio Men, **I**. Waist-Hip Ratio adjusted by BMI Women, **J**. Waist-Hip Ratio adjusted by BMI Men.

F

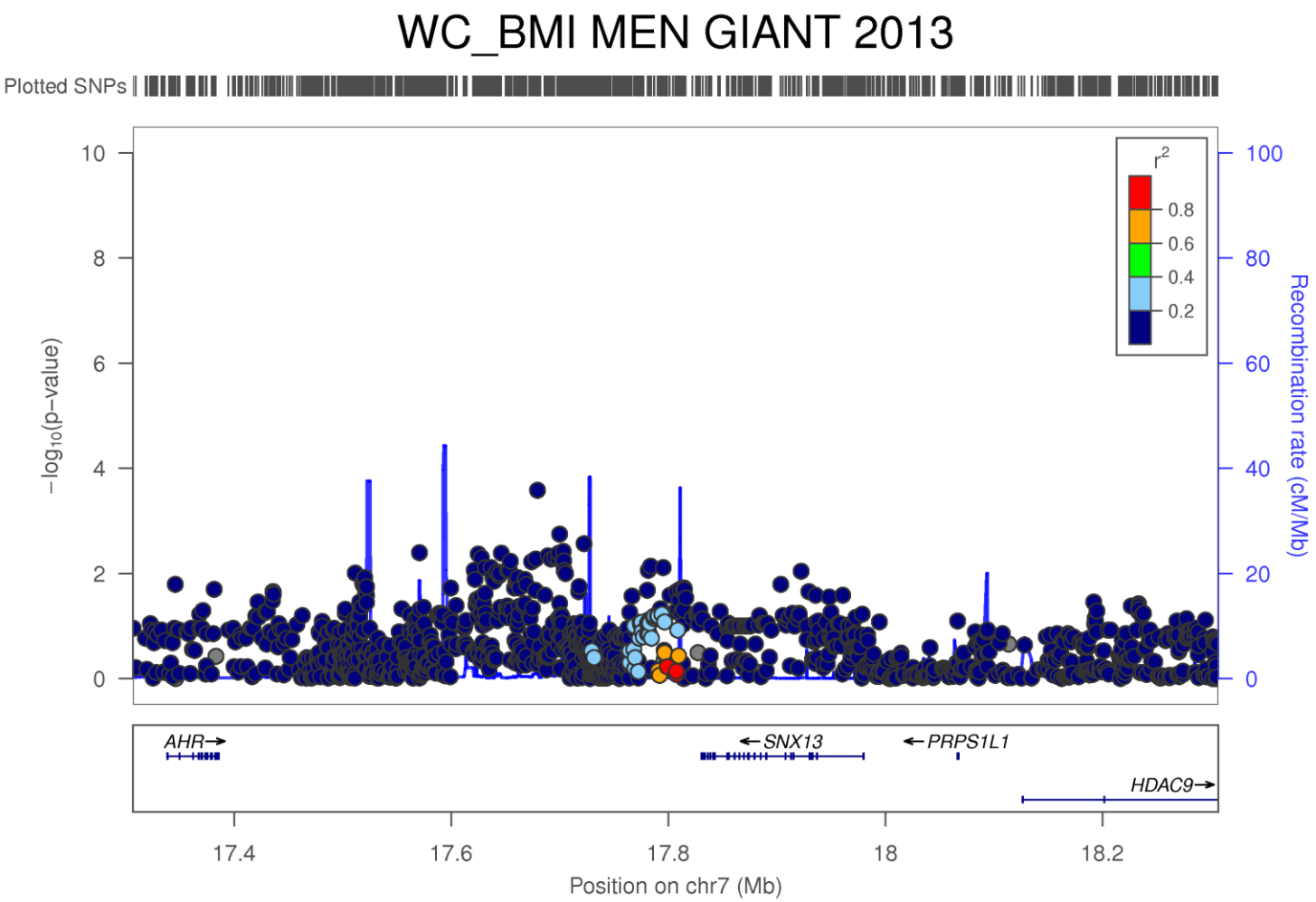

Figure S6. Regional plots for *SNX13* locus from GIANT. **A**. Waist Circumference Women, **B**. Waist Circumference Men, **C**. BMI Women, **D**. BMI Men, **E**. Waist Circumference adjusted by BMI Women, **F**. Waist Circumference adjusted by BMI Men, **G**. Waist-Hip Ratio Women, **H**. Waist-Hip Ratio Men, **I**. Waist-Hip Ratio adjusted by BMI Women, **J**. Waist-Hip Ratio adjusted by BMI Men.

G

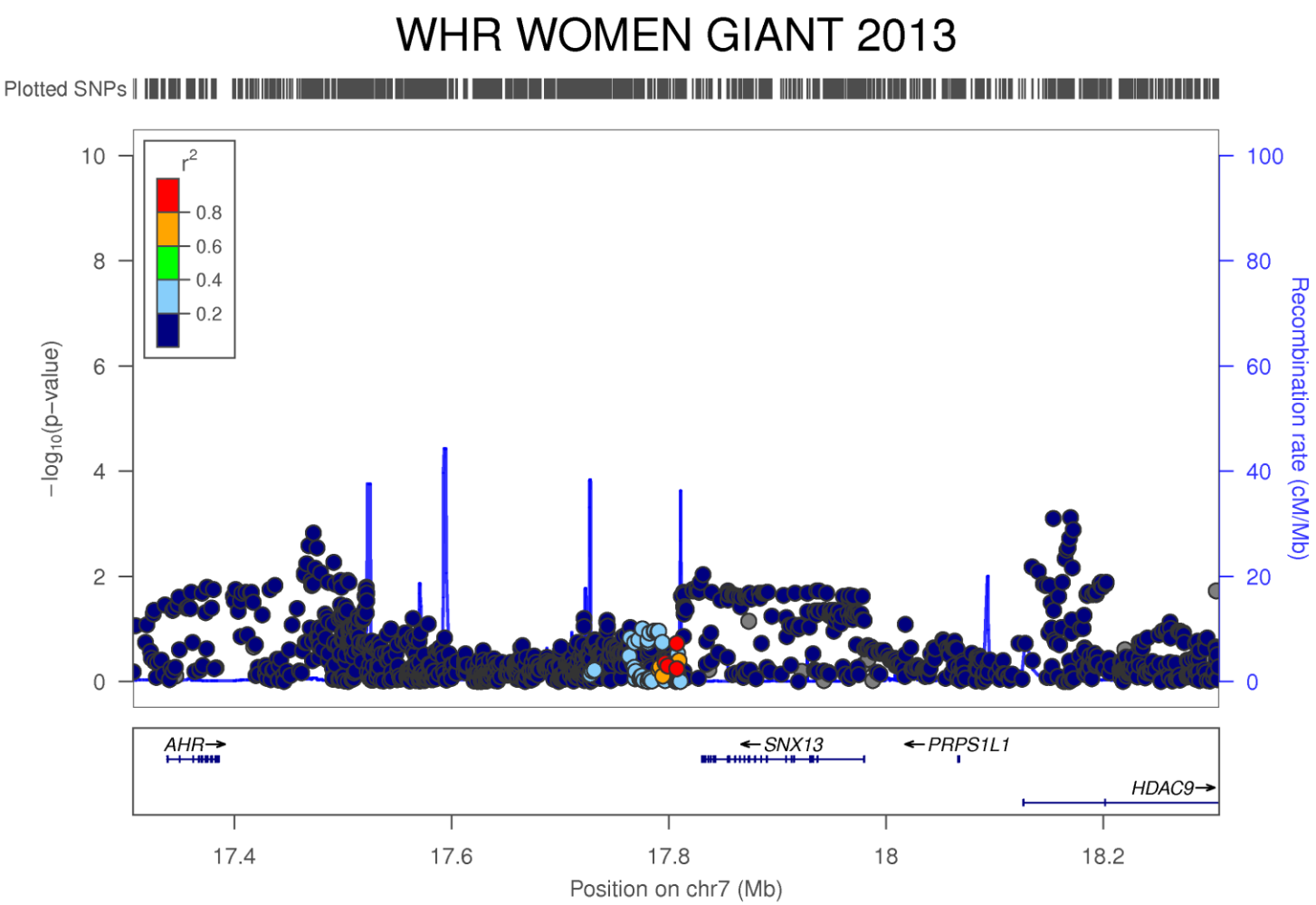

Figure S6. Regional plots for *SNX13* locus from GIANT. **A**. Waist Circumference Women, **B**. Waist Circumference Men, **C**. BMI Women, **D**. BMI Men, **E**. Waist Circumference adjusted by BMI Women, **F**. Waist Circumference adjusted by BMI Men, **G**. Waist-Hip Ratio Women, **H**. Waist-Hip Ratio Men, **I**. Waist-Hip Ratio adjusted by BMI Women, **J**. Waist-Hip Ratio adjusted by BMI Men.

H

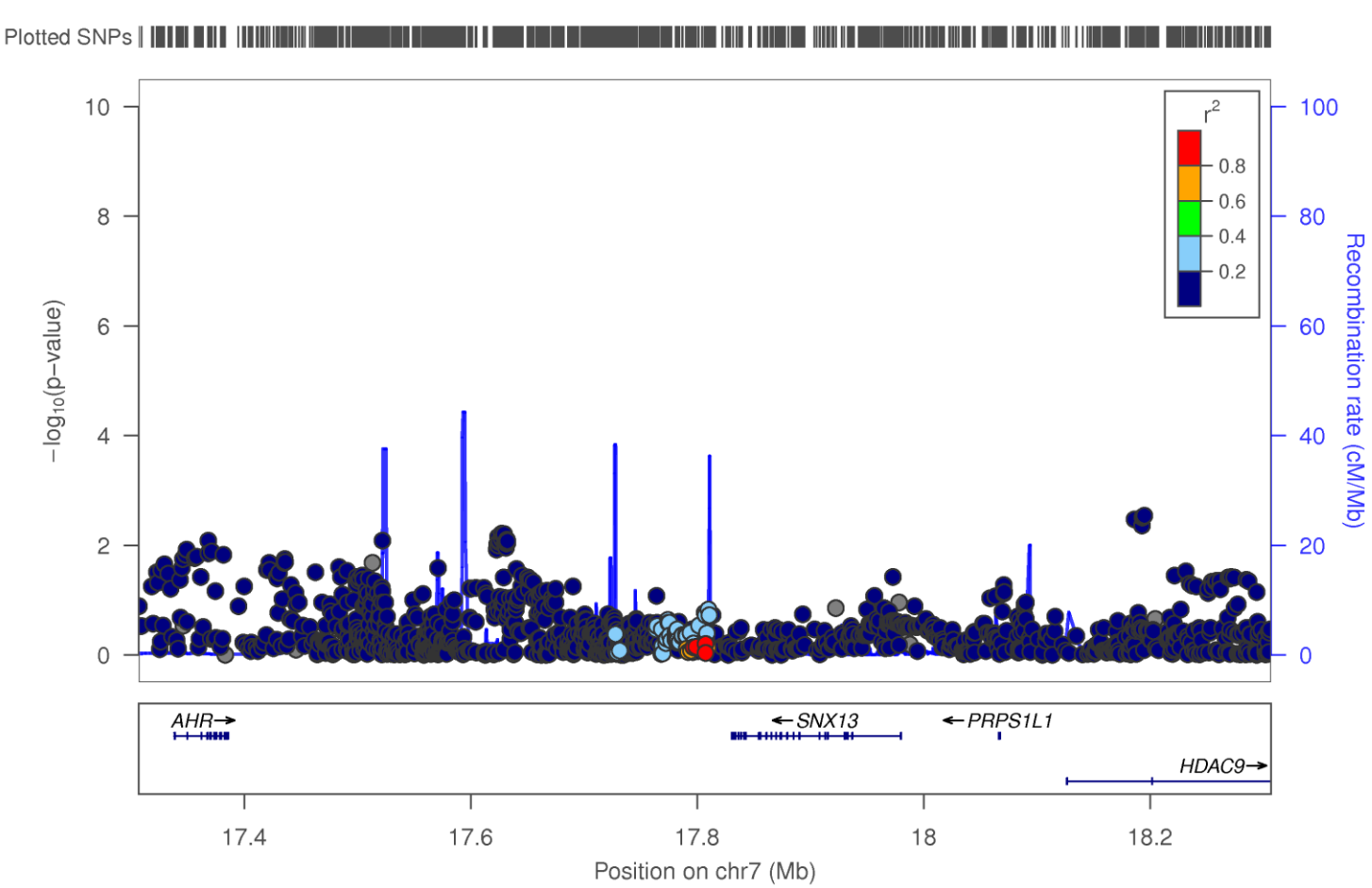

Figure S6. Regional plots for *SNX13* locus from GIANT. **A**. Waist Circumference Women, **B**. Waist Circumference Men, **C**. BMI Women, **D**. BMI Men, **E**. Waist Circumference adjusted by BMI Women, **F**. Waist Circumference adjusted by BMI Men, **G**. Waist-Hip Ratio Women, **H**. Waist-Hip Ratio Men, **I**. Waist-Hip Ratio adjusted by BMI Women, **J**. Waist-Hip Ratio adjusted by BMI Men.

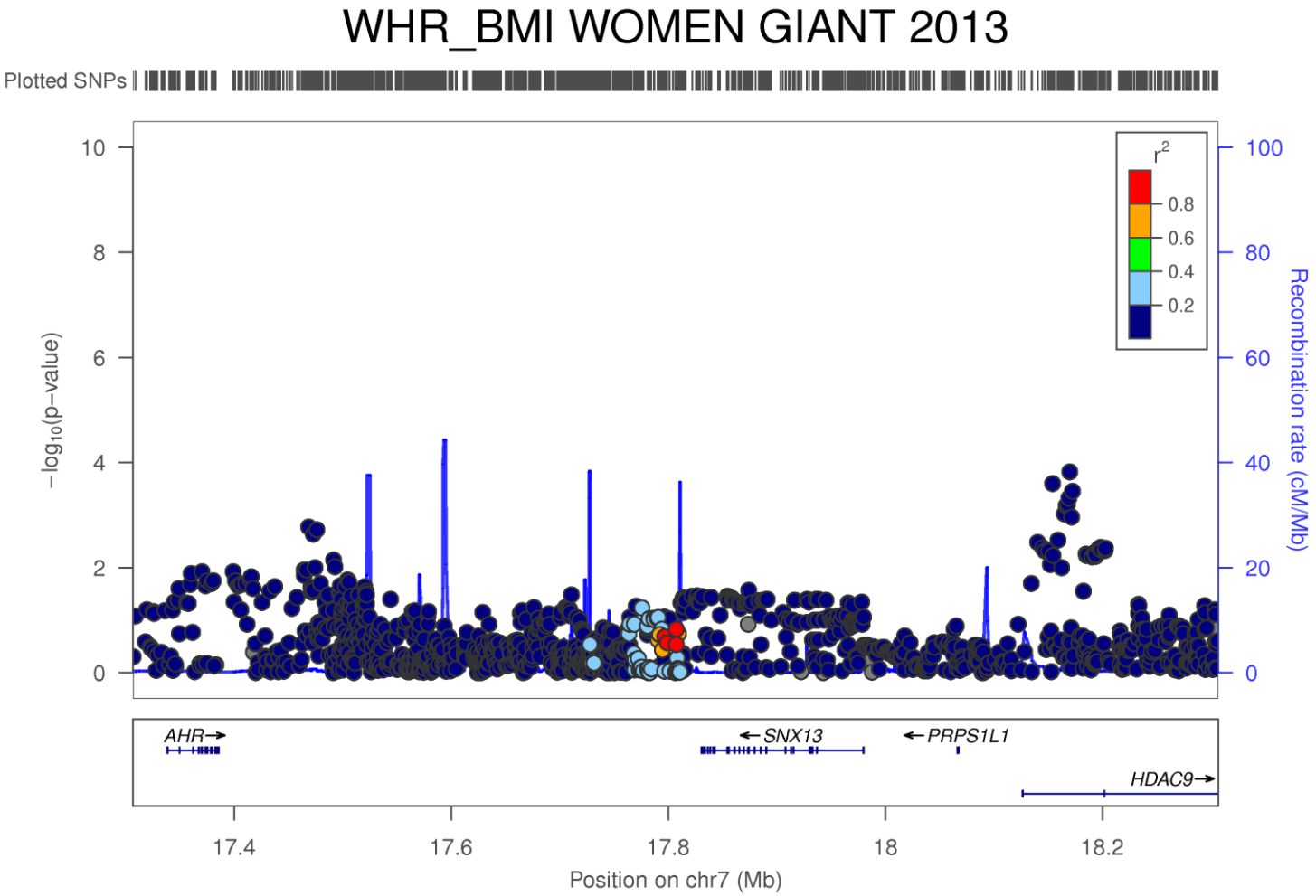

Figure S6. Regional plots for *SNX13* locus from GIANT. **A**. Waist Circumference Women, **B**. Waist Circumference Men, **C**. BMI Women, **D**. BMI Men, **E**. Waist Circumference adjusted by BMI Women, **F**. Waist Circumference adjusted by BMI Men, **G**. Waist-Hip Ratio Women, **H**. Waist-Hip Ratio Men, **I**. Waist-Hip Ratio adjusted by BMI Women, **J**. Waist-Hip Ratio adjusted by BMI Men.

J

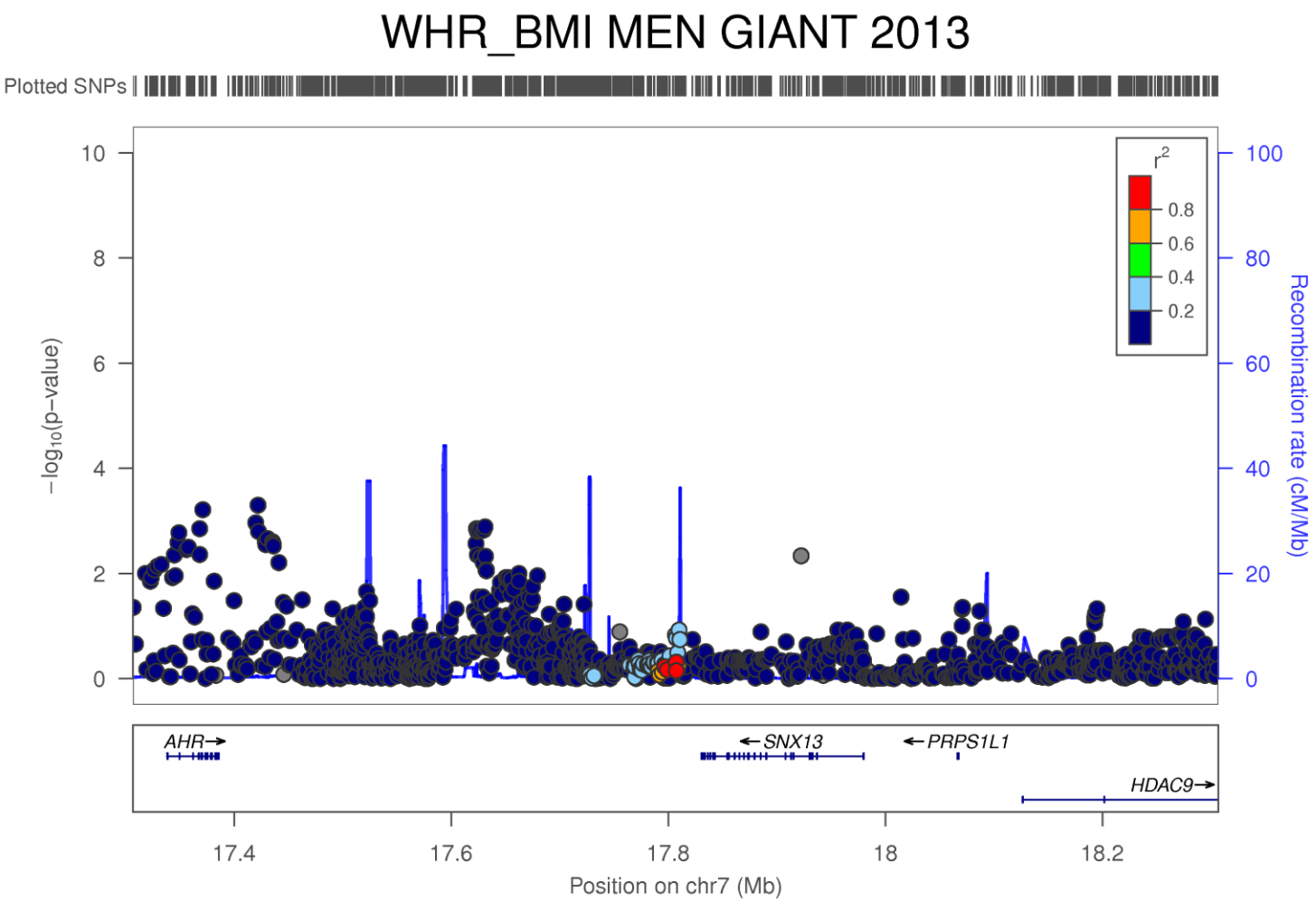

Figure S6. Regional plots for *SNX13* locus from GIANT. **A**. Waist Circumference Women, **B**. Waist Circumference Men, **C**. BMI Women, **D**. BMI Men, **E**. Waist Circumference adjusted by BMI Women, **F**. Waist Circumference adjusted by BMI Men, **G**. Waist-Hip Ratio Women, **H**. Waist-Hip Ratio Men, **I**. Waist-Hip Ratio adjusted by BMI Women, **J**. Waist-Hip Ratio adjusted by BMI Men.

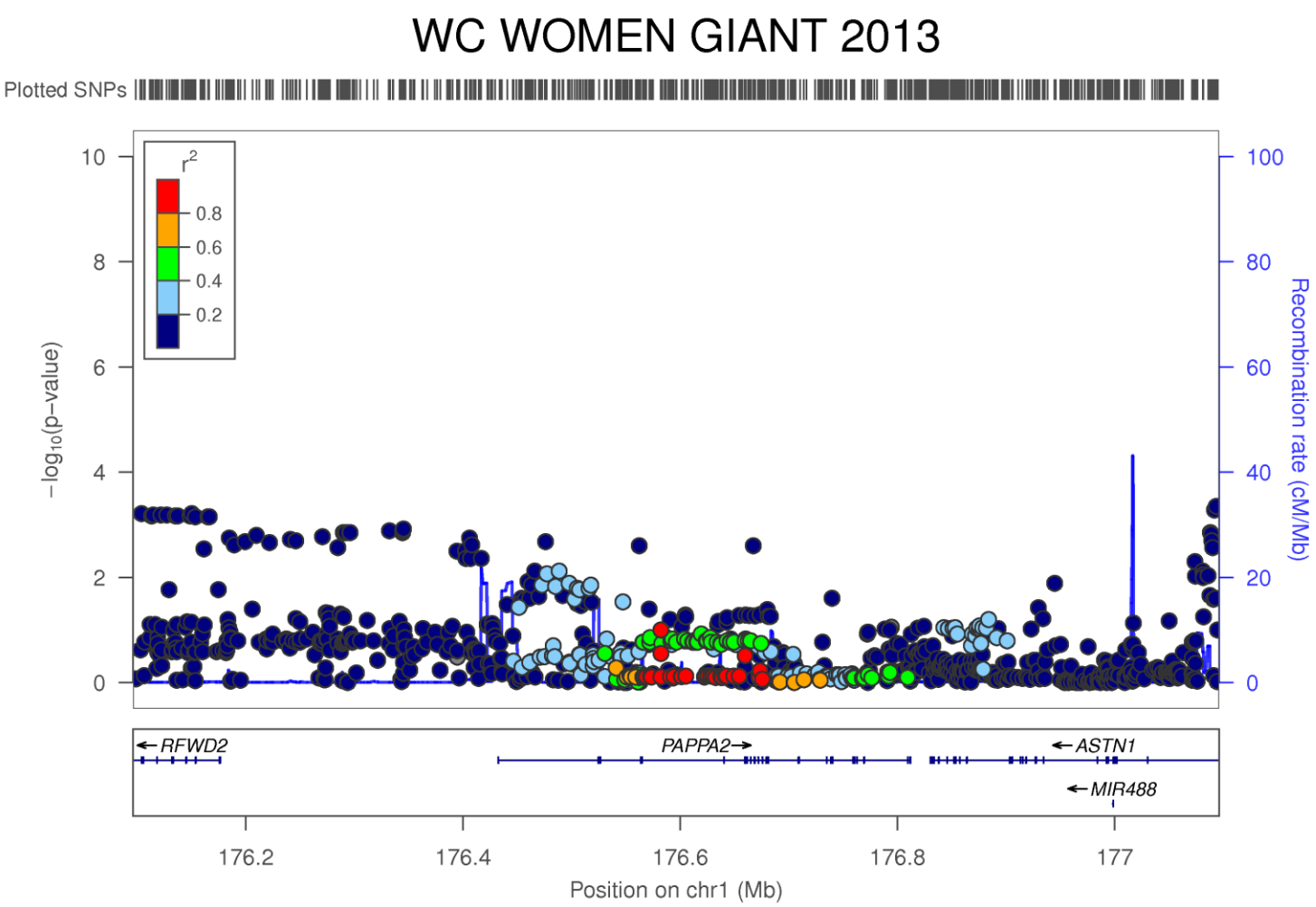

Figure S7. Regional plots for *PAPPA2* from GIANT indexed by interaction analysis significant SNP rs12090061 (6.28×10^{-8}). **A**. Waist Circumference Women, **B**. Waist Circumference Men, **C**. BMI Women, **D**. BMI Men, **E**. Waist Circumference adjusted by BMI Women, **F**. Waist Circumference adjusted by BMI Men, **G**. Waist-Hip Ratio Women, **H**. Waist-Hip Ratio Men, **I**. Waist-Hip Ratio adjusted by BMI Women, **J**. Waist-Hip Ratio adjusted by BMI Men.

Schneider Drive, 375 Greenbrier Drive, Charlottesville, VA, 22903

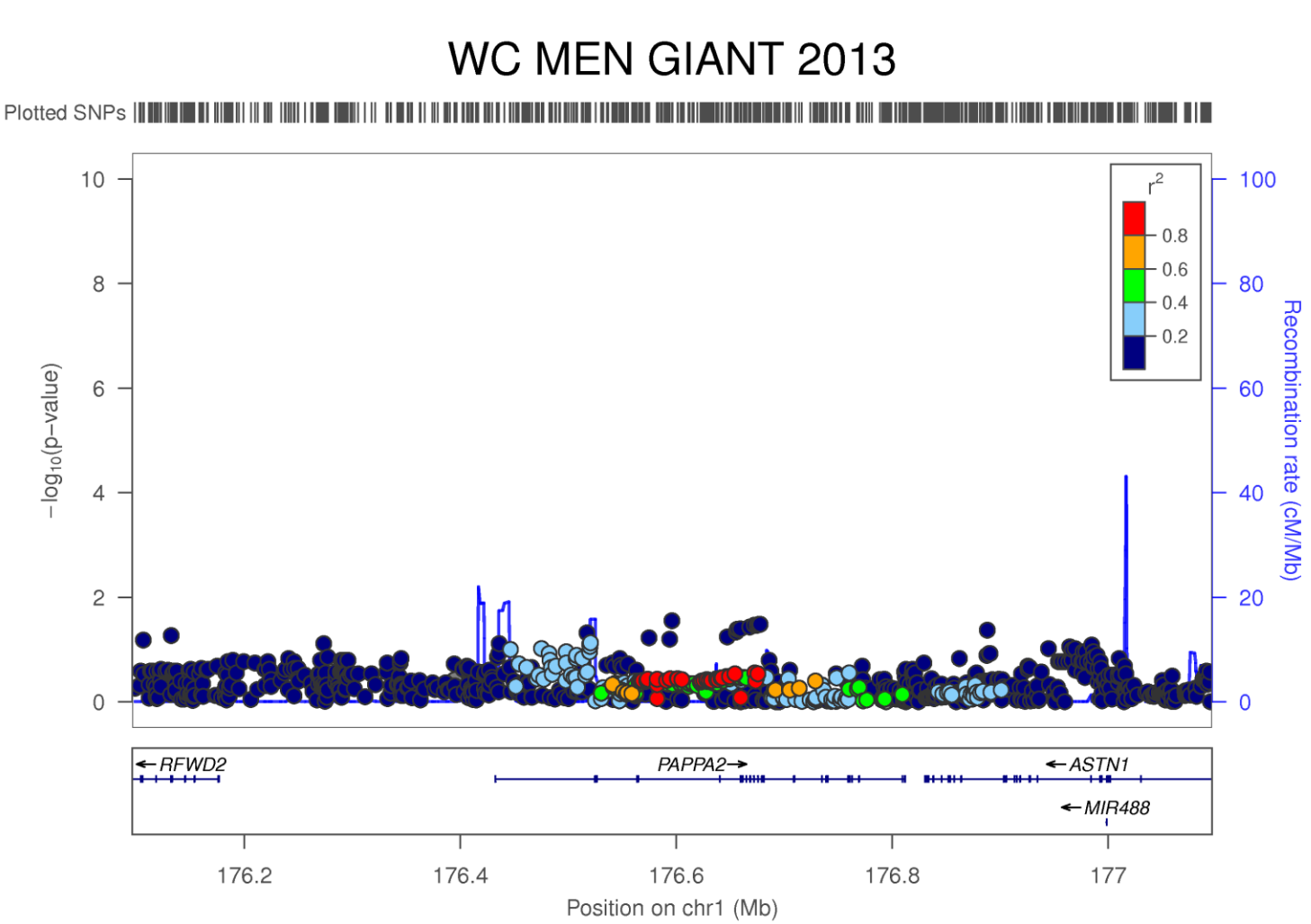

Figure S7. Regional plots for *PAPPA2* from GIANT indexed by interaction analysis significant SNP rs12090061 (6.28×10^{-8}). **A**. Waist Circumference Women, **B**. Waist Circumference Men, **C**. BMI Women, **D**. BMI Men, **E**. Waist Circumference adjusted by BMI Women, **F**. Waist Circumference adjusted by BMI Men, **G**. Waist-Hip Ratio Women, **H**. Waist-Hip Ratio Men, **I**. Waist-Hip Ratio adjusted by BMI Women, **J**. Waist-Hip Ratio adjusted by BMI Men.

C

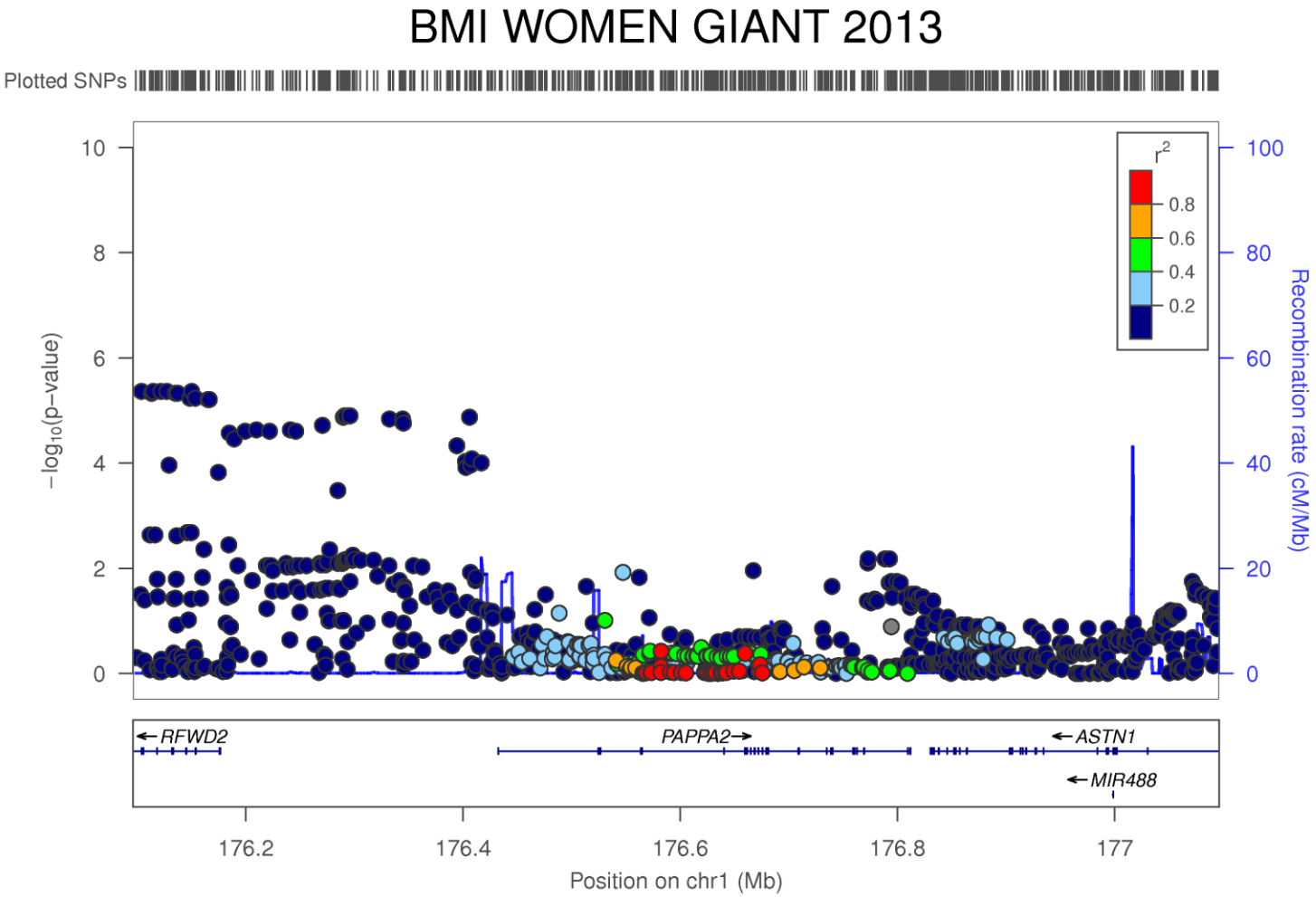

Figure S7. Regional plots for *PAPPA2* from GIANT indexed by interaction analysis significant SNP rs12090061 (6.28×10^{-8}). **A**. Waist Circumference Women, **B**. Waist Circumference Men, **C**. BMI Women, **D**. BMI Men, **E**. Waist Circumference adjusted by BMI Women, **F**. Waist Circumference adjusted by BMI Men, **G**. Waist-Hip Ratio Women, **H**. Waist-Hip Ratio Men, **I**. Waist-Hip Ratio adjusted by BMI Women, **J**. Waist-Hip Ratio adjusted by BMI Men.

D

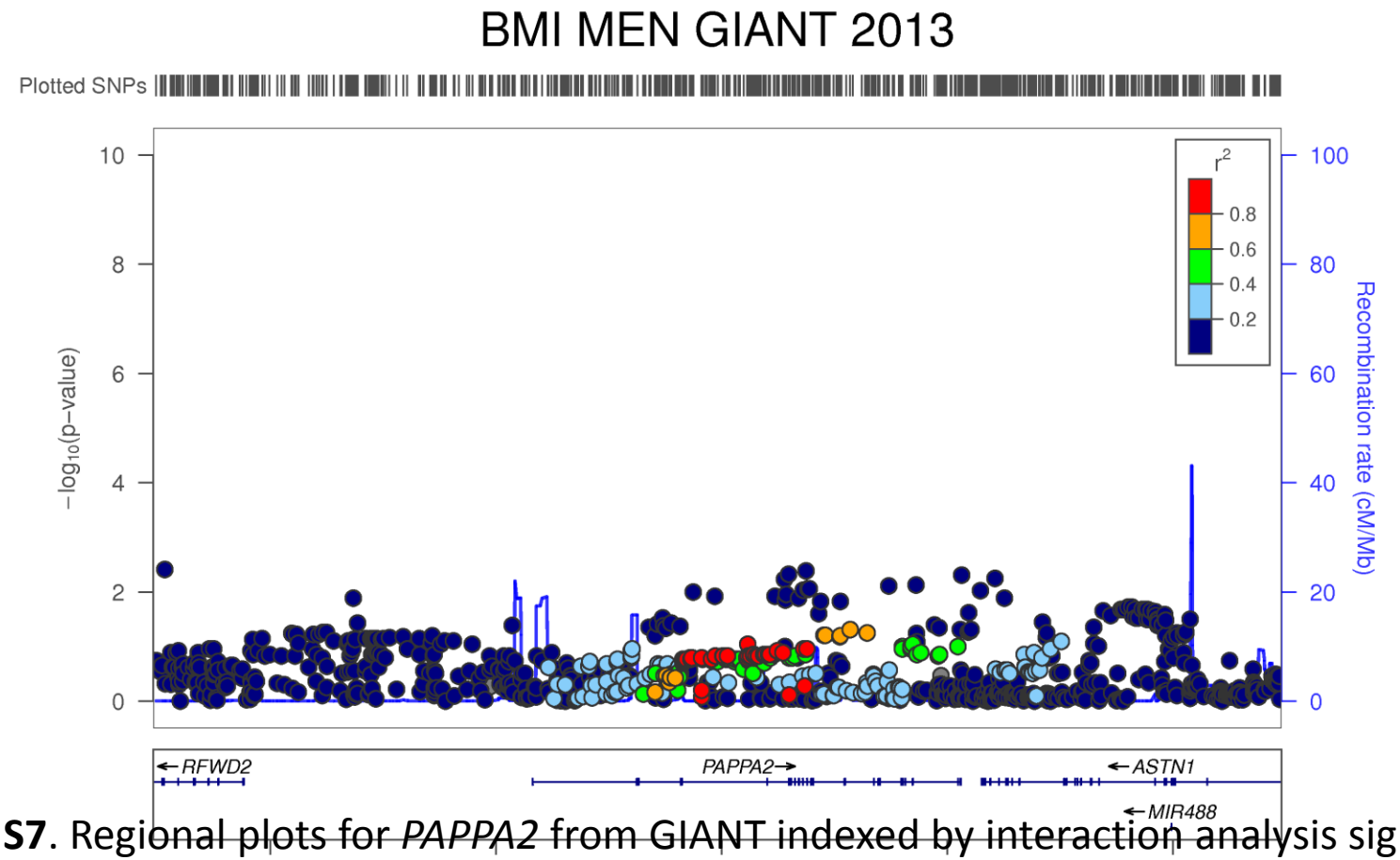

Figure S7. Regional plots for *PAPPA2* from GIANT indexed by interaction analysis significant SNP rs12090061 (6.28×10^{-8}). **A**. Waist Circumference Women, **B**. Waist Circumference Men, **C**. BMI Women, **D**. BMI Men, **E**. Waist Circumference adjusted by BMI Women, **F**. Waist Circumference adjusted by BMI Men, **G**. Waist-Hip Ratio Women, **H**. Waist-Hip Ratio Men, **I**. Waist-Hip Ratio adjusted by BMI Women, **J**. Waist-Hip Ratio adjusted by BMI Men.

E

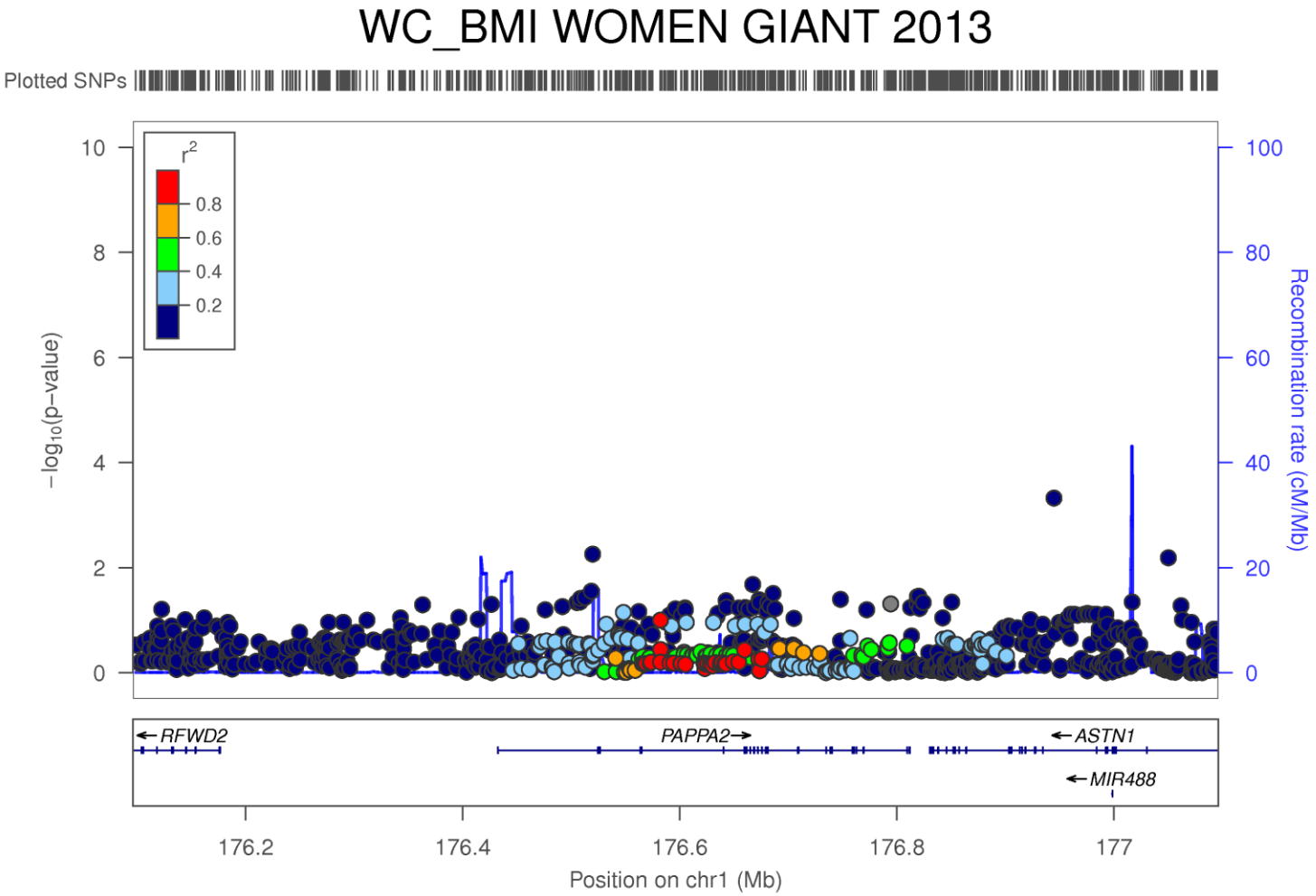

Figure S7. Regional plots for *PAPPA2* from GIANT indexed by interaction analysis significant SNP rs12090061 ($6.28x10^{-8}$). **A**. Waist Circumference Women, **B**. Waist Circumference Men, **C**. BMI Women, **D**. BMI Men, **E**. Waist Circumference adjusted by BMI Women, **F**. Waist Circumference adjusted by BMI Men, **G**. Waist-Hip Ratio Women, **H**. Waist-Hip Ratio Men, **I**. Waist-Hip Ratio adjusted by BMI Women, **J**. Waist-Hip Ratio adjusted by BMI Men.

F

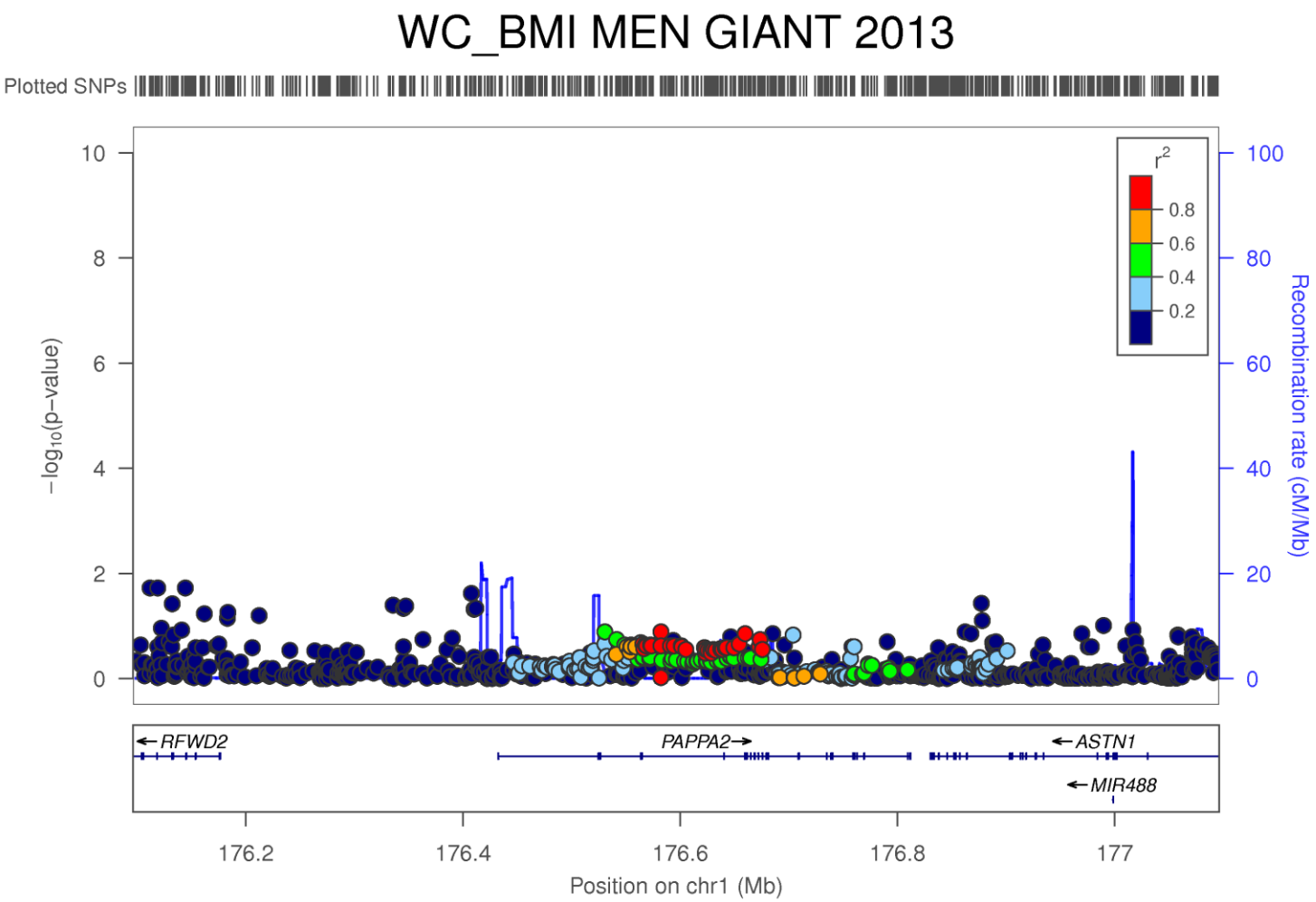

Figure S7. Regional plots for *PAPPA2* from GIANT indexed by interaction analysis significant SNP rs12090061 ($6.28x10^{-8}$). **A**. Waist Circumference Women, **B**. Waist Circumference Men, **C**. BMI Women, **D**. BMI Men, **E**. Waist Circumference adjusted by BMI Women, **F**. Waist Circumference adjusted by BMI Men, **G**. Waist-Hip Ratio Women, **H**. Waist-Hip Ratio Men, **I**. Waist-Hip Ratio adjusted by BMI Women, **J**. Waist-Hip Ratio adjusted by BMI Men.

Schlauch, 375 Greenbrier Drive, Charlottesville, VA, 22903

G

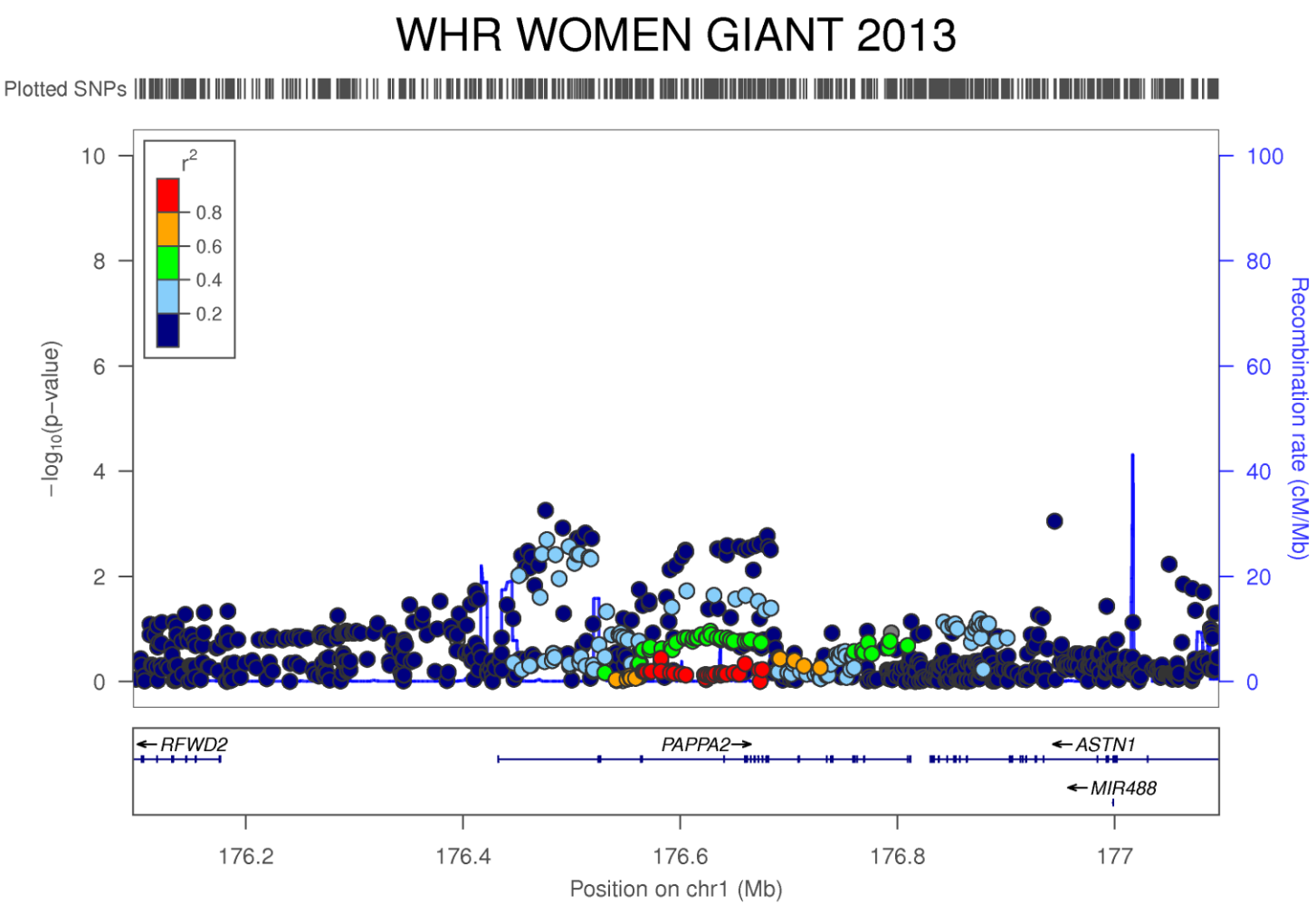

Figure S7. Regional plots for *PAPPA2* from GIANT indexed by interaction analysis significant SNP rs12090061 (6.28×10^{-8}). **A**. Waist Circumference Women, **B**. Waist Circumference Men, **C**. BMI Women, **D**. BMI Men, **E**. Waist Circumference adjusted by BMI Women, **F**. Waist Circumference adjusted by BMI Men, **G**. Waist-Hip Ratio Women, **H**. Waist-Hip Ratio Men, **I**. Waist-Hip Ratio adjusted by BMI Women, **J**. Waist-Hip Ratio adjusted by BMI Men.

H

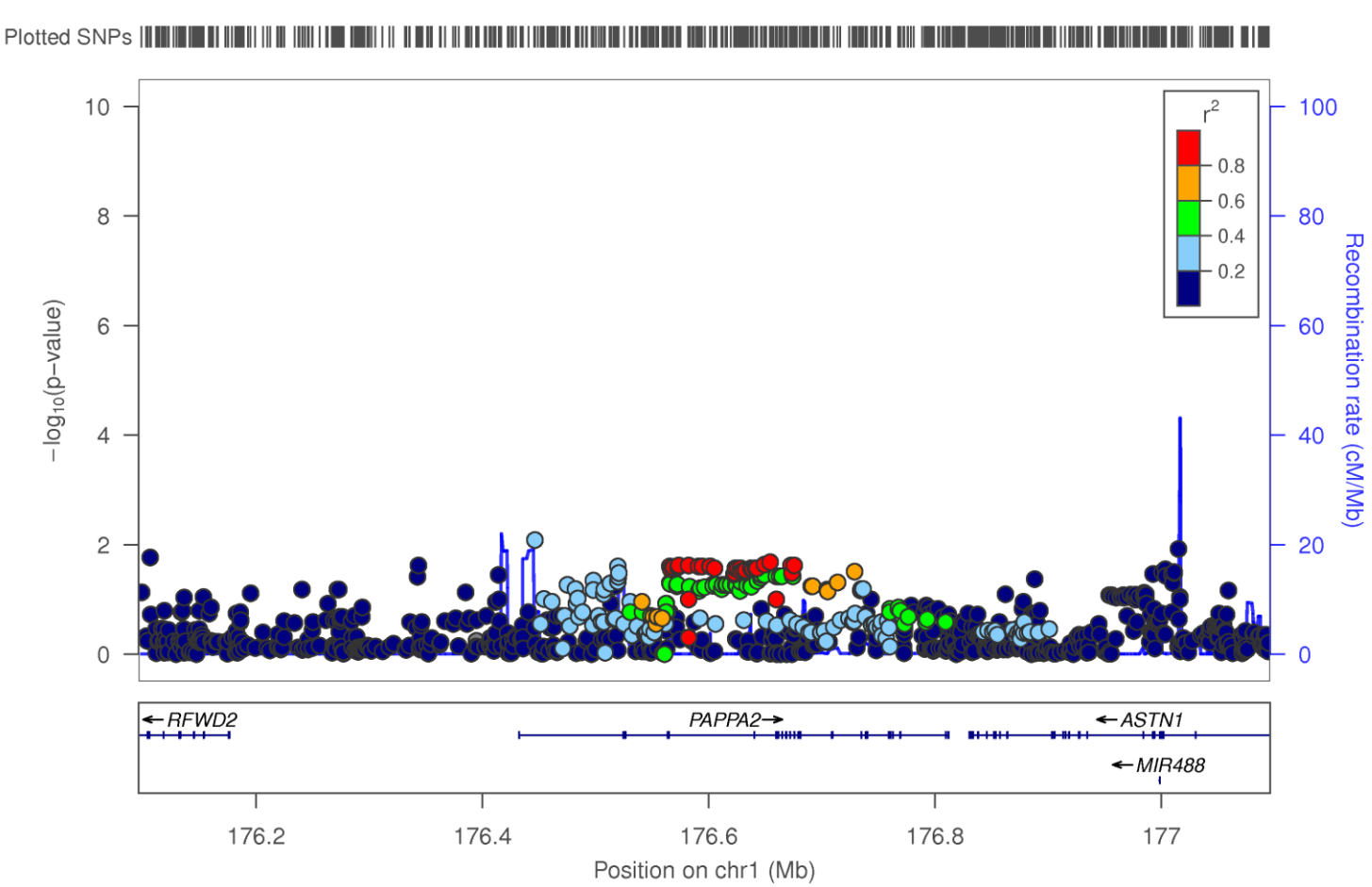

Figure S7. Regional plots for *PAPPA2* from GIANT indexed by interaction analysis significant SNP rs12090061 ($6.28x10^{-8}$). **A**. Waist Circumference Women, **B**. Waist Circumference Men, **C**. BMI Women, **D**. BMI Men, **E**. Waist Circumference adjusted by BMI Women, **F**. Waist Circumference adjusted by BMI Men, **G**. Waist-Hip Ratio Women, **H**. Waist-Hip Ratio Men, **I**. Waist-Hip Ratio adjusted by BMI Women, **J**. Waist-Hip Ratio adjusted by BMI Men.

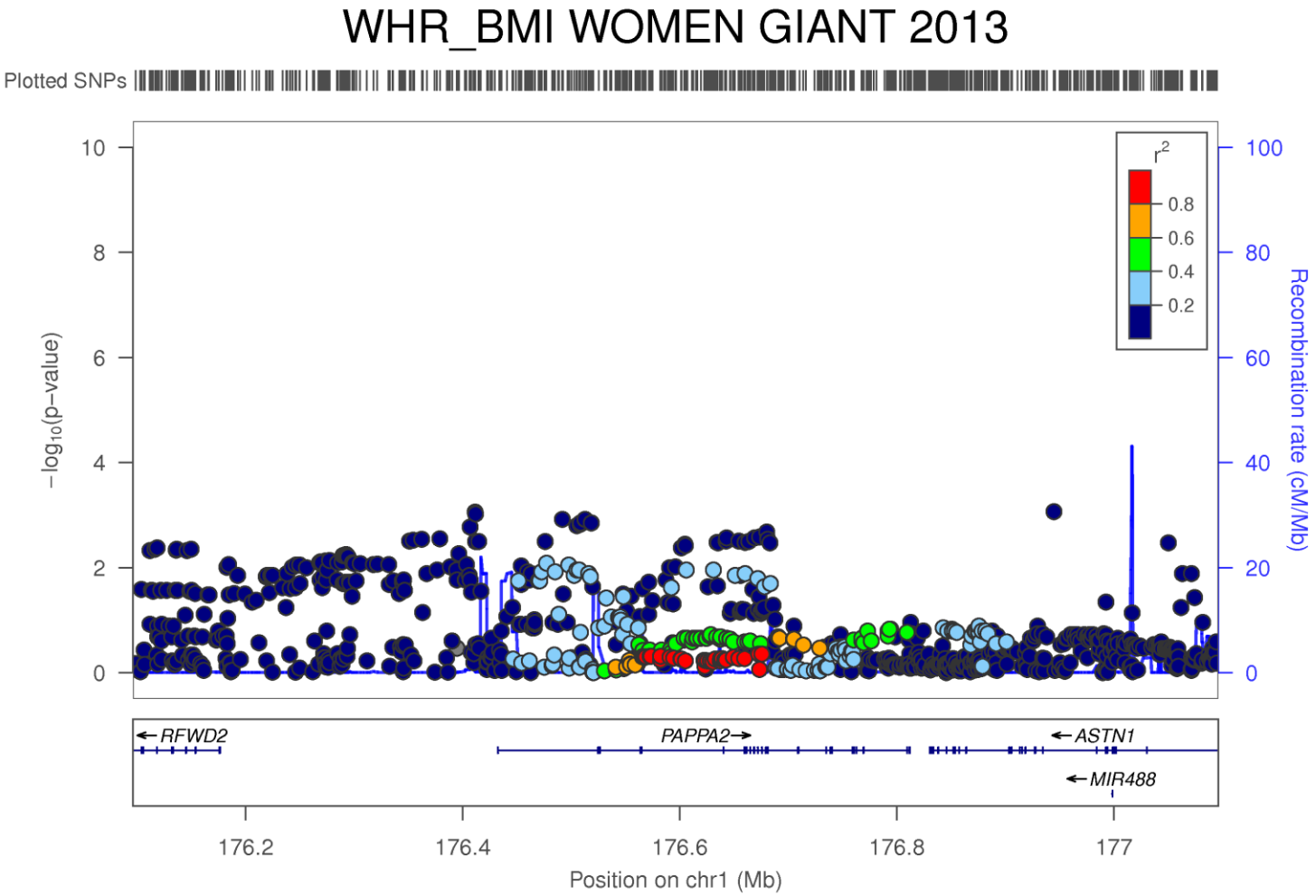

Figure S7. Regional plots for *PAPPA2* from GIANT indexed by interaction analysis significant SNP rs12090061 (6.28×10^{-8}). **A**. Waist Circumference Women, **B**. Waist Circumference Men, **C**. BMI Women, **D**. BMI Men, **E**. Waist Circumference adjusted by BMI Women, **F**. Waist Circumference adjusted by BMI Men, **G**. Waist-Hip Ratio Women, **H**. Waist-Hip Ratio Men, **I**. Waist-Hip Ratio adjusted by BMI Women, **J**. Waist-Hip Ratio adjusted by BMI Men.

Schlauch, 375 Greenbrier Drive, Charlottesville, VA, 22903

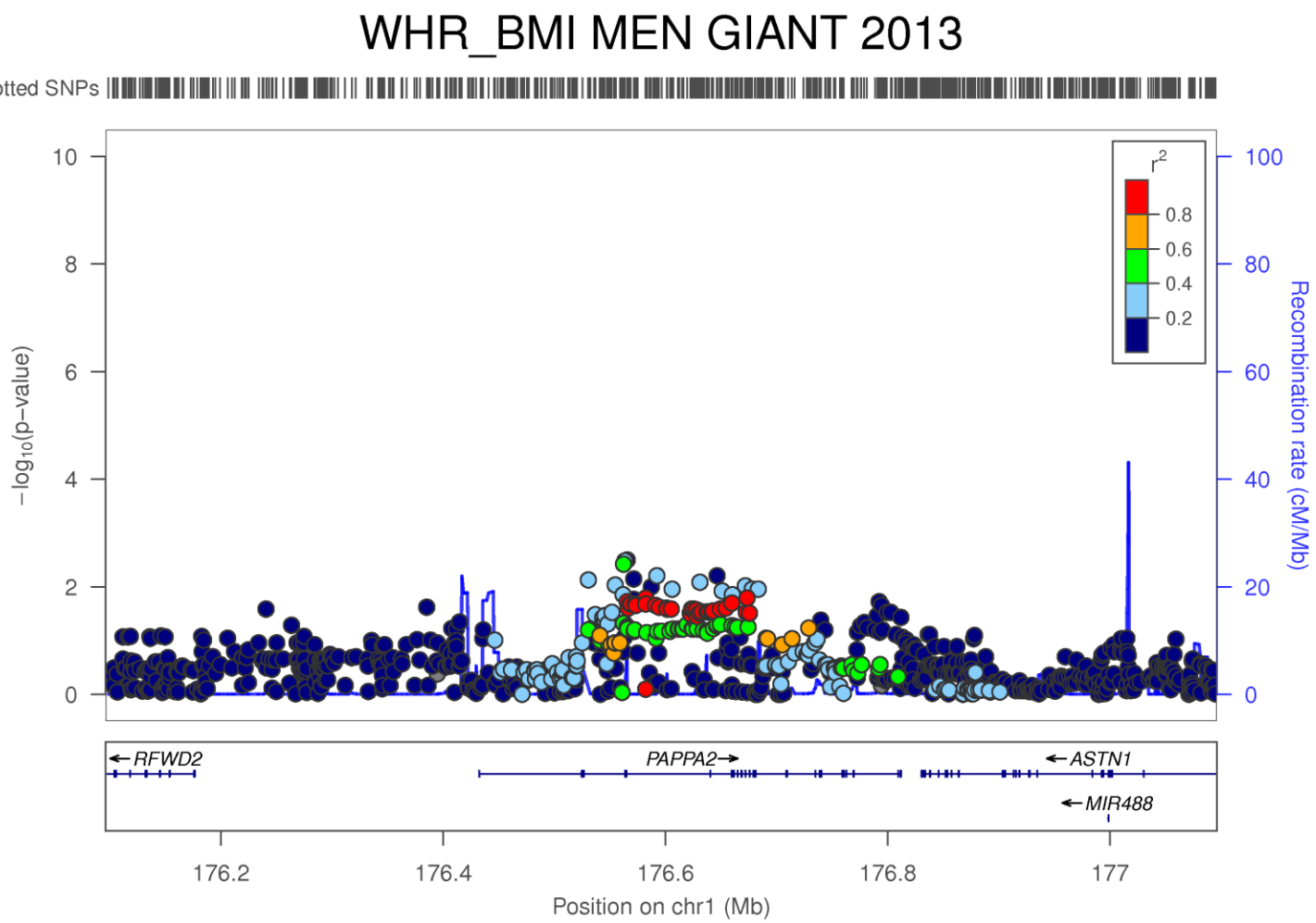

Figure S7. Regional plots for *PAPPA2* from GIANT indexed by interaction analysis significant SNP rs12090061 ($6.28x10^{-8}$). **A**. Waist Circumference Women, **B**. Waist Circumference Men, **C**. BMI Women, **D**. BMI Men, **E**. Waist Circumference adjusted by BMI Women, **F**. Waist Circumference adjusted by BMI Men, **G**. Waist-Hip Ratio Women, **H**. Waist-Hip Ratio Men, **I**. Waist-Hip Ratio adjusted by BMI Women, **J**. Waist-Hip Ratio adjusted by BMI Men.